IDENTIFICATION OF CANCER RELEVANT SYNTHETIC GENETIC INTERACTIONS WITH COHESIN MUTATIONS IN SACCHAROMYCES CEREVISIAE

by

Sivan Reytan

B.Sc., The Hebrew University of Jerusalem, 2014

A THESIS SUBMITTED IN PARTIAL FULFILLMENT OF

THE REQUIREMENTS FOR THE DEGREE OF

MASTER OF SCIENCE

in

THE FACULTY OF GRADUATE AND POSTDOCTORAL STUDIES

(Medical Genetics)

THE UNIVERSITY OF BRITISH COLUMBIA

(Vancouver)

May 2017

ABSTRACT

Cancer therapy is changing. Whole genome sequencing technologies are advancing at an unprecedented pace, opening new opportunities for the genotype-driven personalized treatment of cancer. Synthetic Lethality (SL) based therapeutics have emerged as promising approaches to target cancer-specific somatic mutations, by targeting a second gene that is required for viability in the presence of a tumor-specific mutation. The targetable set of SL partner genes can be expanded by screening for a conditional SL interaction, in which loss of function of two genes results in sensitivity to low doses of a DNA-damaging agent, a concept we have called Synthetic Cytotoxicity (SC). SC also has the potential to expand the number of genotypes that can be treated with existing chemotherapeutics and to improve the efficacy of these therapeutics. In contrast to SL and SC negative genetic interactions, Phenotypic Suppression (PS) describes a genetic interaction in which the double mutant cell is more fit than anticipated based on the fitness of each single mutant.

The model organism, *Saccharomyces cerevisiae* was used to screen for SC interactions with cohesin-mutated genes, with the aim of identifying cross species candidate genes that could be followed up in subsequent studies as SL-based cancer-drug targets. The cohesin complex is frequently mutated across a wide range of tumors and is conserved from yeast to man. We used Synthetic Genetic Array (SGA) technology, a high-throughput genetic method available in yeast, to screen cohesin-mutated strains for synthetic lethal genetic interactions against an array of 310 deletions affecting mainly DNA damage response genes. The screens were done in the presence and absence of four clinically-relevant genotoxic agents. We screened and analyzed 4,650

potential genetic interactions, identifying hundreds of negative and positive interactions, belonging to conserved biological pathways, and potentially relevant to cancer. Using ScanLag, a new validation method, we re-tested and validated several genetic interactions that represent potential therapeutic candidates. These strong SL, SC and PS interactions can be further analyzed in mammalian cells to potentially inform and improve individual cancer therapies as personalized medicine treatments, and lead to the discovery of new pathways or candidates for anti-cancer treatments.

LAY SUMMARY

Cancer cells contain unique DNA alterations that distinguish them from normal cells, representing vulnerabilities that can be exploited for more precise therapy. Currently, cancer therapies heavily rely on DNA-damaging treatments that affect normal cells and lead to various side effects. Exploiting the genetic distinctness of cancer cells to sensitize them to lower doses of DNA-damaging therapy has the potential to improve cancer treatment while minimizing side effects. The cohesin complex of proteins is frequently altered in cancer and can contribute to the initiation and progression of the disease. Since cohesin, and many cancer-relevant processes are similar in yeast and humans, yeast could be used to model cancer and anti-tumor therapy and allow for large scale testing that is impractical in higher organisms. Here, I identified combinations of potential therapeutic targets with specific DNA-damaging agents in yeast, that could guide current cancer treatments.

.

PREFACE

This thesis is original, unpublished work by Sivan Reytan.

Dr. Philip Hieter conceptualized this project along with Dr. Nigel O'Neil and Sivan Reytan. All experiments were performed by Sivan Reytan. The creation of the DDR mutant array (DDR-MA) was a combined effort of Hunter Li, Megan Kofoed, Erik Tammpere and Sivan Reytan. Collection and analysis of data was completed by Sivan Reytan under the guidance of Hunter Li, Dr. Nigel O'Neil and Dr. Philip Hieter.

TABLE OF CONTENTS

LIST OF TABLES

LIST OF FIGURES

LIST OF SYMBOLS

Δ: deletion

LIST OF ABBREVIATIONS

AUC: area under the curve

CIN: chromosome instability

CPT: camptothecin

DDA: DNA-damaging agent

DDR: DNA damage response

DDR-MA: DNA-damage response mutant array

DMSO: dimethyl sulfoxide

DSB: double-strand DNA break

G418: geneticin

HR: homologous recombination

LOF: loss of function

M: cell cycle mitotic phase

MMS: methyl methanesulfonate

ND: no drug

NI: negative (genetic) interaction

OD: optical density

PARP: poly (ADP ribose) polymerase

PI: positive (genetic) interaction

PS: phenotypic suppression

S: cell cycle synthesis phase

SC: synthetic cytotoxicity

SD: standard deviation

SGA: synthetic genetic array

SL: synthetic lethality

SS: synthetic sickness

SSB: single-strand DNA break

SSC: sister chromatid cohesion

SS/L: synthetic sickness/ lethality

ts: temperature sensitive

WT: wild type

ACKNOWLEDGEMENTS

I would like to thank my supervisor, Dr. Philip Hieter, for the opportunity to pursue this project under his supervision and for his highly appreciated support, guidance and generosity.

Thank you to my committee members, Dr. Michel Roberge, Dr. William Gibson and Dr. Marco Marra, for their willingness to oversee my scientific progress despite their busy schedule, and for their valuable intellectual contributions.

I would like to express my sincere gratitude to the wonderful past and present members of the Hieter Lab: Nigel O'Neil, Megan Kofoed, Hunter Li , Leanne Amitzi, Akil Hamza, Frank Ye, Tejomayee Singh, Shay Ben-Aroya, Supipi Duffy, Joshua Regal, Melanie Bailey, Sidney Ang, Walid Omar and Jan Stoepel, for steering me in the right direction and offering useful comments, remarks and engagement through the learning process of this master thesis.

A special thanks to Cheryl Bishop, graduate secretary of the Medical Genetics program, for her admirable care for the graduate students of the program, beyond her professional requirements.

I offer my enduring gratitude to Dr. Shay Ben-Aroya and his lab, and professor Nathalie Balaban and her lab, for their valuable guidance in establishing ScanLag in the Hieter lab.

Finally, I would like to thank my beloved family and friends for your continuous encouragement and love that helped me overcome hardships and accomplish my goals.

Thank you all, for supporting me throughout my years of study in Canada and through the process of researching and writing this thesis.

DEDICATION

Thank you, my dear parents, for providing me the opportunity to follow my ambition and chase my dreams. This accomplishment would not have been possible without you.

Thank you, from the bottom of my heart.

למשפחתי האהובה והיקרה,

תודה לכם, הוריי היקרים, ורד ויגאל, על שנתתם לי את האמצעים לרדוף אחרי השאיפות שלי ולנתב את חיי בדרך שבחרתי. תודה על השורשים העמוקים שנטעתם בי ועל הכנפיים שהענקתם לי, על האהבה, התמיכה, ההקשבה והעזרה חוצי-הגבולות.

תודה ליאור, אחי היקר, על הדאגה והעידוד מרחוק.

תודה לכן, סבתות יקרות, על האהבה המתמדת, האכפתיות והברכות הרבות.

אני מקדישה את התזה הזו לכם, משפחתי הנפלאה.

Chapter 1: INTRODUCTION

1.1 Overview

Cancer is regarded as a global epidemic and is among the leading causes of death worldwide. Cancer is not a single disease, but rather, a collection of perhaps hundreds of diseases, in which the accumulation of specific sets of genetic alterations enables a number of abnormal phenotypes that define a particular cancer subtype[1]. Genome instability, which results in increased frequency of alterations in chromosome number, structure and sequence, is a key tumor-enabling process that drives the accumulation of genetic changes that facilitate tumor survival and progression[2]. The cohesin complex, when mutated, leads to genome instability and is frequently mutated across a variety of cancer types[3], making cohesin an attractive genetic vulnerability to target with new anti-cancer therapeutics.

Synthetic Lethality (SL)-based therapeutics have emerged as a promising approach to target cancer specific somatic mutations[4,5]. SL exploits the genetic distinctness of cancer cells by targeting a second gene that is required for viability in the presence of a tumor specific mutation, resulting in specific killing of the tumor cells while normal cells remain viable. Another approach to leverage genetic interactions to specifically kill cancer cells is Synthetic Cytotoxicity (SC), in which the disruption of two gene products results in increased sensitivity to low dose of a cytotoxic agent[6]. SC has the potential to expand the number of genotypes that can be treated in combination with existing cytotoxic therapies, and to substantially improve their efficacy, which could result in lower effective doses of potentially harmful cytotoxic drugs. However, SC genetic interactions have not been broadly explored.

SL/SC genetic interactions are rare and large scale screening is needed in order to find relevant interactions. The budding yeast, *Saccharomyces cerevisiae*, has been proven to be a

valuable model organism for studying eukaryotic gene function and interaction[7]. Nearly 20% of yeast genes are members of orthologous gene families associated with human disease[8], and together with advanced genetic technologies available for yeast, this organism serves as a powerful model to screen for conserved genetic interactions with yeast homologs of known cancer-associated mutated genes, and for sensitivity to clinically-relevant DNA-damaging agents (DDAs). This, in turn, has the potential to identify therapeutic candidates in humans that can improve current cancer treatment.

The aim of my thesis is to use the cohesin complex as a test case to screen for SC genetic interactions in yeast, and discover how SC can broaden the number of genes that can be targeted in the context of specific DDAs. In the course of this study, a new growth measurement system, ScanLag, was assessed as a method to validate genetic interactions discovered in large-scale genetic screens.

In this chapter, I will introduce the concept of targeted therapy in cancer, describe how genetic interactions can be used to develop new anti-cancer therapeutics, and describe the yeast genetic technology that allows for the high-throughput screening of genetic interactions. I will also provide an introduction to the function and cancer-mutation frequencies of the cohesin complex. The genetic approaches discussed here, have implications for both the advancement of personalized medicine in the field of cancer, as well as in the field of rare genetic diseases associated with mutations in the cohesin complex.

1.2 Cancer: disease and therapeutics

Cancer is the second leading cause of death worldwide, accounting for 8.8 million deaths in 2015, and for which the number of new cases is expected to rise by ~70% over the next 2 decades[9].

Cancer is a genetic disease

Cancer is a complex genetic disease, that is caused by the genetic composition of the cell, as well as by epigenetics and environmental factors (e.g. diet and lifestyle). It describes a situation in which certain cells in the body acquire certain capabilities that enable them to become tumorigenic and ultimately malignant, via a series of enabling mutations and genomic alterations[2]. The genomic landscape of cancer cells usually consists of two distinct types of mutations: 1) several driver mutations (accumulation of as many as 20 mutations per individual cancer[10]), which are genetic alterations that provide a selective proliferative advantage (directly or indirectly) to the malignant cell, and, 2) many passenger mutations, which confer no selective growth advantage[11,12]. Driver mutations can be further distinguished by the type of gene affected, either oncogenes or tumor-suppressor genes. Oncogenes are altered genes (proto-oncogenes) that have acquired mutations that drive the process of tumorigenesis when activated, usually by a dominant gain-of-function mutation[11,13]. On the other hand, tumor-suppressor genes can drive tumorigenesis when inactivated, usually by a recessive loss-of-function mutation, as their expression inhibits cell-proliferation and the development of cancer[11,13]. The unique accumulation of genomic changes and mutations among malignant cells, between and within patients, contributes to cancer heterogeneity and the complexity of the disease.

Hallmarks of cancer

Despite being heterogeneous, several common phenotypes, known as "the hallmarks of cancer" [2], characterize cancer. These phenotypes include: eluding growth suppressors, which includes the bypassing of negative regulation of cell proliferation, mainly via LOF mutations in tumor-suppressor genes; continued proliferative signaling, which is characterized by the ability of cancer cells to sustain chronic proliferation, independent of external growth signals (either by

an autocrine proliferative stimulation, stimulation of surrounding cells to secrete various growth factors, or by dysregulated receptor signaling); resistance to apoptosis, which is the avoidance of cell death by circumventing or limiting the effects of intrinsic (e.g. due to DNA damage) or extrinsic (e.g. via Fas receptor) cell-death signals; angiogenesis, which is the formation of new blood vessels that help sustain the expanding neoplastic growth via delivery of oxygen and nutrients, as well as enabling cells to secrete metabolic waste and carbon dioxide; enabled invasion and metastasis, which is the ability of tumor cells to migrate to other tissues and spread throughout the body (e.g. via loss of cell adhesion); genome instability and mutation, which is an enabling feature of cancer cells that is due to the acquisition of genomic alterations that contribute to an increased aneuploidy rate and/or mutation-rate; tumor-promoting inflammation, that is an enabling feature of cancer cells in which the attempt of the immune system (mainly the innate system) to eradicate the tumor results in the opposite effect, leading to other hallmark features (e.g. by releasing mutagenic reactive oxygen species); escaping immune detection and eradication; reprogrammed energy metabolism, which describes the adjustments of energy metabolism inside the tumor cell to support cell growth and division (e.g. switching to glycolysis as the primary energy source, especially under hypoxia (Warburg effect)); and finally, uncontrolled replication leading to immortality, such as by protection of telomere length. These hallmarks of cancer cells, which differentiate them from normal cells, also represent potential vulnerabilities that can be leveraged to kill cancer cells selectively.

Cytotoxic anti-cancer therapeutics

While some cancers (specifically those that form solid tumors) can be treated locally with surgery, others require taking a different approach, including the use of radiation and pharmaceutical compounds. Chemotherapy (i.e. the use of drugs) and radiation were

incorporated into cancer treatment in the 20th century, when clinical scientists discovered the negative effects of certain compounds (e.g. nitrogen mustard and aminopterin) and x-ray irradiation on one of the known abnormal phenotypes of cancer cells- uncontrolled proliferation[14]. While accomplishing the goal of killing cancer cells, these traditional therapeutics target important cellular processes, such as DNA replication and cell division, that are essential for both cancer and normal cells, especially rapidly dividing cells[14,15]. Thus, chemotherapy and radiation therapy can be classified as cytotoxic therapy, as they are toxic to both healthy and malignant cells and can be accompanied by a range of negative side effects.

Major classes of current standard (or traditional) cytotoxic chemotherapy include: 1) Alkylating agents (e.g. temozolomide, lomustine, oxalaplatin), which damage DNA bases by cross linkage, disrupting abnormal base pairing, or by attaching an alkyl group to DNA bases. 2) Antimetabolites (e.g. 5-FU, 6-MP), which are pyrimidine or purine analogues that interfere with the biosynthesis of DNA and RNA. 3) Anti-tumor antibiotics (e.g. doxorubicin, bleomycin), which function by altering the DNA of cancer cells, for example, by introducing double-strand breaks. 4) Topoisomerase inhibitors (e.g. topotecan, etoposide), which bind to either topoisomerase I or II, stabilize the complex onto the DNA, and stimulate DNA cleavage. 5) Mitotic inhibitors (e.g. paclitaxel, vinblastine, ixabepilone), which interfere with microtubule stability and structure, thus, preventing the completion of cell division during M-phase.[15]

Next generation cancer therapies

A new generation of chemotherapeutic drugs was designed to exploit other hallmarks of cancer cells besides rapid cell division. These treatments can be general or more specific as part of the concept of targeted therapy based on cancer sub-typing[16]. Examples for non-sub-typed treatments that target cancer hallmarks include: drugs that induce apoptosis (e.g. infliximab,

oncrasin-1) to address the hallmark capability of escaping cell death, and angiogenesis inhibitors (e.g. bevacizumab) to address the hallmark capability of forming new blood vessels to provide a tumor with oxygen and necessary nutrients. Treatments that target more specific hallmarks are usually based on tumor-profiling and include: specific growth signal inhibitors (e.g. erlotinib, gefitinib) to address the hallmark of dysregulated signaling pathways of cancer cells[17], and immunotherapy, that has become an exciting and promising method to treat cancer, to address the hallmark capability of avoiding immune destruction[18].

As more has been learned about the biology underlying tumor development and progression, treatments have been developed based on molecular classification of tumors in order to stratify them and choose a more specific therapy. Breast cancer, for example, can be classified by the presence or absence of specific hormone receptors on the tumor cell surface that are associated with the development of this type of cancer[19]. If the cancer cells have estrogen (ER) or progesterone (PR) receptors, they are classified as either ER+ or PR+, respectively, and can be treated with hormonal therapy to limit or inhibit the level of hormone signaling[19]. However, if the cells are ER- or PR- (i.e. hormone-receptor negative), hormonal therapy will most likely not be effective. In addition, breast cancer cells can be tested for human epidermal growth factor receptor 2 (HER2) status, another receptor that when overexpressed, contributes to cancer development and to more aggressive malignancy[19,20]. Cancers that are HER2+ can also be specifically treated. However, 10-20% of breast cancers test negative for all three receptors, hence classified as triple-negatives, and require a different treatment that can involve chemotherapy, radiotherapy, or a combinational therapy of specific inhibitors such as PARP inhibitors (discussed later) and cytotoxic agents[19,20,21]. More recently, breast cancers have been further stratified by DNA sequencing or microarray profiling, in which specific genes (known to

be associated with the disease) are being assayed for predisposing mutations. BRCA status assays, for example, are designed to screen for cancer-predisposing *BRCA1* and *BRCA2* mutations[22]. Mutations in *BRCA1* or *BRCA2* can result in sensitivity to certain DNA damaging therapeutics[23].

The advancement of next-generation sequencing, that has facilitated low cost sequencing of whole genomes and exomes, has expanded the mutational profiling of tumors and has directly contributed to the rise of personalized medicine, allowing to identify cancer vulnerabilities including mutations in oncogenes and tumor- suppressors of specific cancer types, at an unprecedented pace[16]. Cancer cells accumulate a unique set of genomic alterations and mutations, contributing to the different response to treatment between cancer patients, even those who are diagnosed with the same type or subtype of cancer[11]. Personalized medicine addresses this challenge by taking into consideration the unique genetic composition of the individual tumor and tailoring specific cancer treatments and preventive measures based on the tumor genotype[16,24]. One example of a genotype-associated cancer vulnerability is oncogene addiction, which describes a situation in which tumor cells depend on a certain oncogene (and its gain-of-function mutation) for survival[25]. Exploiting oncogene addiction, as part of targeted therapy, aims to inhibit the expression of that specific oncogene to selectively kill the tumor cells[25]. An example of a therapeutic that targets oncogene addiction is the drug Gleevec (generic imatinib mesylate) in the treatment of chronic myeloid leukemia (CML)[26]. The BCR-ABL fusion protein is the product of the Philadelphia (Ph+) chromosome, a reciprocal translocation between chromosome 9 (ABL gene) and chromosome 22 (BCR gene), and is present in >90% of CML patients[27]. The fused parts of the two genes generate a tyrosine kinase protein that causes an irregular signaling inside hematopoietic stem cells that alters their normal function. Gleevec

revolutionized CML treatment by specifically inhibiting the oncogenic tyrosine kinase, resulting in a significant improvement of patient outcome and survival[28].

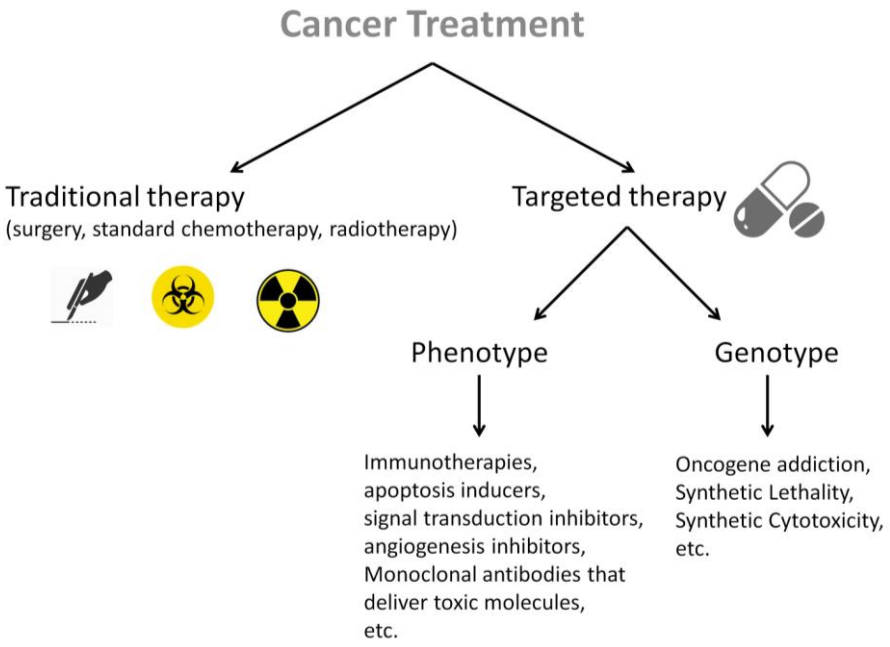

Figure 1-1. Types of cancer therapies.

Cancer can be treated in a non-targeted manner via surgery, chemotherapy or radiation therapy. Targeted therapy can be directed to either a general phenotype of cancer cells or to a specific genotype.

1.2.1 Synthetic Lethality (SL)

Not all cancers have identified targetable oncogenes. Targeting tumor-suppressor gene mutations poses a greater challenge than targeting oncogenes because tumor-suppressor gene mutations are usually loss- or reduction-of-function and, therefore, are not targets for inhibition[5]. However, it may be possible to exploit tumor specific mutations by identifying and utilizing synthetic lethal interactions between tumor-suppressor gene mutations and a synthetic lethal partner.

Synthetic Lethality (SL), a concept first developed in model organisms, is a genetic interaction between two mutated genes in which a mutation in either gene alone is viable yet mutations in both genes simultaneously is lethal[29,30,31–33] (Figure 1-2). The protein product of a gene that, when mutated, has a SL interaction with a known cancer mutation should be an excellent anti-cancer drug target[4,5,34]. An example of a cancer-relevant SL interaction is between mutated BRCA genes (*BRCA1* or *BRCA2*) and Poly (ADP-ribose) polymerase (PARP) inhibitors. PARP1 and PARP2 are active at single-strand break (SSB) sites, where they contribute to efficient repair[35]. BRCA1 and BRCA2 are key proteins in the homologous recombination (HR) repair pathway, and account for the majority of families with hereditary susceptibility to ovarian and breast cancers[36]. Mutation in either *BRCA1* or *BRCA2*, results in a compromised or non-functional HR pathway, leading to DNA-damage repair via an error-prone pathway and to genetic instability. Deficiency in either pathway, HR or PARP-mediated repair, is viable, however, loss of both repair pathways was found to result in cell death[37,38]. The implementation of PARP inhibitors in the clinic[39,40], has stimulated attempts to identify other SL interactions.

1.2.2 Synthetic Cytotoxicity (SC)

Genetic interactions are condition-dependent and can depend on or be suppressed by intrinsic (e.g. genetics, cellular metabolism, cellular microenvironment) and extrinsic (e.g. exposure to cytotoxic therapy) conditions. In the case of tumor cells, therapeutic exposure can affect SL interactions and conversely, genetic interactions can affect the cellular sensitivity to therapeutics. Studies in yeast have shown that genetic interactions can ‘re-wire’ the DNA damage response pathway resulting in increased or decreased sensitivity to DNA damaging agents[41,42]. Genetic interactions resulting in sensitivity to a DNA damaging agent is a class of

conditional SL that we have called Synthetic Cytotoxicity (SC)[6] (Figure 1-2). Genetic interactions resulting in resistance to DNA damaging agents would be characterized as Phenotypic Suppression (PS), or conditional viability.

SC, the combining of an inhibitor of a secondary gene and lower doses of cytotoxic therapies, in the context of a specific cancer mutation, has the potential to expand targetable tumor specific mutations beyond those for which SL interactions can be found. A proof-of-concept screen used a *tel1* null mutant, the yeast orthologue of the human tumor-suppressor *ATM*, to identify SC interactions in yeast, using the topoisomerase I inhibitor camptothecin (CPT)[6]. There are few SL interactions with *tel1* in yeast. However, the SC screen found several SC interactions that were not present in the absence of the cytotoxic agent, thereby demonstrating that SC, in principle, could be used to expand the number of genetic interaction partners that could be targeted to affect the specific killing of *ATM* mutated tumors[6]. Another example of SC is the effect of inhibiting PARP in cohesin-mutated glioblastoma cells in the presence of temozolomide (alkylating agent)[43]. Bailey and colleagues, used matched glioblastoma cell lines, with either a mutated *STAG2* (a cohesin core subunit) or a restored wild-type *STAG2*, to investigate the combined effect of PARP inhibitor and temozolomide. It was found that using a monotherapeutic approach of only PARP inhibitor, can affect genome stability of *STAG2*-mutated glioblastoma cells. However, the combination of a temozolomide and PARP inhibitor, enhanced the killing of *STAG2* mutated cells. Thus, a SC combination, consisting of an inhibitor and a cytotoxic agent, was more effective in killing cohesin-mutated cells compared to the presence of only the inhibitor.

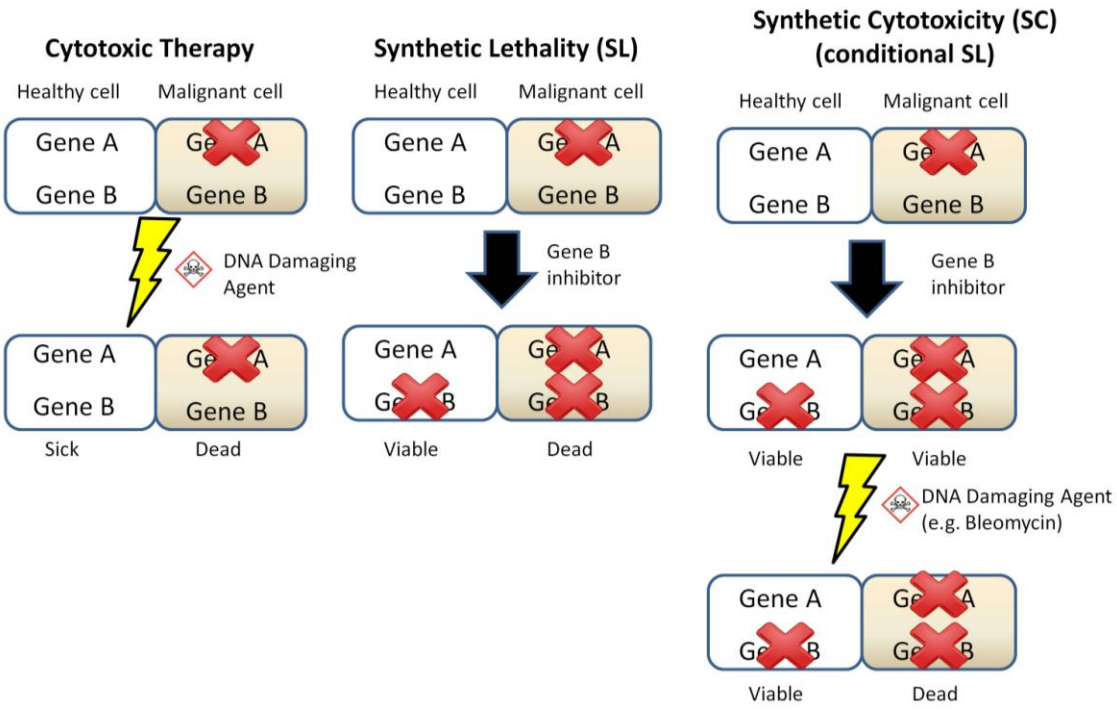

Figure 1-2. The concept of SL and SC.

For the purpose of this project, gene A is a CIN-causing gene that is frequently mutated in tumors (e.g. cohesin gene), and gene B is a negative interaction partner gene (e.g. DNA-damage response gene). *This figure was adapted from Xuesong L *et al.* 2014[6].

The main goal of cancer treatment is to selectively eliminate the malignant cells (maximizing the therapeutic effect) while reducing adverse reactions (minimizing the toxic effect). Finding a secondary gene, that upon inhibition, will sensitize only cancer cells to lower dose of a cytotoxic agent, is highly valuable in terms of minimizing side effects while maintaining efficacy and, in principle, expanding the spectrum of cancer genotypes that can be targeted.

1.3 The cohesin complex

The cohesin complex is involved in various essential cellular functions which, when mutated, can contribute to tumorigenesis. These functions include DNA repair, DNA replication, chromosome segregation, chromatin structure and gene expression[44,45]. Somatic mutations in cohesin-encoding genes occur frequently across many tumor types, including colorectal cancer (one of the leading cancers), acute myeloid leukemia (AML), bladder cancer, glioblastoma, Ewing's sarcoma, melanoma, and Down syndrome related acute megakaryocytic leukemia[3,44] (Figure 1-4). These somatic cohesin mutations could thereby, represent an excellent genetic vulnerability for SC-based therapeutic approaches. The high frequency of cancer mutations in cohesin, an essential protein complex, combined with SL data that is available for its mutated subunits, make cohesin a good candidate for SC screening with DNA damaging agents. To date, no therapeutics have been identified that exploit cohesin mutations in cancer cells.

The cohesin complex is highly conserved from yeast to humans and is composed of four core subunits, including SMC3, SMC1A, RAD21 and STAG1/2 in human somatic cells[46,47] (Figure 1-3). Cohesin-associated proteins support the function and regulation of the cohesin complex[46,47] (**Table 1-1**).

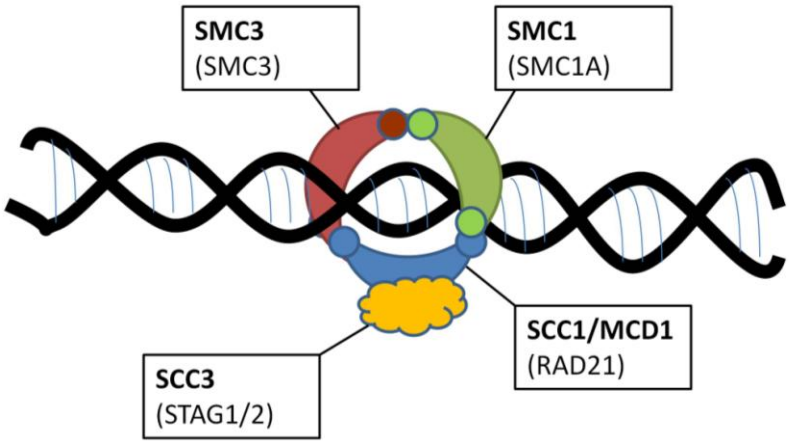

Figure 1-3. The cohesin complex in yeast (bold) and human.

The SMC protein family displays both a hinge domain at one end of the protein and an ATPase head domain at the other end. SMC1 and SMC3 bind together in a V shape through their hinge domains, and interact with SCC1 (RAD21) through their head domains. The SCC3 protein (either STAG1 or STAG2 in humans) binds to the central region of SCC1.

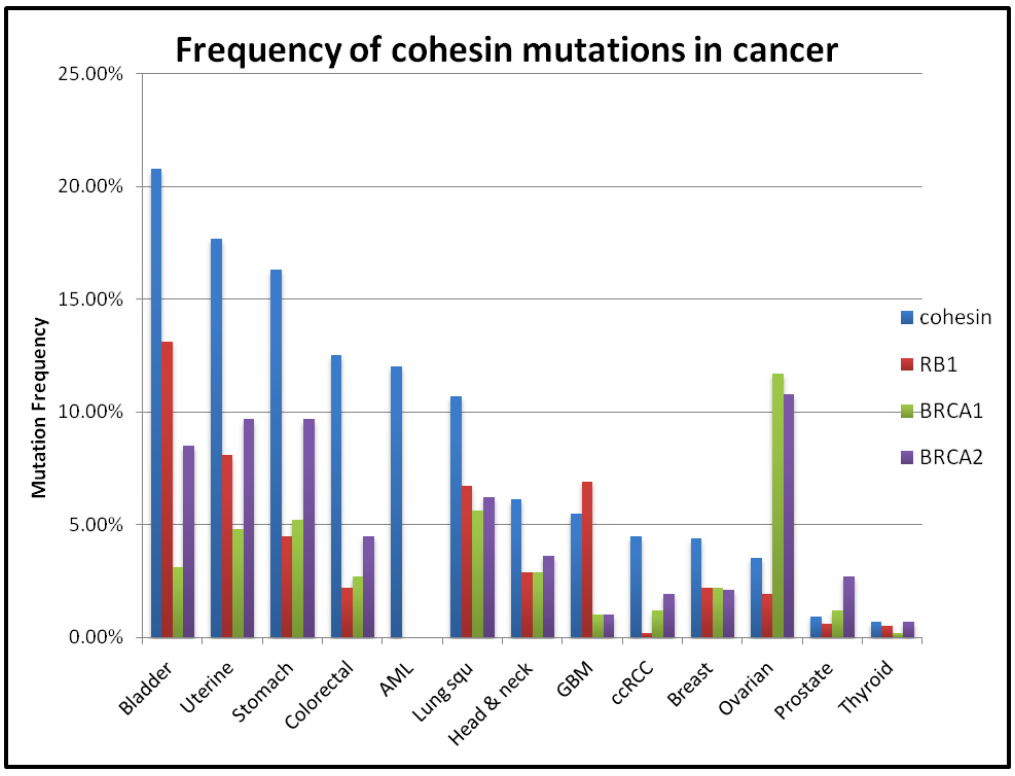

Figure 1-4. Frequency of cohesin mutations in human cancers.

Based on all current TCGA published data from cBioPortal database, the graph shows the percentage of cases in which an altered gene was identified in a given study, organizing the data based on cancer type and plotting it into charts using Excel. Cohesin mutations include mutations in the core subunits of the complex, SMC1A, SMC3, RAD21, STAG1 and STAG2.

The frequency of mutations in the cohesin core subunits is notably higher than other well described tumor-suppressors for many cancer types. For example, more samples of breast cancer contain mutations in cohesin as compared to *BRCA1* or *BRCA2* genes. In breast and ovarian cancers, cohesin gene alteration frequencies are even higher when including copy number variations, due to amplifications of the *RAD21* subunit (Figure 1-5). Recurrent mutations in the cohesin genes, especially in *STAG2*, are associated with different myeloid neoplasms such as AML, and were found to coexist frequently with common mutated epigenetic modifiers in the initiation of this type of cancer[48–51]. Although AML and glioblastoma have relative low mutation rates[52], cohesin mutations are found in more than 10% and 5% of the number of samples studied, respectively, consistent with an important contribution to the development of these cancers.

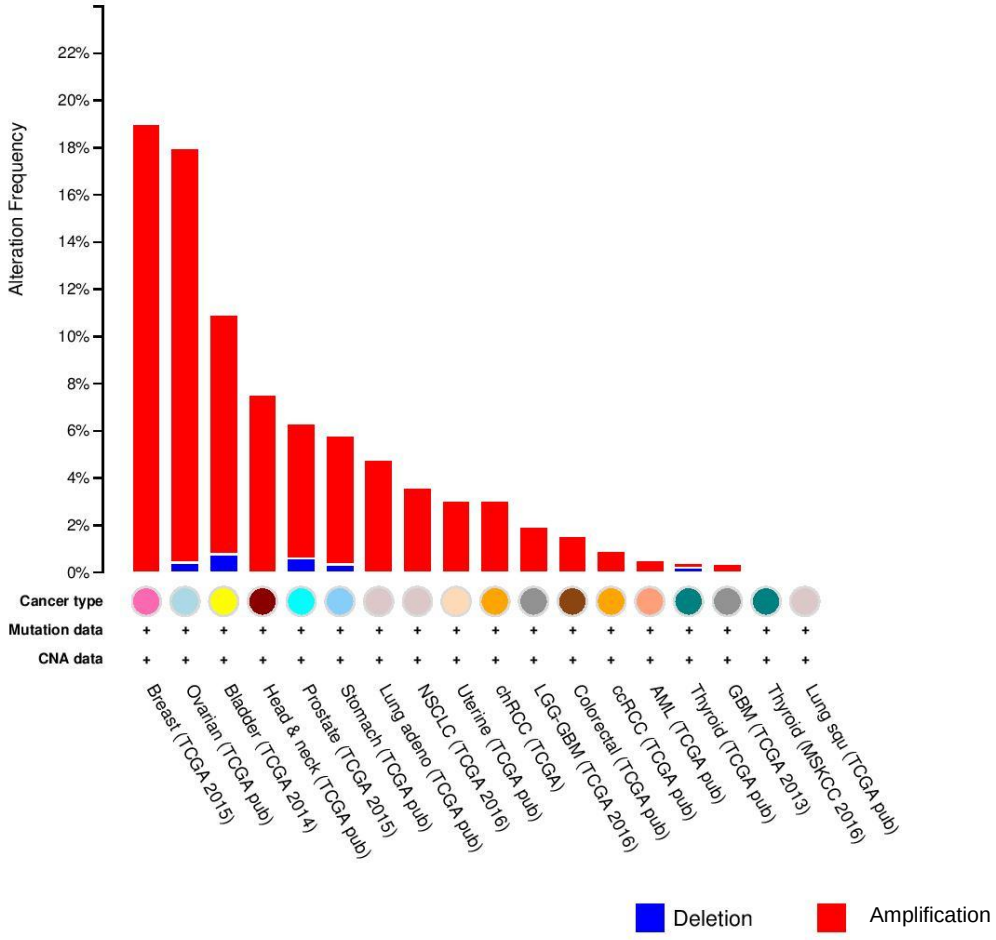

Figure 1-5. Copy number variations (CNA) of RAD21 across a variety of cancer types.

Data was extracted from cBioPortal database and was based on TCGA published data.

Cohesin is essential for cell viability, therefore, most cohesin subunit genes that are mutated in tumors carry hypomorphic mutations which most likely lead to a reduced function rather than a complete loss of function. The exception is *STAG2*, which does exhibit frequent loss-of-function mutations in tumors. This can be explained by the fact that *STAG2* has a paralog, *STAG1*[44]. In vertebrates, the two somatic cohesin complexes are differentiated by the presence of either STAG1 or STAG2, and can vary in their cellular abundance, between cell types, and/or the stage of development[44]. The *STAG2* gene is among the most frequently mutated

genes in at least four tumor types[44], and is highly mutated in bladder cancer (10-30%)[53,51,54,55]. Due to its location on the X-chromosome, only one copy is being expressed in each cell, therefore, a loss of STAG2 requires only a single mutational event. Loss of STAG2 is not lethal because STAG1 is thought to have some overlapping function with STAG2[44].

Mutations in cohesin and cohesin-associated genes can also result in a spectrum of rare inherited human diseases, termed cohesinopathies. The cohesinopathies include Cornelia de Lange syndrome, Roberts syndrome, Wilson-Turner syndrome, Warsaw breakage syndrome, and other medical conditions such as premature ovarian failure and chronic atrial and intestinal dysrhythmia[56–60]. Table 1-1, summarizes the association of the different cohesin subunits with these conditions.

Table 1-1. Cohesin subunits, regulatory proteins and associated cohesinopathies.

S. cerevisiae	Human	Function	Disease
Smc1	Smc1a	Cohesin subunit	Cornelia de Lange syndrome
	Smc1b	Cohesin subunit (meiosis)	
Smc3	Smc3	Cohesin subunit	Cornelia de Lange syndrome
Mcd1/Scc1	Rad21	Cohesin subunit (α-kleisin)	Cornelia de Lange syndrome
Rec8	Rad21L1	Cohesin subunit (meiotic α-kleisin)	
Scc3/Irr1	STAG1	Cohesin subunit	
	STAG2		
	STAG3	Cohesin subunit (meiosis)	Premature ovarian failure
Pds5	Pds5a	Cohesin maintenance	
	Pds5b		
Wpl1/Rad61	Wapal	Cohesin dissociation	
Scc2	Nipbl	Cohesin loading	Cornelia de Lange syndrome
Scc4	Mau2	Cohesin loading	
Eco1/Ctf7	Esco1	Cohesin establishment	
	Esco2		Roberts syndrome

S. cerevisiae	Human	Function	Disease
Esp1	Espl1	Separase	
Pds1	Pttg1	Securin	
Hos1	HDAC8	Smc3 deacetylase	Wilson-Turner syndrome, Cornelia de Lange syndrome
Sgo1	Sgol1	Protection of centromeric cohesin	Chronic Atrial and Intestinal Dysrhythmia
	Sgol2		

Interestingly, an increased risk of cancer among patients with these rare cohesinopathies is not obvious[56,61]. These congenital disorders are very rare (1:10,000 live births for Cornelia de Lange syndrome, unknown prevalence for Roberts syndrome and <1:1,000,000 live birth for both Wilson-turner and Warsaw breakage syndromes), and patients often die young from other medical complications before tumors can be identified. However, in a retrospective analysis done on 295 deceased Cornelia de Lange individuals with a known cause of death, it was found that 2% of death cases were accounted by cancer (1 lymphoma out of 117 children, 4 gastrointestinal and 1 unspecified cancer deaths out of 97 adults)[62]. In addition, two cases of Cornelia de Lange syndrome associated with infantile hemangioendothelioma of the liver and Wilms' tumor were also reported[63].

1.4 Yeast genetics, cohesin and cancer therapeutics

Yeast is a single-cell eukaryotic organism that shares many fundamental genes and pathways with humans. Studies in yeast have provided major insights on gene function, cellular pathways and interactions relevant to human cancer[64–66]. Of particular relevance to this thesis, many human CIN-causing genes were first found in yeast, demonstrating the power and benefit of using model organisms for studying biological mechanisms[67–71]. For example, the cohesin complex was initially discovered in yeast[72,73], and later was found to be mutated in colorectal cancer samples exhibiting a CIN phenotype[74,75], and several other tumor types (see above). In

1997, Hartwell suggested that model organisms, such as yeast, could be harnessed to discover cancer-relevant SL interactions, which could identify potential anti-cancer therapeutic targets[4]. Using the highly conserved cohesin genes as queries for high-throughput synthetic lethal genetic interactions screening, yeast can serve as a platform to identify genetic interactions of value for the development of novel cancer drug targets for selective killing of tumors carrying cohesin somatic mutations[74,76].

1.4.1 Synthetic Genetic Array (SGA)

Finding potential SL and SC targets requires large scale unbiased screening. Yeast affords the opportunity for high-throughput genetic screening to identify therapeutically-relevant genetic interactions using approaches such as Synthetic Genetic Array (SGA)[77,78]. SGA is a powerful genetic screening technique in yeast that can identify a vast number of genetic interactions, both positive and negative, in a fast and systematic way. It involves using robotics to efficiently mate and manipulate high-density arrays of yeast single mutants in order to construct double mutants for a reference query gene mutation of interest, via a sequence of replica-pinning procedures[78,79]. By observing the differences in growth rate between the single and the double mutants under diverse conditions (e.g. chemical compounds), quantitative scores can be generated to reflect the magnitude of genetic interactions. Negative genetic interactions (i.e. SL and SC) will result in a more severe fitness defect than anticipated under a certain condition (Figure 1-6), while positive genetic interactions (i.e. PS) will result in a better fitness than anticipated. Another important benefit of SGA is its flexibility, as any genetic alteration can be used as the reference query mutation (e.g. point mutation, knockout, gene over expression, etc.), and genetic interactions can be tested under various conditions (different temperatures, media, drugs, etc.).

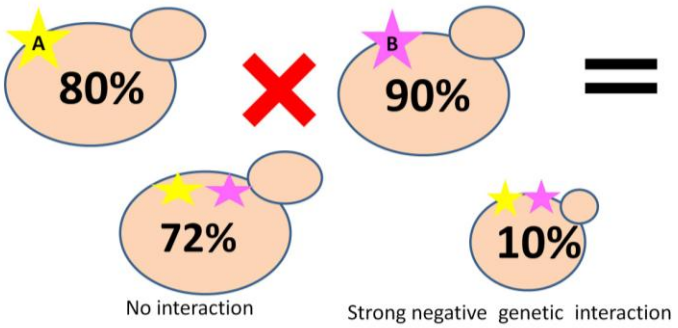

Figure 1-6. Quantitative genetic interactions determination.

In the absence of a genetic interaction, the fitness of a double mutant is expected to be the product of the individual fitness values of the corresponding single mutants. For example, a yeast strain that carries a mutation in gene A, which confers a defective response and consequent increased sensitivity to a certain DNA-damaging agent (DDA), demonstrates 20% growth rate reduction compared to wild-type strain at the same dose of the DDA. Likewise, mutant B shows a sensitivity with a 10% growth-rate reduction. The double mutant, however, grows 90% slower than the wild-type in the presence of the DDA, indicating that the genetic combination is more than additive (i.e. causes a greater growth defect than expected for the combination of mutation A and B) (0.8 *0.9 = 0.72, or a 28% expected reduced growth rate). One interpretation of this type of genetic interaction is that both genes might be involved in the same biological process, such as DNA repair, but occur in separate pathways. The cell can tolerate loss-of-function mutations in either pathway but not both.

In a typical SGA screen (Figure 1-7), a haploid query yeast strain, harboring the reference mutation of interest, is mated to an array of haploid mutants. Diploid cells are selected for the selective markers of both query gene and array null mutation. After two rounds of diploid selection, the diploid strains are induced to go through meiosis and produce spores (via nutrient starvation). Sporulated haploids are then selected based on their genotype. Haploid double mutants bearing the query mutation and the array deletion, are analyzed based on strain spot size on the final plate relative to the array single mutant. SL genetic interactions are identified based on the non-drug condition, while SC interactions are identified in the presence of sub-lethal

doses of DDAs. Comparing the area of the strain spots between the single and the double mutants, will demonstrate the growth rate differential of each single and double mutant strain under the specific environment. SC genetic interactions are those for which the double mutants demonstrates a greater growth defect in the presence of DDA compared to each single mutant or to the double mutant in the absence of a DDA.

These genetic interactions, identified by SGA, can indicate functional dependency and pathway redundancy in yeast that might be conserved in humans. This, in turn, can be exploited for developing new inhibitory drugs or guiding the modification of current medical therapies[16]. SGA technology enables an investigator to collect and analyze large sets of genetic interaction data[77,78,80] that can be used to construct and map a large number of genetic interactions into networks, all in an efficient and robust way.

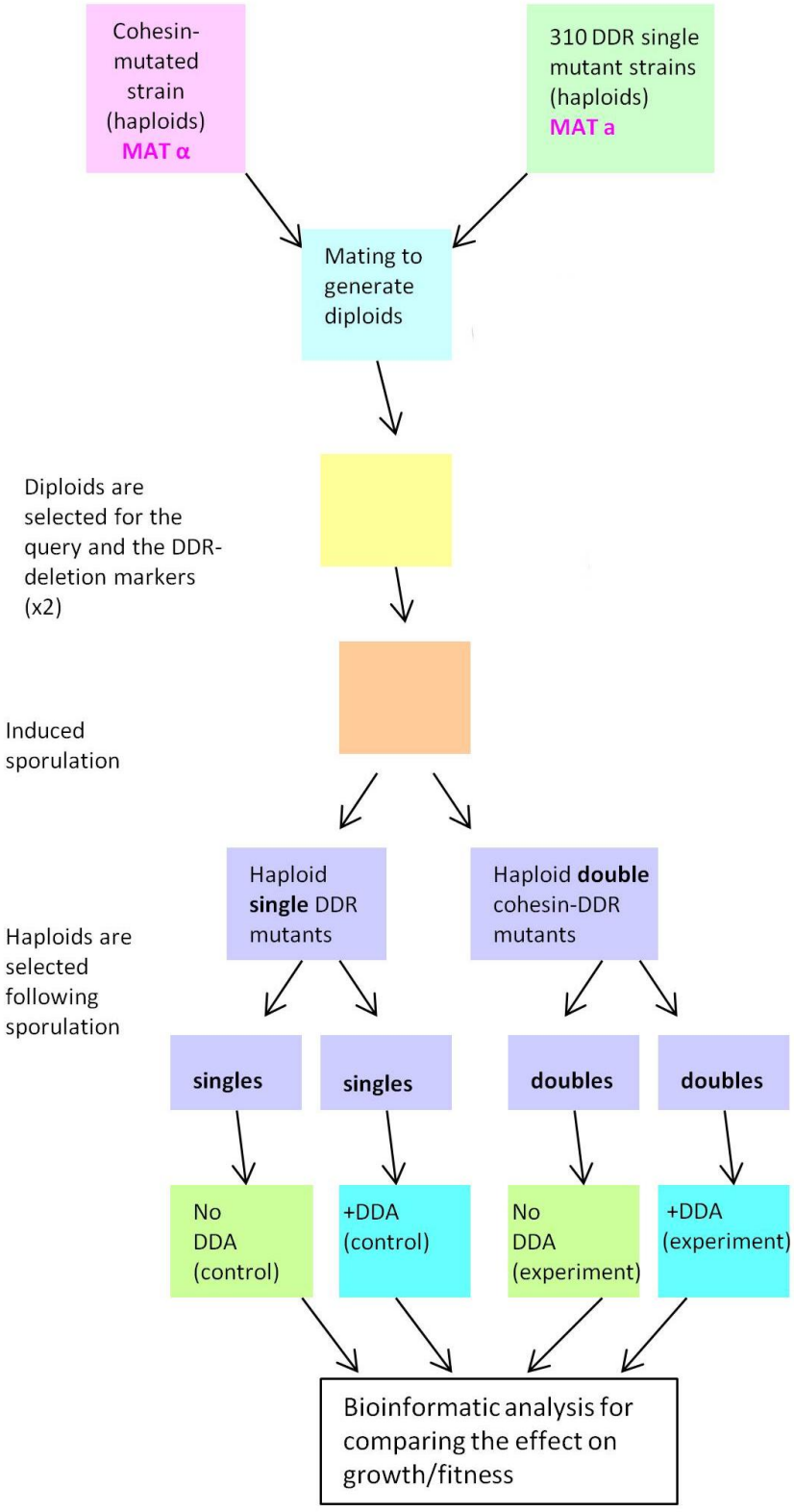

Figure 1-7. The structure of the SGA screen conducted in this project.

1.5 Thesis objective

The aim of my project was to identify novel genetic interactions, both negative (SL, SC) and positive (PS), with the frequently-mutated cohesin complex genes in yeast using SGA. Over the span of a decade, this technology has been used to screen genome-wide for SL genetic partners of all non-essential and essential yeast genes, under a defined laboratory condition[81]. Screening for SC is a powerful and an innovative concept with potential clinical relevance. By using different conditions, including the presence of four distinct cytotoxic agents (MMS, CPT, bleomycin, and benomyl), SC interactions could be assessed for frequency and strength of the negative interaction. We also wanted to determine whether cohesin mutations affect the efficacy of these DDAs and whether any gene mutations could suppress the sensitivity of cohesin mutations to the DDAs (i.e. act as phenotypic suppressors, PS).

High-throughput methods such as SGA generate false positives and false negatives, and therefore, SGA data needs to be validated to identify bona fide genetic interactions. A new method, called ScanLag, was also assessed for validating initial genetic interaction hits, as captured in the SGA screens. The ScanLag method was compared to liquid growth curves, that have been used as the gold standard in the field for validating genetic interactions. ScanLag score data was also compared to the magnitude of genetic interactions from the preliminary SGA score data to understand the correlation between the two.

The SGA genomic technology can enable the identification of many SL and SC genetic interactions with a mutated cohesin gene, that can be tested for evolutionary conservation in mammalian cells. Creating maps of these interactions can further expand our knowledge about the biological importance of these genes and their potential role in cancer.

Any SL and SC genetic interactions that are validated in mammalian cells have the potential to provide improved individual cancer therapies for tumors carrying cohesin gene mutations, while PS genetic interactions can indicate potential molecular mechanism for chemotherapy resistance and potential targets for treating the cohesinopathies.

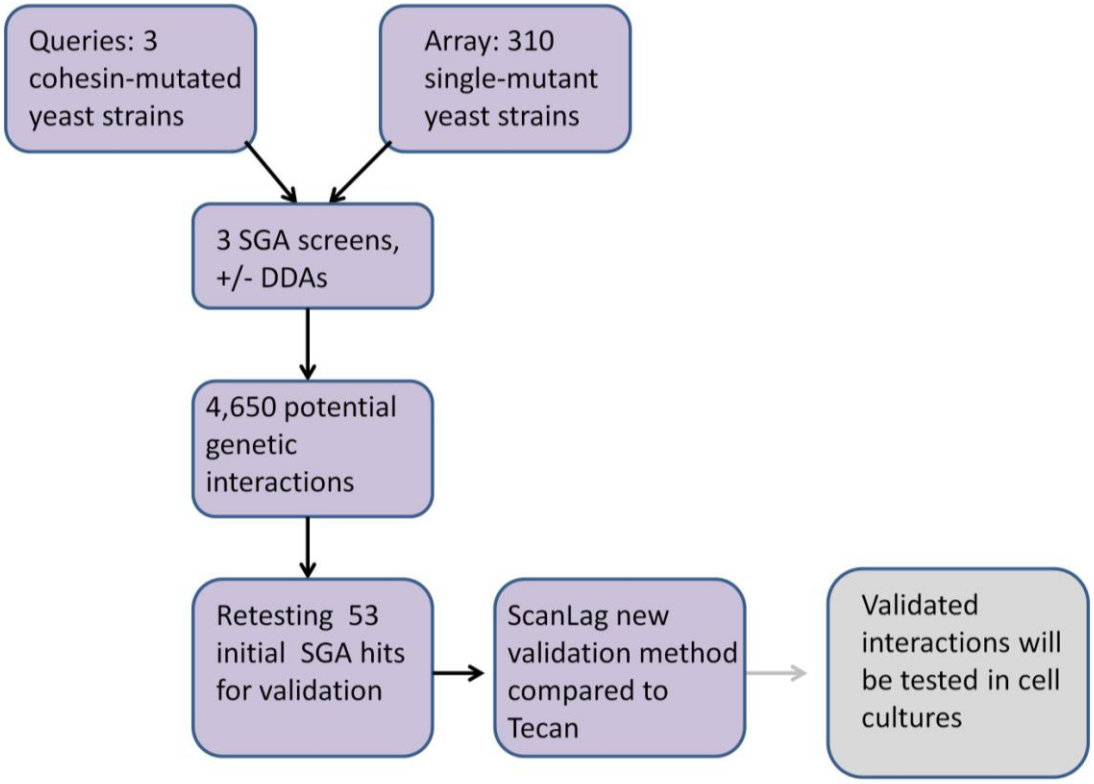

Figure 1-8. Thesis project flow.

Chapter 2: MATERIALS AND METHODS

2.1 Yeast strains

Strains used are BY4743 background[82]. All strains used in this project were confirmed by PCR and were checked for temperature-sensitive (ts) phenotype and auxotrophic markers. Temperature-sensitive cohesin subunit alleles, *smc1-259* and *scc1-73*, and cohesin loader allele *scc2-4*, are marked with URA3[83] and were used as the query genes in the SGA screens, as an expansion of a previously published screen[76]. The full genotypes of the haploid query strains are: *scc1-73::URA3/SCC1* or *smc1-259::URA3/SMC1* or *scc2-4:URA3/SCC2*, ura3*Δ0* his3*Δ1 LYS2* can1*Δ*::STE2pr_pombeHIS5 lyp1*Δ.* All query strains are MATα haploids *met15Δ0 orMET15* in addition to the genotype specified.

For validation, double mutants from the *scc1-73* screen were retested, as the *scc1-73* data captured many previously reported hits. In addition, the *scc1-73* strain exhibits a better fitness than the *smc1-259* strain, and we wished to follow-up with one of the core subunits of the complex. The scc1-double mutants, that were retested for validation, originated from SGA screen plates following re-sporulation and haploid selection of the original screen double heterozygous diploids. The double mutant spot on the haploid double-selection SGA plate, containing a mixed population, was streaked for single colonies on a -URA+G418 selective plate. One single colony was chosen for retesting and validation to ensure a cloned population of cells with a homogeneous genetic background. To generate MATa single mutants from the DDR-MA carrying both selective markers, double heterozygotes were generated through a separate SGA screen with a "WT query", marked with the NatMX cassette inserted into the URA3 gene. Following sporulation, single mutants representing the array deletion were picked from the final haploid double selection plate. This separate SGA procedure was needed since the

spots on the single haploid selection plates generated in the cohesin allele SGA screens contain a mixed population of single and double mutants (due to selection of only the array marker). SGA spots were streaked for single colonies on double-selection plates, from which one single colony was chosen for validation. Haploid double mutant strains were tested simultaneously with both single mutant strains (i.e. array deletion and query mutated parental strains). All strains, tested in both SGA and in the validation process, were grown at 25°C until the final experimental stage (to prevent long exposure to cellular stress), unless otherwise indicated.

2.1.1 DDR-MA

In order to focus on highly conserved genes and pathways associated with a CIN phenotype and relevant to cancer survival and progression (rather that the whole-genome array), we built the DNA-damage response mutant-array (DDR-MA), which is a collection of 310 haploid yeast strains, bearing knock-outs of non-essential genes which function or are mainly associated with the cellular process of DDR. These strains are marked with a KanMX cassette, which confers resistance to the drug G418. The overall genotype of the haploid gene deletion strains is MATa *ura3Δ leu2Δ his3Δ lys2Δ met15Δ ykoΔ*::KanMX.

The DDR-MA was arrayed in a 384 density format for the SGA screen. Many of these genes, when mutated, are known to cause a CIN phenotype[71] and almost all genes have at least one human homolog or functional analog (Table 4-1). Array strains were either originated from the Deletion Mutant Array (DMA) Collection[84] or the Heterozygous Diploid Collection[85].

Before any screen could be conducted, quality control (QC) of the array strains used in the build of the new DDR-MA was performed. This was accomplished by a group effort that included making genomic DNA preparations of 313 array yeast strains, and confirming that the gene deletions were correct by using PCR to identify the specific deleted gene, and compiling a

collection of correct strains. The goal of this process was to verify the identity of the mutated strains on the array. Sixty-two strains were incorrect in the genome wide DMA (obtained from a commercial source) and were, therefore, needed to be re-created. Out of these 62 strains, 11 were created via direct DNA-mediated transformation, and the other 51 were generated from the heterozygous collection (via tetrad dissection) and were incorporated into the new array (Table 2-1).

Table 2-1. The physical map of the new DDR-MA

1	2	3	4	5	6	7	8	9	10	11	12	13	14	15	16	17	18	19	20	21	22	23	24
WT	YER051W	YDL155W	YLR247C	WT	YLL019C	YBR158W	YLR085C	WT	YLR107W	YER016W	YML011C	WT	#REF!	YJR047C	/MR186W	WT	YMR216C	YER070W	YDR014W	WT	Blank	Blank	WT
WT	JHD1	CLB3	IRC20	WT	KNS1	AMN1	ARP6	WT	REX3	BIM1	RAD33	WT	#REF!	ANB1	HSC82	WT	SKY1	RNR1	RAD61	WT	Blank	Blank	WT
WT/Blank	YOR025W	YDL013W	YOL072W	YDL042C	YPL241C	YDL070W	YPL129W	YER164W	YDR378C	YER169W	YEL003W	YER179W	YEL061C	YDR523C	YGR171C	YFL003C	YGR184C	YGR271W	YCR008W	YIL018W	Blank	WT	Blank
WT/Blank	HST3	SLX5	THP1	SIR2	CIN2	BDF2	TAF14	CHD1	LSM6	RPH1	GIM4	DMC1	CIN8	SPS1	MSM1	MSH4	UBR1	SLH1	SAT4	RPL2B	Blank	WT	Blank
WT/Blank	/MR284W	YAR002W	YNL330C	YLL002W	YOR073W	YML061C	YOR304W	YML032C	YOR351C	/MR167W	YOL006C	YMR190C	YOL043C	YMR201C	YOL068C	YNL299W	YPL240C	YNL246W	YPL181W	YOR026W	YPL096W	YOR080W	WT
WT/Blank	YKU70	NUP60	RPD3	RTT109	SGO1	PIF1	ISW2	RAD52	MEK1	MLH1	TOP1	SGS1	NTG2	RAD14	HST1	TRF5	HSP82	VPS75	CTI6	BUB3	PNG1	DIA2	WT
WT	YLR418C	YJL013C	YGL066W	WT	YKR024C	YGL100W	YDR289C	WT	YGR270W	YML028W	YML124C	WT	YJL115W	YOR308C	YJR063W	WT	YBR009C	YOL012C	YBR189W	WT	YDL082W	YGR180C	WT
WT	CDC73	MAD3	SGF73	WT	DBP7	SEH1	RTT103	WT	YTA7	TSA1	TUB3	WT	ASF1	SNU66	RPA12	WT	HHF1	HTZ1	RPS9B	WT	RPL13A	RNR4	WT
WT/Blank	YBR186W	YOL004W	YBR195C	YPL164C	YBR223C	YBR231C	YBR228W	YDR075W	YDR121W	YDR092W	YDR379W	YDR363W	YEL056W	YDR364C	YAL019W	YDR369C	YGR129W	YGR163W	YHL022C	YHR120W	YHR086W	YCL016C	WT/Blank
WT/Blank	PCH2	SIN3	MSI1	MLH3	TDP1	SWC5	SLX1	PPH3	DPB4	UBC13	RGA2	ESC2	HAT2	CDC40	FUN30	XRS2	SYF2	GTR2	SPO11	MSH1	NAM8	DCC1	WT/Blank
WT/Blank	YGL240W	YHR066W	YJL006C	YCL029C	YBR026C	YKL117W	YAL040C	YGR108W	YHR154W	YPR141C	YLR210W	YBL058W	YJL176C	YGL003C	YDR176W	YGR285C	YPR119W	YHR064C	YGL043W	YNL252C	YJR104C	YJR074W	WT/Blank
WT/Blank	DOC1	SSF1	CTK2	BIK1	ETR1	SBA1	CLN3	CLB1	RTT107	KAR3	CLB4	SHP1	SWI3	CDH1	NGG1	ZUO1	CLB2	SSZ1	DST1	MRPL17	SOD1	MOG1	WT/Blank
WT	YHR200W	YKL057C	WT	YGR056W	YCR014C	YLR357W	WT	YLR270W	YLR135W	YLR288C	WT	YLR320W	YKL017C	YGL194C	WT	YGL211W	YKL025C	YPL042C	WT	YPL008W	YKL190W	YPR164W	WT
WT	RPN10	NUP120	WT	RSC1	POL4	RSC2	WT	DCS1	SLX4	MEC3	WT	MMS22	HCS1	HOS2	WT	NCS6	PAN3	SSN3	WT	CHL1	CNB1	MMS1	WT
WT/Blank	YKR028W	YNR023W	PL183W-/	YKL114C	YJL101C	YBL019W	YNR052C	YML060W	YER177W	YMR106C	YJR066W	YOR005C	YDL047W	YIL132C	YGL070C	YHL006C	YCR044C	YDR078C	YGR252W	WT/Blank	YPL256C	WT/Blank	WT/Blank
WT/Blank	SAP190	SNF12	RTC6	APN1	GSH1	APN2	POP2	OGG1	BMH1	YKU80	TOR1	DNL4	SIT4	CSM2	RPB9	SHU1	PER1	SHU2	GCN5	WT/Blank	CLN2	WT/Blank	WT/Blank
WT/Blank	YOR144C	DR363W-	YOR191W	YBL088C	YOR258W	YGL033W	YLR376C	YGL086W	YAL015C	YGL087C	YLR265C	YNL201C	YLR306W	YKL213C	YGL251C	YOL090W	YPL046C	YER095W	YBL046W	YHL025W	YGL090W	YHR191C	WT/Blank
WT/Blank	ELG1	SEM1	ULS1	TEL1	HNT3	HOP2	PSY3	MAD1	NTG1	MMS2	NEJ1	PSY2	UBC12	DOA1	HFM1	MSH2	ELC1	RAD51	PSY4	SNF6	LIF1	CTF8	WT/Blank
WT	YPL022W	YBR245C	YGR258C	WT	YEL037C	YER045C	YNL082W	WT	YCR092C	YHR082C	YDR097C	WT	YDR419W	YMR156C	YOR346W	WT	YPL167C	YGR109C	YGL058W	WT	YCR066W	YOR156C	WT
WT	RAD1	ISW1	RAD2	WT	RAD23	ACA1	PMS1	WT	MSH3	KSP1	MSH6	WT	RAD30	TPP1	REV1	WT	REV3	CLB6	RAD6	WT	RAD18	NFI1	WT
WT/Blank	YGL094C	YLR032W	YNL218W	YLR035C	YKR056W	YML102W	YDR314C	YPR018W	YDR334W	YPR101W	YFR014C	YJL047C	/FR031C-A	YGR188C	YIR019C	YJR043C	YOL115W	YDL101C	YPR052C	YDL116W	YJL030W	YNL021W	WT/Blank
WT/Blank	PAN2	RAD5	MGS1	MLH2	TRM2	CAC2	RAD34	RLF2	SWR1	SNT309	CMK1	RTT101	RPL2A	BUB1	MUC1	POL32	PAP2	DUN1	NHP6A	NUP84	MAD2	HDA1	WT/Blank
WT/Blank	YIL139C	YLR233C	YMR224C	YLR318W	YNL250W	YDR225W	YOR033C	YGL229C	YGL163C	YGR003W	YDR076W	YPL001W	YDR004W	YFR040W	YJL092W	YFR034C	YER041W	YBL003C	YDR386W	YBL067C	YBR098W	YNL230C	WT/Blank
WT/Blank	REV7	EST1	MRE11	EST2	RAD50	HTA1	EXO1	SAP4	RAD54	CUL3	RAD55	HAT1	RAD57	SAP155	SRS2	PHO4	YEN1	HTA2	MUS81	UBP13	MMS4	ELA1	WT/Blank
WT	YJR082C	YNL025C	WT	YBR073W	YKR092C	YIL112W	WT	YIL128W	YML021C	YNL107W	WT	YGR063C	YDL230W	YKL139W	WT	YBR289W	YDR030C	YGL115W	WT	YGL173C	YBR274W	YGL175C	WT
WT	EAF6	SSN8	WT	RDH54	SRP40	HOS4	WT	MET18	UNG1	YAF9	WT	SPT4	PTP1	CTK1	WT	SNF5	RAD28	SNF4	WT	KEM1	CHK1	SAE2	WT
WT/Blank	YDR217C	YDR263C	YER173W	YIL009C-A	YPL194W	YMR080C	YOR368W	YOL087C	YCL061C	YER098W	YNL273W	YMR127C	/MR048W	YJL065C	YDL200C	YDL216C	YPR135W	YMR036C	YKL113C	/MR199W	YHR031C	YNL030W	WT/Blank
WT/Blank	RAD9	DIN7	RAD24	EST3	DDC1	NAM7	RAD17	DUF1	MRC1	UBP9	TOF1	SAS2	CSM3	DLS1	MGT1	RRI1	CTF4	MIH1	RAD27	CLN1	RRM3	HHF2	WT/Blank
WT/Blank	YBR278W	YER116C	YCR065W	YER142C	YDL154W	YER162C	YBR010W	YDL074C	YIL153W	YLR240W	YIR002C	YLR399C	YNL068C	YPL024W	YBR272C	YJR090C	YMR137C	/DR079C-A	YNL138W	YAL021C	YPR023C	YOR014W	WT/Blank
WT/Blank	DPB3	SLX8	HCM1	MAG1	MSH5	RAD4	HHT1	BRE1	RRD1	VPS34	MPH1	BDF1	FKH2	RMI1	HSM3	GRR1	PSO2	TFB5	SRV2	CCR4	EAF3	RTS1	WT/Blank
WT	WT/Blank	YNL031C	WT	YBR034C	WT/Blank	YNL136W	WT	YNL116W	WT/Blank	YLR394W	WT	/MR173W	WT/Blank	YER176W	WT	YOR386W	WT/Blank	YIL066C	WT	YBL002W	WT/Blank	YNL307C	WT
WT	WT/Blank	HHT2	WT	HMT1	WT/Blank	EAF7	WT	DMA2	WT/Blank	CST9	WT	DDR48	WT/Blank	ECM32	WT	PHR1	WT/Blank	RNR3	WT	HTB2	WT/Blank	MCK1	WT

The new DDR-MA, was designed to also account for certain artifacts that could affect growth fitness such as the position of the strains on the plate and their growth characteristics (slow or fast growers). The new array, DDR-MAv1, now contains 289 DDR genes, 21 CIN genes, 63 WT strains (his3*Δ* and met15*Δ*) as control, and 4 empty spots as contamination control. Every strain, except WT, is represented once (i.e. one spot) on the array plate.

2.2 SGA screen

Ts cohesin-mutated alleles, marked with URA3[76], were used as queries to perform three high-throughput SGA screens (Figure 2-1). These mutants were screened against the DDR-MA using a Singer ROTOR automated method[79]. During the SGA pinning steps, all strains were grown at 25^{o}C until the final step, in which the *smc1-259* strain was screened at 25^{o}C while *scc1-73* and *scc2-4* were screened at 30^{o}C, based on their growth defects, as described[76].

Using the ROTOR robotic arm, each haploid MATα query strain (bearing a cohesin mutation) was pinned to mate with every MATa haploid array strain to generate heterozygous diploid cells. The mating plate was put in the 25^{o}C incubator for 1 day. A single mating plate was split into three biological replicates for the next step, in which diploids were selected for the presence of both the URA3 (marking the cohesin query gene) and the KanMX (marking the array deletion) markers, by growing them on SC-URA+G418 media. Plates were put in the 25^{o}C incubator for 1 day. This step was repeated twice to increase confidence (with second diploid selection plate being put in the 25^{o}C incubator for 1.5 days). By pinning to sporulation media and inducing nutrient starvation, the cells on each of the three plates were triggered to sporulate and generate haploid spores. Sporulation plates were put in the 25^{o}C incubator for 7 days. Following sporulation, cells on each plate were pinned onto 2 plates: single-selection (synthetic complete medium lacking histidine, lysine and arginine but containing 50μg/ml thialysine and 50μg/ml canavanine, and 200μg/ml G418) and double-selection (synthetic complete medium lacking uracil, histidine, lysine and arginine but containing 50μg/ml thialysine and 50μg/ml canavanine, and 200μg/ml G418) haploid media plates. In this step, two important selections are performed: 1.Selecting against diploids by providing the recessive resistance to canavanine and thialysine through CAN1 and LYP1 KO genes. 2. Via HIS3 haploid selection marker, selecting for MATa

haploids to prevent selfing/mating between different mating type germinated spores that could result in new diploids. Single haploid selection media (selecting for ura+ cells) enables the growth of both the single mutants carrying a cohesin ts-allele::URA3, and the double mutants carrying a cohesin ts-allele::URA3 and the DDRΔ:: KanMX allele. Double haploid selection media (selecting for ura+ and G418 resistant cells) enables only cohesin ts-allele::URA3 DDRΔ:: KanMX double mutants to grow. Plates were put in the 25^{o}C incubator for 3 days. This step of haploid selection was repeated twice to increase confidence, where each plate was pinned onto 2 plates, containing the same-media (either single or double haploid selection). Plates were put in the 25^{o}C incubator for 2 days. Final step involved each biological replicate non-drug (ND) plate being replicated onto 3 plates, representing technical replicates to increase statistical power. Plates were put at 25^{o}C or 30^{o}C, depending on the semi-permissive temperature for the particular query strain, for 1-2 days. Another copy of the haploid selection ND plate was pinned onto a similar haploid selection media (either single or double selection), containing 1 of 4 DNA-damaging agents (DDAs) in 1 of 2 different sub-lethal concentrations (high or low), to test sensitivity. Plates were put in the 25^{o}C incubator for 1 day. Final step for the drug plates includes every DDA plate being replicated into 3 identical selection plates (technical replicates) to increase statistical power and incubated at semi-permissive temperature, either 25^{0}C or 30^{0}C, for 1-2 days.

All SGA plates were scanned after 48 hours from the incubation time point of the final steps, and analyzed using the bioinformatic tools Balony and R software.

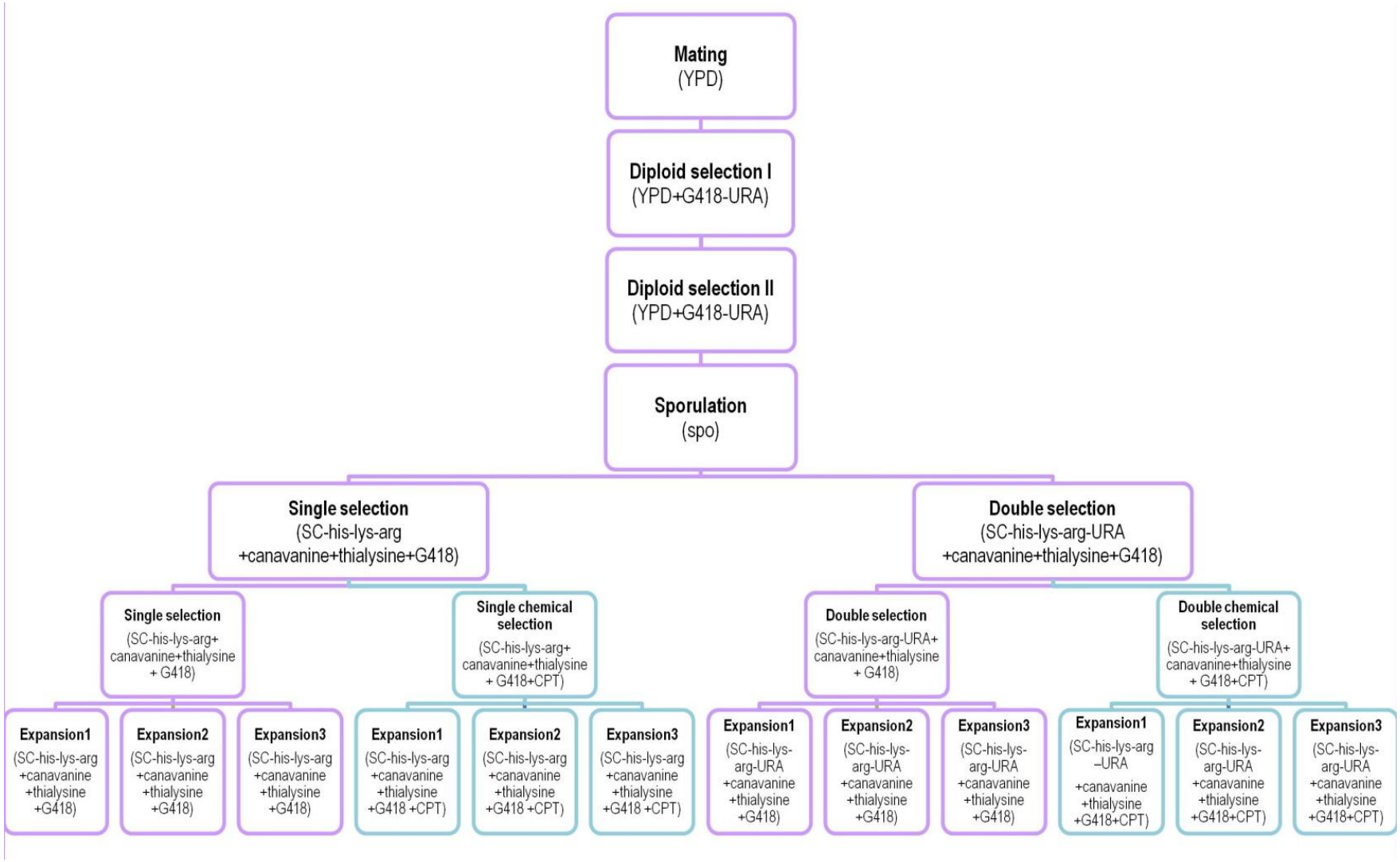

Figure 2-1. SGA screen structure scheme.

2.2.1 SGA bioinformatic analysis

Using well established bioinformatics methodologies (Balony and R softwares), I quantified the effect of the genetic interaction on the growth of each double mutant yeast strain compared to the relevant single mutant strains. The analysis involved 3 steps: Balony, Excel (normalization), and the R software.

Balony[86], a freely available software, follows a multi-step process, starting with the preparation of plate scans. The strain spots on each plate are identified and the pixel area of each is measured to provide a raw score. Scores are copied to a designated Excel template, ordered by the type of mutants on the plate (single mutants or double mutants), the number of biological replicate (out of 3), and the number of technical replicate (out of 3). Normalizing the raw score of each mutated strain relative to either WT (on haploid single selection plate) or cohesin query (on haploid double selection plate) strains, is then performed manually in Excel.

Using the raw scores acquired from Balony, 36 of the WT or query spot scores are averaged and compared to the raw score of each single or double mutant on the plate, respectively (by dividing the score of the mutant strain in the parental spots average). Though the Balony software can also be used for normalization, it is not used because it will normalize the score of each spot relative to all the spots on the specific plate. This will not suit an array such as the DDR-MA, where many strains are slow growers, because it will lead to a distorted normalization.

Normalized values are further processed in Excel to generate an **(e-c)/c** score, by averaging the normalized scores of all 9 replicates (3 biological x 3 technical) of each strain, in the **c**ontrol (single mutants) and in the **e**xperimental (double mutants) plates, per condition (-/+ DDA). The e-c/c score is used to determine SGA initial hits. In a previous SGA screen, which

used the same cohesin-mutated queries[76], initial hits were determined based on an e-c calculation (rather than e-c/c), using a whole-genome yeast array. A whole-genome array will mainly consist of strains that grow similar to WT, therefore, there is no need to take into account the fitness of the array strains. However, the smaller DDR-MA, consists of ~56% sensitive and slow growing strains (based on unpublished data), therefore, (e-c)/c calculation is more appropriate. This type of calculation enables the capture of more genetic interactions that otherwise would not have passed the cutoff. In addition, the (e-c)/c formula also enables comparison of double mutants between conditions without having to take into account the change in fitness of the query strain (see Figure 4-1). However, the limitation of this calculation is that it can also increase the false positive rate.

Using R, we compared the scores of all 9 replicates of the double mutants to all 9 replicates of the single mutants to check for variability and reproducibility. Via R, we generated the significance of the SGA results (i.e. P value). P value was determined by comparing the variability between replicates (technical and biological) and between the experiment and the control sets (detailed in Stoepel *et al*.- manuscript in preparation). R requires 3 files, including a data file with normalized pixel counts obtained from Balony, a plate information file containing information about whether each plate is a control or an experimental plate, and information about biological and technical replicates, and a script file.

2.3 DDAs

For this project, four DDAs were used, as summarized in Table 2-2.

Table 2-2. DNA damaging agents used in the project.

Agent name	Action	Standard drug stock	Low SGA concentration	High SGA concentration
Camptothecin (CPT)	topoisomerase I inhibitor	5mg/mL DMSO	1 µg/mL	4 µg/mL
Bleomycin	SSB and DSB via free radicals	10mg/mL H_2O	2.5 µg/mL	10 µg/mL
Methyl methanesulfonate (MMS)	alkylating agent	100%	0.00001%	0.00005%
Benomyl	Destabilizing microtubules (mitotic inhibition)	25mg/mL DMSO	5 µg/mL (0.02%DMSO)	20µg/mL (0.08%DMSO)

High concentration was defined as the concentration that results in ~80% fitness of the wild-type strain. Low concentration was defined as the concentration that results in ~80% averaged fitness of the top 30 sensitive strains on the array for that condition, while having no effect on the wild-type strain. The three query strains are not hypersensitive under these concentrations.

2.4 Tecan liquid growth curves

Strains were grown to saturation at 25^{o}C in 5ml YPD. The next day, 100µl of the saturated over-night culture was diluted into fresh 5ml YPD and was incubated at 25^{o}C for ~3 hours. OD600 measurements were taken and each culture was diluted to an OD of 0.1 in a 96-well plate containing YPD or YPD+DDA to reach a final volume of 200µl. The plate was inserted into Tecan M200 plate reader, where OD600 measurements are taken at 30 minute intervals for 24 or 48 hours at 30^{o}C. To analyze the growth curves, the area under the curve (AUC) was calculated for each curve and compared to WT strain for that specific condition.

Each strain was tested in triplicate. Each replicate generated an independent growth curve that was averaged to generate an average AUC value per strain and condition.

2.5 ScanLag solid growth curves

Using ScanLag software[87], the program serves as a communication method between a designated computer and a scanner to periodically acquire images of the spot of cells growing on the plate. Scanning intervals were set to two hours over the period of 48 hours (overall, 25 scans including 0 time point). Preparation of strains is the same as for liquid growth curves using Tecan. Each tested strain was inoculated into 5ml YPD media and grown overnight at 25^0C. The next day, 100µl of the saturated culture was inoculated into a fresh 5ml YPD media and incubated for 3 hours at 25^0C. Each culture was measured for OD600 and was diluted into YPD-containing 96-well plate to reach an OD600 of 0.1. Diluted strains were then spotted in a volume of 4µl onto solid media plates (-/+ DDA) (**Table 2-3**) in triplicates, and were placed onto the scanner surface with lids on facing up, inside the 30^0C incubator for 48 hours.

Table 2-3. DDAs and concentrations used for ScanLag validation process.

DNA-damaging agent	Concentration used
methyl methanesulfonate (MMS)	0.00005%
Camptothecin (CPT)	4 µg/mL
bleomycin	10 µg/mL, 3 µg/mL
benomyl	20µg/mL

2.5.1 ImageJ analysis

The software ImageJ[88], relying on the Time Series Analyzer plugin, was used to analyze the 2D time-lapse scans and to measure the increase in brightness over time. The intensity of each yeast spot of interest on the plate was monitored using a particle tracking tool, for which the dimensions stay consistent for the analysis of every strain spot and every plate in the course of a certain experiment. Periodic scores for each spot were obtained and analyzed in Excel to create growth curves over time and the AUC was calculated. Each strain was tested in triplicate. Each replicate generated an independent growth curve that was averaged to generate an average AUC value per strain and condition. For every plate, the scores of a blank spot (i.e. a spot on the plate that does not contain yeast) over time were obtained and subtracted from the scores of every yeast spot at that time point.

2.6 AUC calculation

AUC calculation was performed on normalized values, by reducing each periodic score from the first score of a specific strain replicate, averaging of every two sequential scores divided by 2 (averaging serves as multiplying by 2, which is the time difference between every score), summing all values per replicate and averaging final values per triplicate. The final averaged value of the WT strain, for every condition, was set to 1. The final averaged value of every other strain replicate was compared to that value. High values of AUC, compared to WT, are associated with increased growth and hence high strain fitness of the mutant strain, and vice versa.

Chapter 3: RESULTS

3.1 Systematic identification of cohesin genetic interactions

Synthetic Genetic Array (SGA) technology was used to screen temperature sensitive alleles of two cohesin core-subunits (*smc1-259, scc1-73*) and a cohesin loader subunit (*scc2-4*)[76], against a curated array of 310 yeast strains carrying gene deletions affecting DNA damage response (DDR) genes, termed DDR-MA (MATERIALS AND M). The screens were done in the presence and absence of 4 distinct genotoxic agents, representing commonly used chemotherapeutic classes: Benomyl (microtubule inhibitor), Bleomycin (radiomimetic), Camptothecin (CPT) (TOP1 inhibitor), and Methyl Methanesulfonate (MMS) (alkylating agent) (MATERIALS AND M). Therefore, each SGA screen consisted of five conditions; four DDAs and one no-DDA control (termed no-DDA condition, ND). Thus, 4,650 potential genetic interactions (3 query genes X 310 array genes X 5 conditions) were generated and analyzed. SGA screens were performed as previously described (MATERIALS AND M).

Using Balony and R software (MATERIALS AND M), SGA data was sorted using two criteria to identify potential interactions. In concordance with the goal of identifying novel SC genetic interactions that could be translated to human cancers, the focus was on the magnitude of the genetic interaction. Potential interactions were defined as double mutants with an e-c/c score (experimental set value – control set value/ control set value) of $\leq$-0.2 for negative genetic interactions (NI) with the cohesin mutation, or $\geq$0.2 for positive genetic interactions (PI) (Table 3-1). The experimental set represents the overall growth of the double mutant spots (normalized to the cohesin query), while the control set represents the overall growth of the array single mutant spots (normalized to WT), per condition. The formula uses the fitness of the two parental

strains (i.e. each single mutant) and calculates the growth of the double mutant colony relative to the predicted growth based on the growth of the combined two single mutations (i.e. the multiplicative model). In the analysis of a typical SGA screen, most double mutants would not exhibit an interaction. This is expressed in an e-c/c score of 0. However, we focused on the tails of the distribution that passed the cutoffs (Figure 3-1). These initial hits represent double mutants that due to the genetic interaction and the condition used, exhibit a reduced growth rate that is lower than expected (i.e. SL or SC, classified as negative genetic interactions) or an improved growth rate that is greater than expected (i.e. PS, classified as positive genetic interaction).

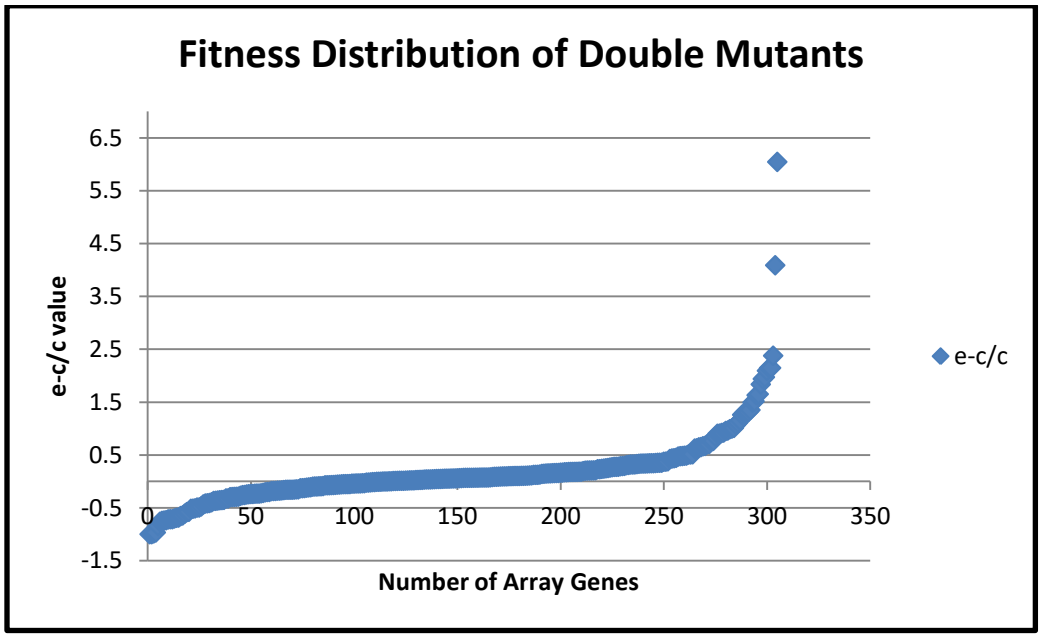

Figure 3-1. Example for fitness-defect distribution.

e (experiment) represents the fitness of the double mutant, c (control) represents the fitness of the single array mutant. e-c/c=0 means no interaction, e-c/c>o means positive interaction, e-c/c<0 means negative interaction. Each dot on the graph represents one double mutant yeast strain. This graph was based on the results of the *scc1-73* screen using camptothecin (CPT) (analyzed after 48 hours). There are, overall, 59 negative interaction hits and 96 positive interaction hits.

Due to the high-quality and small size of the array, we used a less stringent cutoff value of ≤-0.2, relative to the cutoff chosen for a previous SL screen using these queries against a whole-genome array which was ≤-0.3[76]. This cutoff was chosen based on experience with previous SGA screens done in the Hieter lab using the DDR-MA (H. Li, personal communication).

	SMC1										SCC1										SCC2									
	ND		MMS		CPT		BEN		BLE		ND		MMS		CPT		BEN		BLE		ND		MMS		CPT		BEN		BLE	
Gene	ec/c	pval	ec/c	pval	ec/c	pval	ec/c	pval	ec/c	pval	ec/c	pval	ec/c	pval	ec/c	pval	ec/c	pval	ec/c	pval	ec/c	pval	ec/c	pval	ec/c	pval	ec/c	pval	ec/c	pval
ACA1	0.02	0.66	-0.01	0.91	-0.18	0.01	-0.07	0.26	-0.09	0.30	N/A	NA	N/A	NA	N/A	NA	N/A	NA	N/A	NA	0.12	0.12	0.10	0.19	0.12	0.18	0.07	0.33	0.04	0.71
AMN1	0.10	0.02	0.01	0.64	-0.10	0.04	0.05	0.51	0.13	0.03	0.01	0.91	-0.19	0.09	-0.04	0.29	0.09	0.41	-0.22	0.18	-0.11	0.09	-0.18	0.06	-0.06	0.73	-0.05	0.45	0.31	0.11
ANB1	-0.01	0.76	0.07	0.20	-0.03	0.61	0.00	1.00	0.09	0.27	0.01	0.75	-0.03	0.55	0.07	0.65	0.04	0.63	0.17	0.05	-0.09	0.05	-0.15	0.15	-0.08	0.54	-0.01	0.65	0.25	0.02
APN1	0.01	0.63	-0.35	0.00	-0.25	0.00	0.11	0.40	-0.06	0.67	0.11	0.03	-0.27	0.03	0.10	0.04	0.08	0.10	0.07	0.47	-0.06	0.14	-0.20	0.04	-0.01	0.85	-0.03	0.40	-0.05	0.38
APN2	-0.02	0.61	-0.07	0.13	-0.23	0.01	-0.13	0.12	-0.20	0.04	0.12	0.12	-0.08	0.39	0.05	0.42	0.03	0.51	0.07	0.47	-0.02	0.36	-0.16	0.00	-0.04	0.12	-0.07	0.01	-0.11	0.07
ARP6	0.09	0.67	1.19	0.07	0.29	0.56	-0.02	0.95	0.09	0.90	-0.25	0.02	1.67	0.46	0.35	0.68	-0.42	0.09	-0.74	0.07	-0.32	0.01	1.50	0.00	1.66	0.00	0.53	0.08	1.14	0.01
ASF1	0.10	0.17	0.63	0.51	-0.66	0.05	-0.05	0.43	-0.65	0.00	-0.26	0.40	0.14	0.86	0.34	0.79	0.15	0.62	-0.74	0.04	-0.33	0.00	-0.12	0.66	-0.33	0.67	-0.25	0.00	-0.59	0.03
BDF1	0.16	0.53	0.73	0.16	0.40	0.45	-0.33	0.48	0.04	0.88	0.52	0.55	1.80	0.27	1.35	0.32	1.14	0.36	1.19	0.37	0.34	0.00	1.16	0.00	1.57	0.00	0.10	0.33	0.73	0.00
BDF2	-0.01	0.68	-0.03	0.24	-0.13	0.02	-0.04	0.42	0.06	0.60	-0.01	0.81	0.71	0.45	0.18	0.60	0.00	0.96	-0.03	0.89	-0.07	0.15	0.11	0.42	0.16	0.26	-0.08	0.19	0.19	0.05
BIK1	-0.03	0.57	0.00	0.99	0.08	0.80	-0.18	0.09	-0.07	0.33	-0.17	0.00	-0.08	0.08	-0.04	0.67	-0.33	0.01	-0.32	0.01	-0.15	0.02	-0.01	0.94	0.12	0.55	-0.38	0.00	0.09	0.69
BIM1	-0.33	0.01	0.22	0.32	-0.22	0.23	-0.53	0.13	-0.56	0.00	0.15	0.76	0.66	0.59	0.27	0.66	-0.63	0.02	0.26	0.81	-0.62	0.05	-0.55	0.03	-0.53	0.00	-0.92	0.00	-0.75	0.02
BMH1	-0.08	0.33	0.35	0.03	-0.21	0.01	-0.15	0.29	-0.06	0.85	0.20	0.06	1.17	0.00	0.18	0.06	0.02	0.84	1.15	0.01	0.07	0.58	0.48	0.21	0.30	0.55	-0.32	0.06	-0.35	0.40
BRE1	0.37	0.00	-0.20	0.20	-0.18	0.41	0.60	0.01	0.00	0.99	0.08	0.13	0.00	0.98	-0.77	0.00	0.42	0.00	-0.33	0.06	0.40	0.14	2.02	0.06	2.39	0.01	-0.18	0.01	0.80	0.19
BUB1	-0.22	0.01	-0.50	0.01	-0.02	0.81	2.89	0.01	-0.80	0.00	-0.17	0.68	0.85	0.55	0.11	0.87	-0.41	0.24	0.33	0.80	-0.76	0.00	-0.24	0.59	-0.11	0.87	-0.01	0.98	-0.88	0.00
BUB3	-0.65	0.00	-0.64	0.00	-0.36	0.00	0.49	0.62	-0.76	0.00	0.71	0.30	1.21	0.29	0.70	0.43	1.84	0.33	1.20	0.39	-0.25	0.41	-0.28	0.17	-0.57	0.01	4.33	0.32	-0.24	0.65
CAC2	0.09	0.03	0.19	0.63	-0.09	0.70	0.07	0.26	0.04	0.79	-0.30	0.16	1.26	0.51	0.29	0.69	-0.28	0.01	0.06	0.92	-0.02	0.82	-0.06	0.67	0.08	0.64	-0.05	0.23	-0.14	0.61
CCR4	0.06	0.21	0.17	0.03	0.30	0.01	0.25	0.09	0.04	0.67	0.16	0.13	0.57	0.05	0.33	0.13	0.08	0.61	0.19	0.08	-0.42	0.13	-0.15	0.56	-0.15	0.72	-0.17	0.59	-0.39	0.25
CDC40	0.85	0.07	0.18	0.34	-0.36	0.02	0.16	0.72	-0.62	0.20	0.14	0.80	0.33	0.76	0.24	0.77	0.10	0.92	-1.00	0.37	0.07	0.93	2.01	0.36	1.77	0.33	0.64	0.17	0.18	0.89
CDC73	N/A	NA	N/A	NA	N/A	NA	N/A	NA	N/A	NA	N/A	NA	N/A	NA	N/A	NA	N/A	NA	N/A	NA	17.98	0.27	5.43	0.24	9.10	0.27	20.33	0.31	14.85	0.22
CDH1	0.18	0.51	0.21	0.67	0.45	0.49	-0.69	0.01	0.39	0.54	-0.06	0.91	0.43	0.75	0.34	0.63	-0.65	0.02	0.28	0.83	-0.57	0.00	-0.50	0.04	-0.52	0.04	-0.76	0.00	-0.78	0.00
CHD1	0.03	0.43	-0.08	0.09	-0.29	0.00	0.16	0.06	0.19	0.16	-0.21	0.02	-0.17	0.10	-0.40	0.00	0.00	0.99	-0.38	0.00	-0.32	0.00	-0.41	0.00	-0.44	0.00	-0.25	0.00	-0.15	0.09
CHK1	0.07	0.05	0.02	0.71	-0.11	0.28	0.04	0.53	-0.05	0.59	0.03	0.24	-0.02	0.69	-0.05	0.17	0.06	0.12	0.08	0.46	-0.15	0.03	-0.11	0.03	-0.22	0.01	-0.05	0.02	0.05	0.47
CHL1	0.37	0.06	1.19	0.03	1.07	0.02	0.07	0.91	0.81	0.08	-0.95	0.00	-1.00	0.00	-0.98	0.00	-1.00	0.00	-1.00	0.00	-0.23	0.59	0.00	1.00	0.53	0.50	-0.09	0.87	-0.26	0.73
CIN2	-0.09	0.04	-0.10	0.04	-0.12	0.00	2.23	0.03	-0.07	0.37	-0.24	0.00	-0.28	0.02	0.03	0.55	-0.45	0.55	-0.70	0.01	-0.32	0.00	-0.37	0.00	-0.29	0.00	-0.14	0.91	-0.28	0.01
CIN8	-0.52	0.00	-0.39	0.15	-0.27	0.02	-0.44	0.20	-0.54	0.05	-0.54	0.00	-0.24	0.01	-0.24	0.01	-0.43	0.00	-0.87	0.00	-0.41	0.05	-0.31	0.39	-0.10	0.74	-0.45	0.04	-0.61	0.05
CLB1	0.12	0.11	0.08	0.30	-0.14	0.36	0.08	0.12	-0.04	0.53	0.18	0.01	0.18	0.04	0.07	0.40	0.17	0.02	0.14	0.12	0.09	0.04	0.02	0.41	0.08	0.14	0.04	0.09	-0.19	0.14
CLB2	-0.18	0.00	-0.42	0.00	-0.79	0.00	-0.64	0.00	-0.97	0.00	-0.61	0.00	-0.65	0.00	-0.72	0.00	-0.60	0.00	-0.97	0.00	-0.31	0.02	-0.08	0.59	-0.24	0.26	-0.43	0.01	-0.58	0.03
CLB3	0.00	0.98	0.05	0.03	-0.16	0.08	0.09	0.30	0.09	0.18	-0.05	0.19	-0.24	0.00	-0.27	0.00	-0.20	0.01	-0.25	0.02	-0.12	0.36	-0.08	0.71	0.08	0.82	-0.20	0.06	0.22	0.09
CLB4	-0.03	0.55	-0.06	0.20	-0.23	0.01	-0.15	0.02	-0.13	0.22	0.12	0.11	-0.04	0.43	-0.01	0.87	0.06	0.34	-0.11	0.19	-0.05	0.20	-0.11	0.10	-0.19	0.00	-0.16	0.01	-0.39	0.03
CLB6	0.13	0.04	0.05	0.40	-0.16	0.01	0.05	0.31	0.02	0.70	0.30	0.00	0.40	0.00	0.31	0.01	0.17	0.04	0.39	0.01	0.03	0.65	0.10	0.20	0.21	0.11	0.14	0.01	-0.09	0.25

	SMC1										SCC1										SCC2									
	ND		MMS		CPT		BEN		BLE		ND		MMS		CPT		BEN		BLE		ND		MMS		CPT		BEN		BLE	
Gene	ec/c	pval	ec/c	pval	ec/c	pval	ec/c	pval	ec/c	pval	ec/c	pval	ec/c	pval	ec/c	pval	ec/c	pval	ec/c	pval	ec/c	pval	ec/c	pval	ec/c	pval	ec/c	pval	ec/c	pval
CLN1	0.02	0.64	0.11	0.39	0.20	0.29	0.11	0.07	0.03	0.60	0.10	0.06	0.21	0.02	0.09	0.07	0.06	0.34	0.52	0.03	-0.13	0.12	-0.05	0.41	-0.12	0.08	-0.07	0.09	0.09	0.12
CLN2	0.22	0.00	0.38	0.00	0.09	0.40	0.55	0.00	0.20	0.02	0.48	0.00	0.52	0.00	0.47	0.00	0.59	0.00	0.47	0.02	0.16	0.02	0.20	0.01	0.24	0.01	0.24	0.00	0.29	0.09
CLN3	0.11	0.26	0.18	0.44	-0.02	0.92	0.02	0.87	-0.14	0.15	-0.15	0.14	-0.27	0.04	-0.15	0.02	-0.09	0.22	-0.84	0.00	-0.05	0.35	-0.04	0.33	-0.06	0.02	-0.13	0.00	-0.28	0.09
CMK1	0.06	0.20	0.03	0.78	-0.07	0.72	-0.03	0.54	0.09	0.63	-0.01	0.89	0.11	0.45	0.01	0.81	0.03	0.35	-0.20	0.30	-0.05	0.04	-0.07	0.13	-0.17	0.00	-0.10	0.02	-0.29	0.01
CNB1	-0.03	0.19	-0.18	0.01	0.05	0.77	0.12	0.09	-0.08	0.32	0.17	0.05	-0.17	0.00	0.04	0.18	0.11	0.02	-0.13	0.25	-0.10	0.09	-0.16	0.02	-0.02	0.65	-0.04	0.17	-0.03	0.71
CSM2	0.00	0.94	0.07	0.61	-0.10	0.35	-0.04	0.36	-0.09	0.58	0.10	0.08	-0.39	0.01	-0.23	0.00	0.05	0.38	-0.20	0.25	0.02	0.47	0.00	1.00	-0.04	0.83	-0.01	0.78	-0.09	0.47
CSM3	0.29	0.27	0.12	0.72	0.37	0.11	0.41	0.19	-0.02	0.96	-0.62	0.02	-0.70	0.02	-0.72	0.01	-0.87	0.00	-1.00	0.00	-0.74	0.00	-0.06	0.83	0.30	0.09	-0.11	0.55	-0.97	0.00
CST9	0.13	0.02	-0.17	0.00	-0.09	0.22	0.20	0.04	-0.05	0.39	-0.05	0.29	-0.25	0.01	-0.13	0.13	-0.12	0.03	-0.35	0.15	-0.07	0.40	-0.14	0.06	-0.20	0.06	-0.04	0.45	-0.64	0.00
CTF4	-0.32	0.02	3.16	0.12	6.60	0.00	-0.30	0.52	-0.55	0.08	-0.77	0.00	0.45	0.73	0.37	0.71	-0.89	0.00	-1.00	0.00	0.14	0.76	5.04	0.12	6.37	0.25	0.08	0.50	0.44	0.71
CTF8	-0.11	0.21	0.70	0.16	0.98	0.27	0.18	0.32	-0.45	0.10	0.01	0.98	1.74	0.44	1.00	0.54	-0.12	0.73	0.35	0.80	-0.16	0.40	0.06	0.76	-0.08	0.77	-0.08	0.35	-0.33	0.51
CTI6	-0.08	0.06	-0.09	0.07	-0.24	0.00	-0.31	0.00	-0.32	0.00	-0.07	0.21	0.13	0.41	-0.18	0.02	-0.05	0.31	-0.27	0.02	-0.01	0.93	0.15	0.21	-0.08	0.55	-0.04	0.40	0.06	0.64
CTK1	0.21	0.01	-0.02	0.81	-0.16	0.06	-0.35	0.05	-0.44	0.06	-0.20	0.46	0.94	0.43	0.48	0.51	-0.34	0.15	-0.80	0.12	-0.37	0.05	-0.20	0.20	-0.35	0.03	-0.54	0.00	-0.58	0.19
CTK2	0.45	0.00	0.55	0.02	0.12	0.04	-0.06	0.66	2.84	0.13	0.29	0.26	2.94	0.32	1.11	0.34	0.20	0.21	34.39	0.32	0.01	0.90	0.34	0.08	0.43	0.01	0.05	0.78	0.65	0.37
CUL3	-0.05	0.18	-0.19	0.03	-0.16	0.00	0.08	0.02	-0.07	0.24	0.10	0.14	0.18	0.19	0.17	0.01	0.13	0.06	0.03	0.84	0.02	0.73	-0.01	0.94	-0.07	0.19	-0.03	0.09	-0.17	0.07
DBP7	-0.02	0.85	-0.02	0.93	-0.09	0.69	-0.32	0.01	-0.36	0.19	-0.12	0.31	0.79	0.32	0.62	0.40	-0.25	0.01	0.02	0.98	-0.32	0.01	-0.28	0.01	-0.23	0.00	-0.41	0.00	-0.54	0.04
DCC1	0.00	0.99	0.36	0.16	0.58	0.02	0.14	0.12	0.31	0.16	-0.01	0.91	0.80	0.01	0.42	0.01	-0.07	0.23	0.34	0.01	-0.40	0.22	-0.02	0.96	0.14	0.72	-0.22	0.60	0.43	0.58
DCS1	-0.07	0.15	-0.20	0.01	-0.28	0.00	-0.14	0.05	-0.36	0.01	0.13	0.11	0.06	0.33	0.15	0.10	0.10	0.11	0.21	0.05	0.01	0.76	0.00	0.99	0.11	0.04	0.03	0.19	-0.23	0.07
DDC1	0.03	0.22	-0.52	0.00	-0.65	0.01	-0.09	0.26	-0.26	0.09	0.09	0.11	0.10	0.39	-0.72	0.00	0.10	0.11	-0.37	0.21	0.04	0.61	0.00	0.99	2.69	0.40	0.02	0.52	0.04	0.80
DDR48	0.15	0.01	-0.12	0.08	0.04	0.80	0.19	0.05	0.01	0.87	0.02	0.64	-0.11	0.22	0.05	0.44	0.01	0.84	0.11	0.68	-0.10	0.10	-0.15	0.06	-0.25	0.07	-0.10	0.02	-0.29	0.01
DIA2	0.21	0.04	3.44	0.28	1.00	0.41	-0.03	0.90	-0.10	0.86	-0.24	0.00	-0.58	0.14	-0.58	0.03	-0.17	0.16	-0.90	0.12	-0.19	0.25	0.46	0.60	0.02	0.98	-0.34	0.02	-0.16	0.62
DIN7	0.00	0.97	-0.10	0.03	-0.13	0.05	-0.06	0.11	0.24	0.05	0.09	0.12	-0.01	0.85	0.18	0.12	0.07	0.45	0.01	0.87	-0.03	0.77	-0.10	0.00	-0.12	0.02	-0.06	0.13	-0.13	0.05
DLS1	0.08	0.07	0.22	0.01	0.07	0.39	0.14	0.01	0.06	0.53	0.06	0.02	0.32	0.00	0.21	0.00	0.26	0.01	0.34	0.00	0.02	0.71	-0.01	0.67	0.08	0.25	0.02	0.71	0.10	0.33
DMA2	0.03	0.21	-0.10	0.02	-0.11	0.13	0.13	0.24	0.10	0.10	-0.02	0.70	-0.10	0.04	-0.07	0.39	-0.01	0.85	-0.18	0.15	-0.09	0.18	-0.11	0.11	-0.22	0.02	-0.05	0.08	-0.02	0.84
DMC1	0.12	0.02	0.09	0.22	-0.11	0.05	0.21	0.03	-0.07	0.13	0.07	0.05	-0.04	0.34	0.02	0.73	0.15	0.09	-0.25	0.08	0.05	0.46	0.02	0.89	0.13	0.32	0.08	0.03	0.09	0.60
DNL4	0.03	0.61	-0.09	0.14	-0.09	0.43	0.00	0.94	-0.17	0.03	0.05	0.44	0.08	0.03	0.05	0.26	0.09	0.13	-0.05	0.57	0.02	0.32	0.06	0.49	0.13	0.49	0.01	0.58	-0.02	0.89
DOA1	0.11	0.02	-0.67	0.02	-0.60	0.01	-0.66	0.00	-0.58	0.01	-0.22	0.09	-0.46	0.20	-0.70	0.00	-0.50	0.00	-0.87	0.00	0.23	0.00	-0.13	0.53	-0.36	0.00	-0.20	0.04	-0.56	0.08
DOC1	0.08	0.09	0.04	0.59	0.01	0.98	-0.27	0.50	-0.44	0.01	-0.38	0.03	-0.33	0.16	-0.52	0.09	-0.40	0.01	-0.98	0.00	-0.61	0.00	-0.38	0.11	0.70	0.64	-0.61	0.00	-0.33	0.35
DPB3	0.12	0.00	0.00	0.92	-0.02	0.63	0.02	0.73	0.05	0.41	-0.08	0.07	-0.07	0.21	0.00	0.94	-0.05	0.34	-0.22	0.03	-0.05	0.55	-0.24	0.00	-0.21	0.00	-0.13	0.01	-0.09	0.19
DPB4	0.15	0.02	0.31	0.00	0.01	0.91	0.26	0.00	0.01	0.96	0.09	0.28	0.41	0.02	0.20	0.03	0.20	0.01	0.20	0.48	-0.01	0.75	0.01	0.82	-0.02	0.45	-0.05	0.08	-0.32	0.04
DST1	-0.17	0.01	-0.18	0.05	-0.05	0.79	-0.04	0.78	-0.23	0.11	0.15	0.09	0.52	0.22	0.49	0.03	0.15	0.10	-0.25	0.06	-0.10	0.32	-0.02	0.76	0.00	0.99	-0.13	0.06	-0.15	0.28

	SMC1										SCC1										SCC2									
	ND		MMS		CPT		BEN		BLE		ND		MMS		CPT		BEN		BLE		ND		MMS		CPT		BEN		BLE	
Gene	ec/c	pval	ec/c	pval	ec/c	pval	ec/c	pval	ec/c	pval	ec/c	pval	ec/c	pval	ec/c	pval	ec/c	pval	ec/c	pval	ec/c	pval	ec/c	pval	ec/c	pval	ec/c	pval	ec/c	pval
DUF1	0.16	0.03	0.09	0.11	-0.05	0.70	0.26	0.04	0.06	0.40	0.10	0.04	0.06	0.21	-0.02	0.63	0.07	0.47	0.08	0.57	0.10	0.01	0.01	0.72	0.00	0.98	0.15	0.05	-0.16	0.06
DUN1	0.26	0.06	0.12	0.72	0.41	0.46	0.30	0.01	-0.06	0.75	0.20	0.30	0.31	0.49	0.21	0.56	0.30	0.00	-0.27	0.39	0.04	0.62	-0.23	0.00	-0.27	0.00	0.11	0.01	-0.37	0.32
EAF3	0.21	0.01	0.14	0.22	0.36	0.06	0.28	0.03	-0.05	0.58	0.00	0.99	0.25	0.03	0.12	0.09	0.14	0.14	-0.16	0.07	0.07	0.61	0.13	0.39	0.42	0.07	0.03	0.52	0.29	0.01
EAF6	0.20	0.01	0.19	0.01	0.02	0.51	0.42	0.01	0.23	0.01	-0.02	0.69	-0.21	0.03	0.04	0.30	0.12	0.06	-0.27	0.25	0.06	0.38	0.04	0.51	0.12	0.02	0.16	0.01	-0.08	0.47
EAF7	0.11	0.11	0.19	0.03	0.19	0.07	0.36	0.00	0.00	0.95	-0.09	0.10	-0.05	0.22	0.09	0.28	-0.01	0.91	-0.66	0.08	-0.08	0.44	0.04	0.38	0.24	0.01	0.09	0.09	-0.02	0.90
ECM32	0.00	0.98	0.05	0.72	0.28	0.24	0.01	0.79	0.09	0.26	-0.05	0.19	-0.12	0.02	-0.16	0.00	0.10	0.11	0.32	0.07	-0.10	0.20	-0.10	0.45	0.07	0.83	-0.13	0.04	-0.16	0.11
ELA1	0.03	0.20	0.02	0.52	-0.06	0.31	0.01	0.81	-0.10	0.18	0.04	0.09	0.01	0.86	-0.02	0.37	0.01	0.76	0.05	0.48	-0.06	0.13	-0.09	0.14	-0.15	0.10	-0.09	0.03	0.07	0.45
ELC1	0.11	0.01	0.09	0.04	-0.10	0.05	0.08	0.37	-0.25	0.01	0.03	0.57	0.27	0.03	0.10	0.15	0.03	0.78	-0.20	0.15	0.06	0.23	0.03	0.69	0.02	0.51	0.06	0.08	-0.12	0.36
ELG1	0.00	0.99	-0.07	0.68	-0.11	0.69	-0.13	0.19	-0.30	0.28	0.48	0.25	2.02	0.14	0.90	0.29	0.10	0.65	1.32	0.30	-0.33	0.00	-0.44	0.00	-0.42	0.00	-0.38	0.00	-0.59	0.00
ESC2	0.12	0.17	0.38	0.26	-0.31	0.01	-0.07	0.39	-0.45	0.00	0.18	0.17	0.83	0.00	0.38	0.00	0.10	0.38	-0.76	0.06	0.17	0.00	0.80	0.03	0.17	0.23	0.08	0.04	0.01	0.99
EST1	0.04	0.42	-0.09	0.10	0.00	0.98	0.02	0.86	0.05	0.48	0.17	0.25	0.28	0.43	0.48	0.33	0.04	0.39	0.23	0.56	0.01	0.77	-0.09	0.09	-0.01	0.77	0.03	0.06	-0.12	0.06
EST2	0.13	0.14	0.09	0.47	0.28	0.27	0.15	0.31	0.12	0.07	0.14	0.03	0.02	0.72	0.07	0.29	0.15	0.01	-0.08	0.51	0.01	0.77	-0.09	0.01	-0.10	0.03	-0.01	0.45	-0.33	0.01
EST3	0.09	0.02	-0.01	0.92	0.00	0.98	0.03	0.74	0.11	0.30	0.09	0.01	0.07	0.29	0.25	0.00	0.15	0.09	0.05	0.71	0.04	0.75	0.11	0.51	0.23	0.45	0.03	0.42	0.13	0.29
ETR1	-0.04	0.75	-0.18	0.32	-0.05	0.87	0.12	0.67	-0.24	0.26	0.01	0.94	-0.18	0.21	0.06	0.27	0.24	0.01	-0.68	0.00	0.01	0.88	-0.15	0.02	0.22	0.11	-0.10	0.00	-0.20	0.03
EXO1	0.01	0.65	-0.09	0.11	-0.44	0.00	0.00	0.98	-0.12	0.06	0.06	0.15	0.05	0.62	-0.24	0.00	0.06	0.33	0.02	0.81	0.04	0.14	0.06	0.15	-0.22	0.00	0.01	0.86	-0.02	0.91
FKH2	0.15	0.01	-0.24	0.01	-0.52	0.00	0.27	0.00	-0.40	0.01	-0.03	0.92	0.06	0.92	-0.30	0.49	-0.18	0.01	-0.23	0.65	0.01	0.89	0.16	0.59	0.17	0.64	0.07	0.01	-0.41	0.09
FUN30	0.01	0.77	-0.16	0.00	-0.27	0.00	0.01	0.91	-0.22	0.01	-0.12	0.04	-0.20	0.16	-0.30	0.03	-0.16	0.01	-0.58	0.00	0.07	0.25	-0.04	0.66	-0.11	0.02	0.00	0.88	-0.14	0.08
GCN5	0.33	0.02	1.18	0.01	0.91	0.01	-0.29	0.44	0.68	0.02	0.40	0.50	1.68	0.25	0.96	0.25	0.20	0.76	0.46	0.57	-0.02	0.91	0.31	0.56	0.87	0.09	0.37	0.03	-0.20	0.69
GIM4	-0.25	0.00	-0.12	0.28	-0.05	0.87	0.92	0.30	-0.53	0.04	-0.45	0.00	-0.23	0.05	-0.35	0.06	0.23	0.65	-0.75	0.00	-0.47	0.00	-0.34	0.00	-0.41	0.00	-0.69	0.02	-0.64	0.00
GRR1	0.04	0.94	-0.34	0.48	-0.34	0.43	0.33	0.71	-0.65	0.30	2.47	0.48	5.62	0.44	2.14	0.49	3.66	0.48	-1.00	0.37	-0.20	0.61	0.32	0.64	0.41	0.42	-0.06	0.91	N/A	0.37
GSH1	0.02	0.56	0.06	0.57	0.78	0.01	-0.06	0.78	-0.28	0.16	0.09	0.70	-0.39	0.36	0.21	0.58	-0.41	0.74	-1.00	0.14	0.18	0.36	0.93	0.49	1.32	0.22	0.14	0.64	1.06	0.10
GTR2	0.01	0.70	0.36	0.00	0.02	0.91	0.10	0.21	0.05	0.48	0.36	0.00	0.33	0.00	0.29	0.00	0.24	0.01	0.31	0.01	0.07	0.38	0.12	0.07	0.30	0.00	0.10	0.12	0.52	0.01
HAT1	0.05	0.36	0.07	0.55	0.16	0.39	-0.02	0.57	0.10	0.55	0.18	0.01	0.13	0.05	0.07	0.24	0.11	0.11	0.12	0.19	0.11	0.01	0.11	0.19	0.08	0.21	0.02	0.46	-0.07	0.35
HAT2	0.02	0.60	-0.05	0.13	-0.14	0.02	0.00	0.90	-0.03	0.71	-0.17	0.10	0.06	0.46	0.09	0.37	0.09	0.17	0.16	0.16	0.03	0.31	0.06	0.56	0.12	0.44	0.01	0.91	-0.07	0.45
HCM1	-0.06	0.33	0.06	0.28	0.04	0.46	0.05	0.22	0.00	0.95	-0.05	0.69	0.52	0.39	0.51	0.17	0.01	0.91	0.06	0.93	-0.12	0.17	0.02	0.82	0.15	0.03	0.01	0.90	-0.31	0.04
HCS1	-0.01	0.70	-0.07	0.20	-0.22	0.02	0.01	0.87	-0.20	0.01	0.14	0.06	0.10	0.10	0.04	0.66	0.05	0.40	0.09	0.48	0.05	0.16	-0.05	0.36	-0.09	0.02	-0.05	0.01	-0.25	0.05
HDA1	0.04	0.33	0.16	0.34	-0.18	0.24	0.15	0.04	-0.03	0.50	-0.06	0.44	0.28	0.52	0.17	0.16	-0.06	0.18	-0.26	0.25	-0.13	0.03	-0.32	0.00	-0.35	0.00	-0.22	0.00	-0.03	0.70
HFM1	0.06	0.57	-0.04	0.66	0.00	0.99	-0.01	0.93	-0.11	0.20	-0.03	0.60	-0.04	0.40	0.05	0.45	0.01	0.87	-0.19	0.23	-0.03	0.20	-0.05	0.47	-0.12	0.11	-0.09	0.05	-0.25	0.09
HHF1	-0.06	0.23	-0.01	0.72	-0.04	0.77	-0.08	0.17	-0.08	0.19	-0.06	0.61	0.52	0.38	0.21	0.61	-0.06	0.22	-0.36	0.24	-0.02	0.88	0.16	0.17	0.05	0.66	-0.10	0.08	-0.17	0.03
HHF2	0.05	0.04	0.04	0.50	0.04	0.57	0.25	0.09	-0.04	0.37	-0.11	0.09	0.24	0.18	0.27	0.07	0.21	0.04	0.26	0.10	-0.06	0.27	-0.07	0.26	-0.13	0.08	-0.01	0.85	0.17	0.05

	SMC1										SCC1										SCC2									
	ND		MMS		CPT		BEN		BLE		ND		MMS		CPT		BEN		BLE		ND		MMS		CPT		BEN		BLE	
Gene	ec/c	pval	ec/c	pval	ec/c	pval	ec/c	pval	ec/c	pval	ec/c	pval	ec/c	pval	ec/c	pval	ec/c	pval	ec/c	pval	ec/c	pval	ec/c	pval	ec/c	pval	ec/c	pval	ec/c	pval
HHT1	0.05	0.23	0.02	0.80	0.00	0.99	0.09	0.29	0.06	0.20	-0.18	0.00	-0.07	0.24	-0.16	0.00	-0.13	0.02	-0.38	0.00	-0.07	0.04	0.04	0.77	0.02	0.84	-0.06	0.04	-0.02	0.84
HHT2	-0.02	0.49	-0.03	0.65	-0.01	0.95	-0.09	0.04	0.15	0.07	-0.11	0.00	-0.07	0.19	-0.09	0.04	-0.07	0.12	-0.12	0.22	-0.14	0.10	-0.29	0.01	-0.22	0.00	-0.08	0.07	-0.07	0.48
HMT1	0.12	0.12	-0.01	0.72	-0.04	0.79	0.18	0.02	0.16	0.55	-0.02	0.70	-0.06	0.26	-0.04	0.47	-0.01	0.89	-0.17	0.55	-0.19	0.04	-0.25	0.02	-0.03	0.85	-0.12	0.05	-0.46	0.00
HNT3	0.79	0.01	0.76	0.12	1.04	0.11	0.72	0.63	1.87	0.17	1.11	0.41	2.24	0.26	2.15	0.27	0.29	0.76	1.95	0.30	0.45	0.02	1.25	0.00	1.60	0.00	0.59	0.02	0.82	0.00
HOP2	0.39	0.14	0.35	0.47	1.11	0.12	2.86	0.01	0.75	0.41	-0.71	0.02	-0.48	0.28	-0.29	0.42	-0.38	0.34	-0.98	0.00	0.41	0.08	1.00	0.01	1.33	0.03	0.42	0.18	0.60	0.10
HOS2	-0.03	0.31	-0.32	0.02	-0.26	0.01	-0.32	0.00	-0.50	0.01	0.27	0.02	-0.08	0.65	-0.04	0.37	-0.01	0.87	-0.82	0.00	-0.06	0.39	-0.19	0.27	-0.24	0.02	-0.26	0.01	-0.14	0.41
HOS4	0.09	0.16	0.02	0.73	0.00	0.98	0.19	0.06	0.17	0.07	0.32	0.00	0.44	0.01	0.37	0.00	0.29	0.00	0.45	0.13	0.18	0.01	0.15	0.00	0.17	0.00	0.07	0.04	-0.03	0.77
HSC82	0.05	0.37	0.12	0.51	0.18	0.57	0.21	0.00	0.09	0.74	0.08	0.64	0.36	0.58	0.51	0.42	0.06	0.42	0.51	0.53	-0.03	0.39	-0.20	0.23	0.00	1.00	0.14	0.13	0.39	0.02
HSM3	0.09	0.17	0.01	0.76	-0.03	0.59	-0.03	0.66	-0.06	0.52	0.08	0.37	-0.02	0.87	0.01	0.85	0.11	0.16	0.06	0.57	-0.01	0.78	-0.08	0.06	0.08	0.13	0.11	0.00	0.17	0.19
HSP82	-0.06	0.09	0.09	0.09	0.10	0.71	-0.02	0.76	-0.03	0.43	0.16	0.26	0.85	0.28	0.48	0.24	0.15	0.09	0.69	0.28	-0.01	0.92	0.20	0.21	0.37	0.34	0.03	0.42	0.38	0.10
HST1	-0.01	0.73	-0.16	0.01	-0.24	0.00	-0.16	0.06	0.01	0.68	0.04	0.08	-0.07	0.25	0.02	0.55	0.03	0.54	-0.13	0.02	-0.09	0.29	-0.14	0.13	-0.23	0.01	-0.15	0.02	-0.11	0.10
HST3	0.01	0.86	-0.13	0.10	-0.20	0.02	0.23	0.06	-0.35	0.01	-0.25	0.04	-0.33	0.00	-0.32	0.00	-0.14	0.01	-0.77	0.04	-0.36	0.00	-0.44	0.00	-0.33	0.01	-0.28	0.01	-0.26	0.09
HTA1	0.24	0.02	0.00	0.94	-0.18	0.02	0.07	0.41	0.20	0.26	-0.21	0.04	-0.28	0.01	-0.16	0.01	-0.06	0.31	-0.56	0.10	-0.03	0.34	-0.09	0.24	-0.26	0.00	-0.08	0.02	0.01	0.96
HTA2	0.13	0.03	0.01	0.88	0.06	0.74	-0.05	0.28	0.00	0.94	0.10	0.06	0.07	0.18	-0.04	0.12	0.09	0.16	-0.02	0.92	0.04	0.45	0.28	0.22	0.52	0.07	-0.07	0.13	-0.14	0.09
HTB2	0.04	0.16	0.03	0.56	-0.05	0.20	0.10	0.08	0.07	0.09	-0.15	0.00	-0.13	0.12	-0.17	0.02	-0.11	0.04	0.09	0.37	-0.09	0.09	-0.19	0.07	-0.24	0.03	-0.13	0.01	-0.04	0.65
HTZ1	-0.10	0.02	-0.03	0.81	-0.35	0.00	-0.45	0.05	-0.61	0.01	-0.28	0.00	-0.44	0.02	-0.50	0.00	-0.58	0.01	-0.91	0.03	-0.22	0.03	-0.18	0.42	0.15	0.50	-0.22	0.12	0.01	0.98
IRC20	-0.07	0.04	-0.04	0.20	-0.11	0.06	0.06	0.39	0.12	0.02	-0.05	0.47	-0.09	0.68	0.01	0.93	-0.10	0.03	0.15	0.31	-0.15	0.10	-0.29	0.01	-0.28	0.01	-0.20	0.04	0.02	0.68
ISW1	0.01	0.79	-0.15	0.09	0.01	0.95	0.02	0.77	0.13	0.04	0.02	0.84	-0.10	0.55	0.05	0.80	0.00	0.99	0.29	0.26	-0.20	0.03	-0.31	0.00	-0.29	0.00	-0.28	0.00	-0.41	0.04
ISW2	0.12	0.02	0.34	0.00	-0.01	0.86	0.42	0.00	-0.05	0.53	-0.05	0.17	0.01	0.92	0.13	0.06	0.26	0.05	-0.26	0.20	-0.08	0.04	0.35	0.21	0.41	0.03	0.19	0.01	0.03	0.83
JHD1	0.00	0.95	0.02	0.44	-0.11	0.07	0.07	0.33	0.17	0.02	-0.10	0.01	-0.18	0.00	-0.13	0.12	-0.15	0.03	-0.02	0.87	-0.05	0.54	-0.04	0.87	0.03	0.92	-0.05	0.74	0.44	0.03
KAR3	-0.36	0.11	-0.54	0.03	-0.41	0.00	-0.65	0.03	-0.75	0.00	-0.50	0.04	-0.64	0.00	-0.61	0.00	-0.56	0.00	-1.00	0.00	-0.89	0.00	-0.21	0.62	0.12	0.85	-0.74	0.00	-0.99	0.00
KEM1	0.01	0.94	0.04	0.84	-0.04	0.73	-0.02	0.95	-0.60	0.18	-0.25	0.07	0.06	0.63	0.00	0.99	-0.37	0.00	-0.75	0.10	0.91	0.34	1.47	0.23	1.65	0.25	-0.22	0.60	3.07	0.23
KNS1	-0.01	0.61	0.00	0.96	-0.15	0.02	-0.11	0.17	0.08	0.11	-0.08	0.14	0.03	0.42	-0.24	0.00	-0.01	0.91	0.19	0.44	-0.13	0.15	0.04	0.69	-0.08	0.67	-0.21	0.03	0.18	0.05
KSP1	0.17	0.01	0.02	0.64	-0.10	0.16	0.21	0.00	0.10	0.34	0.13	0.04	0.20	0.17	0.02	0.73	0.19	0.00	-0.15	0.02	0.07	0.02	0.01	0.85	-0.06	0.60	-0.01	0.64	-0.12	0.19
LIF1	-0.01	0.87	0.03	0.56	-0.04	0.81	-0.01	0.90	-0.12	0.20	0.03	0.45	-0.07	0.01	-0.05	0.24	-0.01	0.67	-0.14	0.09	0.00	0.93	-0.10	0.16	-0.16	0.04	-0.10	0.01	-0.11	0.26
LSM6	0.02	0.72	-0.08	0.19	0.03	0.89	0.01	0.96	0.19	0.18	-0.21	0.00	-0.43	0.00	-0.36	0.00	-0.01	0.89	-0.70	0.00	-0.36	0.11	-0.11	0.86	0.15	0.85	-0.46	0.00	0.23	0.65
MAD1	-0.11	0.15	-0.08	0.42	0.34	0.31	-0.12	0.62	-0.61	0.02	0.24	0.00	0.41	0.01	0.23	0.06	-0.17	0.16	0.62	0.01	-0.31	0.00	0.02	0.88	-0.06	0.78	-0.54	0.00	-0.36	0.01
MAD2	-0.14	0.01	-0.07	0.12	-0.20	0.01	0.08	0.67	-0.64	0.00	0.17	0.00	0.31	0.20	0.15	0.35	-0.28	0.04	0.07	0.72	0.14	0.45	0.11	0.68	0.30	0.62	-0.33	0.03	-0.34	0.04
MAD3	-0.13	0.01	-0.11	0.02	-0.23	0.01	0.14	0.13	-0.18	0.01	0.21	0.01	0.17	0.02	0.19	0.00	-0.14	0.02	0.23	0.08	-0.28	0.01	-0.17	0.04	-0.22	0.00	-0.35	0.00	-0.27	0.00
MAG1	0.01	0.85	-0.07	0.74	-0.10	0.03	-0.05	0.25	0.14	0.05	0.09	0.12	2.12	0.25	0.07	0.02	0.03	0.56	0.05	0.68	-0.03	0.65	0.42	0.05	-0.11	0.01	-0.06	0.08	-0.05	0.21

	SMC1										SCC1										SCC2									
	ND		MMS		CPT		BEN		BLE		ND		MMS		CPT		BEN		BLE		ND		MMS		CPT		BEN		BLE	
Gene	ec/c	pval	ec/c	pval	ec/c	pval	ec/c	pval	ec/c	pval	ec/c	pval	ec/c	pval	ec/c	pval	ec/c	pval	ec/c	pval	ec/c	pval	ec/c	pval	ec/c	pval	ec/c	pval	ec/c	pval
MCK1	0.00	0.97	-0.08	0.66	-0.66	0.00	-0.04	0.38	-0.22	0.14	-0.10	0.17	-0.36	0.00	-0.84	0.00	-0.25	0.01	-0.64	0.12	-0.18	0.03	-0.35	0.01	-0.59	0.00	-0.19	0.01	-0.25	0.22
MEC3	0.06	0.21	-0.15	0.41	0.25	0.79	-0.07	0.25	-0.27	0.25	0.28	0.03	0.09	0.39	-0.47	0.02	0.16	0.02	-0.62	0.13	0.07	0.08	-0.12	0.13	-0.60	0.12	0.01	0.47	0.44	0.44
MEK1	0.04	0.35	0.03	0.53	-0.15	0.00	0.04	0.17	0.08	0.56	0.19	0.06	0.01	0.85	0.35	0.29	0.26	0.21	0.29	0.47	0.05	0.26	-0.13	0.08	-0.08	0.18	-0.07	0.06	-0.19	0.27
MET18	0.04	0.38	-0.02	0.71	-0.09	0.01	0.27	0.08	0.09	0.33	0.10	0.17	0.47	0.20	0.51	0.00	0.18	0.20	0.37	0.43	0.26	0.04	0.04	0.67	0.14	0.10	0.12	0.43	0.11	0.46
MGS1	0.11	0.04	0.00	0.96	-0.08	0.52	0.08	0.11	0.09	0.22	0.20	0.00	0.27	0.03	0.27	0.02	0.21	0.00	0.39	0.05	0.10	0.13	0.08	0.16	0.07	0.02	0.12	0.00	0.10	0.13
MGT1	0.06	0.11	-0.16	0.00	-0.11	0.02	-0.02	0.60	-0.09	0.18	0.09	0.05	0.28	0.54	0.15	0.26	0.08	0.01	0.22	0.27	-0.03	0.23	-0.08	0.24	-0.03	0.62	-0.01	0.64	-0.08	0.11
MIH1	0.20	0.01	-0.02	0.65	-0.20	0.00	0.12	0.04	-0.11	0.28	-0.01	0.88	-0.29	0.00	-0.22	0.01	-0.01	0.82	-0.50	0.05	-0.10	0.03	-0.01	0.70	-0.11	0.10	0.01	0.88	-0.20	0.06
MLH1	0.32	0.07	0.72	0.09	0.55	0.24	-0.01	0.93	0.09	0.79	0.64	0.05	2.77	0.13	1.49	0.07	0.72	0.05	6.08	0.20	-0.10	0.28	0.21	0.31	0.39	0.04	0.10	0.06	-0.19	0.55
MLH2	0.01	0.69	0.03	0.58	0.06	0.62	0.02	0.42	0.10	0.25	0.10	0.06	0.03	0.72	0.10	0.18	0.09	0.08	-0.02	0.91	0.03	0.55	-0.06	0.27	-0.03	0.46	-0.04	0.21	-0.17	0.04
MLH3	-0.02	0.56	0.00	0.99	-0.03	0.88	0.00	0.90	-0.01	0.80	0.05	0.32	0.12	0.02	0.01	0.74	0.09	0.06	-0.06	0.76	-0.01	0.89	-0.06	0.18	-0.05	0.03	-0.06	0.09	-0.13	0.05
MMS1	0.04	0.38	0.60	0.07	-0.45	0.28	0.29	0.01	-0.61	0.01	-0.23	0.04	0.43	0.03	-0.41	0.09	-0.23	0.05	-0.65	0.00	-0.23	0.04	0.27	0.19	0.12	0.81	-0.15	0.00	-0.42	0.06
MMS2	-0.04	0.19	0.85	0.55	0.00	0.99	0.08	0.37	0.03	0.94	0.02	0.78	0.44	0.33	0.07	0.40	0.17	0.00	-0.32	0.02	-0.08	0.12	-0.26	0.39	-0.12	0.03	-0.11	0.01	-0.44	0.01
MMS22	-0.04	0.43	-0.52	0.44	-0.74	0.34	-0.14	0.05	-0.80	0.00	0.38	0.58	20.64	0.36	26.55	0.38	-0.05	0.72	3.86	0.45	-0.09	0.44	-0.76	0.02	-0.98	0.00	-0.21	0.01	0.25	0.83
MMS4	0.06	0.22	0.13	0.34	-0.70	0.01	0.12	0.37	-0.02	0.87	0.06	0.12	0.78	0.00	-0.23	0.31	0.00	0.93	0.02	0.76	-0.03	0.45	0.25	0.16	0.35	0.26	-0.04	0.16	0.21	0.02
MOG1	0.22	0.17	0.29	0.15	0.29	0.51	0.25	0.29	0.88	0.43	-0.04	0.95	0.37	0.73	0.11	0.89	-0.37	0.34	0.00	1.00	0.29	0.19	1.13	0.00	1.95	0.00	-0.14	0.55	2.33	0.00
MPH1	0.11	0.03	-0.03	0.73	-0.11	0.06	0.16	0.03	-0.04	0.44	0.05	0.22	-0.23	0.15	-0.06	0.07	0.01	0.77	-0.35	0.06	0.05	0.37	-0.05	0.22	-0.01	0.92	0.06	0.33	-0.17	0.30
MRC1	0.10	0.58	-0.04	0.82	0.11	0.79	-0.29	0.05	0.06	0.84	-0.26	0.03	-0.11	0.28	-0.26	0.04	-0.33	0.01	0.03	0.95	-0.56	0.00	-0.30	0.06	-0.33	0.27	-0.53	0.00	-0.51	0.01
MRE11	0.13	0.02	0.17	0.60	-0.29	0.58	-0.02	0.79	-0.38	0.34	-0.16	0.09	1.87	0.18	1.01	0.10	-0.14	0.02	1.16	0.02	-0.01	0.92	0.96	0.08	2.54	0.01	-0.18	0.01	-0.13	0.55
MRPL17	0.03	0.86	-0.09	0.47	-0.02	0.87	-0.18	0.02	-0.18	0.40	0.24	0.03	-0.07	0.14	0.35	0.01	0.22	0.02	-0.43	0.22	0.08	0.09	0.11	0.15	0.50	0.12	0.16	0.02	0.35	0.06
MSH1	0.00	0.96	0.04	0.76	0.43	0.40	-0.09	0.19	0.22	0.54	0.33	0.04	0.92	0.13	1.07	0.05	0.39	0.00	1.84	0.46	0.01	0.90	0.25	0.02	0.27	0.02	0.07	0.01	-0.05	0.85
MSH2	0.31	0.04	0.49	0.18	0.56	0.21	-0.10	0.64	0.32	0.40	0.39	0.43	1.55	0.38	0.75	0.44	0.45	0.15	1.65	0.44	0.35	0.18	0.67	0.07	1.19	0.07	0.13	0.04	1.03	0.17
MSH3	0.05	0.30	-0.06	0.11	-0.25	0.01	0.03	0.57	-0.01	0.92	0.05	0.48	0.14	0.06	0.07	0.48	0.07	0.23	0.22	0.04	-0.02	0.54	-0.03	0.49	-0.08	0.04	-0.02	0.30	-0.03	0.33
MSH4	0.11	0.02	0.19	0.05	-0.05	0.69	0.08	0.25	0.01	0.92	0.03	0.42	-0.06	0.43	0.00	0.97	0.00	0.97	-0.32	0.08	-0.10	0.04	0.02	0.90	-0.20	0.21	-0.04	0.16	-0.51	0.01
MSH5	0.04	0.28	-0.10	0.06	-0.16	0.01	-0.09	0.12	0.20	0.05	0.17	0.11	0.11	0.41	0.16	0.07	0.08	0.38	0.22	0.10	-0.01	0.83	0.00	0.98	0.06	0.70	0.00	0.94	-0.07	0.24
MSH6	0.07	0.14	0.08	0.22	-0.17	0.02	0.20	0.01	0.02	0.90	0.00	0.99	0.13	0.20	0.00	0.95	0.06	0.33	0.17	0.41	0.07	0.10	0.11	0.42	0.03	0.70	0.04	0.38	0.02	0.80
MSI1	-0.02	0.59	-0.19	0.06	-0.22	0.13	0.21	0.01	-0.04	0.30	-0.38	0.00	-0.32	0.00	-0.36	0.00	-0.25	0.00	-0.80	0.00	-0.06	0.25	-0.18	0.32	-0.10	0.06	-0.07	0.01	-0.43	0.01
MSM1	0.17	0.08	0.11	0.03	0.28	0.20	-0.08	0.59	0.57	0.00	0.29	0.03	0.03	0.78	0.44	0.00	0.35	0.01	0.10	0.76	0.05	0.74	0.46	0.44	0.99	0.19	0.12	0.05	4.70	0.18
MUC1	0.13	0.03	0.05	0.33	-0.14	0.05	0.00	0.99	0.01	0.91	0.27	0.01	0.30	0.09	0.18	0.12	0.15	0.13	0.43	0.05	0.01	0.82	0.01	0.88	0.02	0.86	0.00	0.92	0.00	0.96
MUS81	0.05	0.06	0.02	0.64	-0.08	0.59	-0.02	0.55	-0.30	0.00	0.07	0.17	0.77	0.00	-0.09	0.63	-0.09	0.06	-0.24	0.15	0.05	0.60	0.63	0.10	2.08	0.32	-0.02	0.20	0.07	0.57
NAM7	0.00	0.93	-0.16	0.01	-0.02	0.56	-0.28	0.01	-0.20	0.01	-0.09	0.05	0.12	0.24	0.09	0.08	-0.01	0.77	-0.46	0.02	-0.03	0.65	0.08	0.10	0.00	0.93	-0.08	0.01	-0.19	0.11

	SMC1										SCC1										SCC2									
	ND		MMS		CPT		BEN		BLE		ND		MMS		CPT		BEN		BLE		ND		MMS		CPT		BEN		BLE	
Gene	ec/c	pval	ec/c	pval	ec/c	pval	ec/c	pval	ec/c	pval	ec/c	pval	ec/c	pval	ec/c	pval	ec/c	pval	ec/c	pval	ec/c	pval	ec/c	pval	ec/c	pval	ec/c	pval	ec/c	pval
NAM8	-0.09	0.10	0.00	0.96	-0.04	0.09	0.05	0.36	-0.07	0.18	0.00	0.91	0.07	0.46	0.05	0.14	0.03	0.41	-0.21	0.03	-0.17	0.01	-0.09	0.29	-0.10	0.04	-0.06	0.07	-0.11	0.08
NCS6	-0.01	0.71	-0.01	0.85	0.07	0.34	0.01	0.93	-0.67	0.00	0.14	0.05	0.05	0.54	0.34	0.02	0.20	0.01	-0.37	0.18	0.17	0.05	0.15	0.31	0.62	0.00	0.28	0.00	0.39	0.62
NEJ1	0.09	0.21	0.23	0.15	0.25	0.50	-0.01	0.67	0.22	0.36	0.07	0.15	0.16	0.07	0.03	0.71	0.06	0.44	0.00	0.97	-0.01	0.84	-0.02	0.70	-0.12	0.06	-0.02	0.36	-0.53	0.06
NFI1	0.00	0.94	-0.09	0.03	-0.03	0.70	0.08	0.13	-0.19	0.01	0.03	0.28	-0.16	0.04	0.04	0.13	0.03	0.40	-0.05	0.54	-0.06	0.01	-0.02	0.85	-0.06	0.60	-0.03	0.49	0.08	0.29
NGG1	0.39	0.01	1.51	0.05	2.22	0.19	0.21	0.13	0.63	0.09	-0.07	0.65	-0.31	0.69	-0.44	0.28	0.21	0.73	-1.00	0.37	0.16	0.84	2.87	0.17	2.85	0.04	0.60	0.08	29.82	0.18
NHP6a	0.07	0.19	0.08	0.14	0.05	0.82	0.02	0.80	-0.23	0.02	-0.13	0.15	0.27	0.42	0.07	0.73	-0.12	0.02	-0.10	0.83	0.12	0.06	0.05	0.26	0.06	0.34	0.04	0.18	-0.06	0.52
NTG1	-0.03	0.48	-0.02	0.49	-0.23	0.01	-0.06	0.32	-0.12	0.16	0.06	0.45	0.40	0.19	0.29	0.18	0.04	0.24	0.33	0.18	0.01	0.86	0.23	0.26	0.17	0.22	-0.02	0.63	-0.08	0.34
NTG2	0.02	0.69	0.02	0.49	0.04	0.85	-0.03	0.65	0.00	0.97	0.14	0.01	0.03	0.42	0.06	0.14	0.12	0.09	-0.13	0.18	-0.01	0.72	-0.08	0.13	-0.03	0.56	-0.03	0.17	-0.07	0.55
NUP120	0.29	0.09	0.33	0.37	0.10	0.69	0.30	0.16	0.14	0.72	-0.02	0.57	0.26	0.16	0.18	0.22	0.23	0.05	-0.17	0.65	-0.24	0.00	-0.18	0.05	0.11	0.64	-0.22	0.00	-0.20	0.10
NUP60	0.18	0.91	-0.03	0.98	0.00	1.00	0.33	0.85	0.25	0.88	0.02	0.99	-0.21	0.88	0.05	0.97	-0.06	0.96	0.06	0.97	2.05	0.28	1.50	0.32	0.97	0.39	0.02	0.97	9.74	0.15
NUP84	0.25	0.05	1.25	0.02	0.17	0.66	0.42	0.01	-0.42	0.13	1.03	0.00	2.74	0.00	1.51	0.00	1.08	0.00	1.50	0.00	-0.27	0.05	-0.01	0.95	0.72	0.03	-0.08	0.10	-0.53	0.01
OGG1	-0.01	0.73	0.06	0.21	-0.10	0.17	-0.02	0.64	-0.04	0.56	0.15	0.02	0.25	0.01	0.23	0.06	0.10	0.02	0.23	0.02	0.01	0.54	0.03	0.59	0.09	0.01	-0.02	0.26	0.05	0.62
PAN2	-0.08	0.05	-0.31	0.00	-0.13	0.55	0.29	0.17	-0.07	0.26	0.17	0.00	0.02	0.50	0.17	0.10	0.06	0.71	0.08	0.48	-0.19	0.01	-0.01	0.95	0.13	0.60	-0.42	0.00	-0.10	0.20
PAN3	-0.10	0.01	-0.28	0.01	-0.06	0.81	-0.14	0.20	-0.14	0.43	0.24	0.01	0.25	0.01	0.16	0.14	0.20	0.42	0.03	0.79	-0.12	0.01	-0.25	0.00	-0.25	0.00	-0.64	0.00	-0.39	0.00
PAP2	0.10	0.13	0.06	0.31	-0.07	0.27	0.06	0.38	-0.11	0.03	0.18	0.08	0.71	0.29	0.45	0.19	0.02	0.82	0.40	0.51	0.04	0.18	-0.03	0.31	0.04	0.55	0.01	0.68	-0.08	0.23
PCH2	-0.06	0.04	-0.10	0.02	-0.16	0.01	0.13	0.22	-0.02	0.44	-0.06	0.11	-0.16	0.00	-0.10	0.05	-0.05	0.24	-0.32	0.06	-0.12	0.07	0.00	0.97	0.08	0.61	-0.17	0.01	-0.13	0.34
PER1	0.06	0.04	0.16	0.01	-0.64	0.00	-0.04	0.28	-0.53	0.04	-0.01	0.82	0.01	0.77	-0.51	0.00	-0.03	0.59	-0.80	0.01	0.06	0.40	0.20	0.04	-0.13	0.44	0.04	0.29	-0.53	0.10
PHO4	0.06	0.08	-0.03	0.46	-0.15	0.00	-0.02	0.68	-0.22	0.02	0.14	0.03	0.18	0.01	0.17	0.37	0.14	0.14	-0.09	0.28	0.06	0.18	0.00	0.91	0.08	0.10	0.01	0.50	-0.09	0.04
PHR1	0.01	0.97	0.62	0.20	0.38	0.19	0.17	0.03	-0.11	0.77	-0.49	0.41	-0.43	0.50	-0.15	0.79	-0.52	0.37	-0.95	0.16	-0.44	0.52	-0.67	0.31	-0.02	0.97	-0.38	0.64	-0.91	0.17
PIF1	0.12	0.04	0.51	0.00	0.37	0.05	0.19	0.04	0.08	0.42	0.21	0.28	1.36	0.03	0.85	0.02	0.41	0.03	0.91	0.01	0.19	0.07	0.88	0.00	1.20	0.00	-0.02	0.72	0.55	0.01
PMS1	0.05	0.41	-0.05	0.34	-0.25	0.01	-0.07	0.16	-0.06	0.26	0.10	0.10	-0.01	0.92	0.01	0.91	0.03	0.47	0.15	0.47	-0.04	0.63	-0.01	0.71	0.05	0.24	0.01	0.74	0.10	0.60
PNG1	0.02	0.60	0.16	0.17	0.06	0.74	-0.12	0.29	-0.03	0.64	-0.02	0.48	-0.11	0.02	-0.10	0.04	-0.11	0.13	-0.11	0.49	-0.02	0.78	-0.14	0.03	-0.22	0.00	-0.13	0.03	0.00	0.97
POL32	0.10	0.05	0.47	0.54	0.20	0.55	0.23	0.08	-0.03	0.94	-0.06	0.19	0.28	0.25	-0.18	0.01	0.04	0.53	-0.79	0.00	-0.01	0.90	-0.48	0.02	-0.04	0.73	-0.05	0.34	-0.65	0.02
POL4	0.04	0.38	0.08	0.04	-0.21	0.00	0.12	0.05	-0.06	0.22	0.12	0.20	0.12	0.11	0.10	0.02	0.09	0.17	-0.12	0.35	0.00	0.96	0.01	0.84	0.07	0.23	0.10	0.03	-0.17	0.19
POP2	0.40	0.32	0.17	0.70	0.25	0.80	3.61	0.18	0.39	0.80	0.33	0.01	0.53	0.01	0.04	0.83	0.44	0.55	1.69	0.08	0.38	0.61	0.52	0.53	1.51	0.31	0.51	0.70	4.62	0.44
PPH3	0.11	0.14	-0.01	0.88	0.10	0.15	0.05	0.56	0.05	0.61	0.24	0.01	-0.29	0.01	0.07	0.32	0.16	0.02	-0.44	0.00	0.01	0.54	-0.17	0.03	0.06	0.17	-0.10	0.02	-0.42	0.09
PSO2	0.16	0.01	0.00	0.95	-0.09	0.03	0.41	0.01	-0.21	0.13	0.04	0.49	-0.17	0.03	-0.11	0.01	-0.13	0.06	-0.27	0.35	-0.08	0.03	-0.01	0.92	-0.11	0.25	0.05	0.39	-0.09	0.58
PSY2	0.10	0.03	0.02	0.95	0.07	0.56	0.06	0.30	-0.36	0.01	0.03	0.74	-0.15	0.73	0.00	1.00	-0.07	0.55	-0.72	0.05	0.05	0.24	-0.10	0.22	0.00	0.99	-0.06	0.33	-0.40	0.15
PSY3	0.09	0.18	0.01	0.96	-0.12	0.61	0.17	0.02	-0.14	0.56	0.05	0.46	-0.41	0.01	-0.29	0.00	0.10	0.09	-0.48	0.02	0.06	0.24	0.11	0.56	0.00	0.97	0.09	0.08	-0.37	0.14
PSY4	0.05	0.33	0.09	0.28	0.09	0.37	-0.01	0.65	-0.10	0.31	0.05	0.44	0.14	0.34	0.02	0.71	0.07	0.15	-0.12	0.06	-0.03	0.47	0.06	0.62	0.06	0.62	-0.09	0.00	-0.20	0.10

	SMC1										SCC1										SCC2									
	ND		MMS		CPT		BEN		BLE		ND		MMS		CPT		BEN		BLE		ND		MMS		CPT		BEN		BLE	
Gene	ec/c	pval	ec/c	pval	ec/c	pval	ec/c	pval	ec/c	pval	ec/c	pval	ec/c	pval	ec/c	pval	ec/c	pval	ec/c	pval	ec/c	pval	ec/c	pval	ec/c	pval	ec/c	pval	ec/c	pval
PTP1	0.03	0.12	0.01	0.96	-0.10	0.64	-0.09	0.07	0.08	0.45	0.31	0.01	0.77	0.04	0.26	0.16	0.21	0.02	0.98	0.03	0.09	0.04	-0.17	0.00	-0.26	0.00	-0.11	0.00	-0.30	0.02
RAD1	0.12	0.02	-0.17	0.01	-0.19	0.00	0.17	0.01	0.15	0.18	-0.02	0.52	-0.25	0.01	0.09	0.25	0.12	0.15	0.04	0.68	0.01	0.92	-0.18	0.01	-0.08	0.04	0.04	0.28	0.00	0.91
RAD14	0.09	0.25	0.02	0.59	-0.04	0.19	0.04	0.64	0.03	0.45	0.29	0.23	1.29	0.44	0.62	0.31	0.10	0.26	0.41	0.63	-0.13	0.10	-0.14	0.22	0.01	0.78	-0.05	0.06	0.04	0.62
RAD17	0.02	0.46	-0.51	0.00	-0.74	0.00	-0.02	0.85	-0.48	0.00	0.11	0.01	0.08	0.36	-0.66	0.02	0.11	0.18	-0.48	0.04	-0.03	0.54	-0.04	0.60	-0.73	0.00	0.02	0.57	-0.10	0.40
RAD18	0.10	0.05	0.39	0.28	-0.08	0.18	0.08	0.04	-0.51	0.02	-0.05	0.47	0.22	0.62	-0.07	0.04	-0.08	0.10	-0.51	0.03	-0.04	0.04	1.48	0.01	0.23	0.28	-0.06	0.12	0.15	0.41
RAD2	0.10	0.01	0.17	0.37	0.23	0.42	0.11	0.28	0.10	0.41	0.06	0.16	-0.09	0.41	0.14	0.09	0.16	0.01	0.23	0.11	0.05	0.49	0.00	0.95	0.04	0.50	0.03	0.61	0.10	0.33
RAD23	0.06	0.12	0.12	0.29	0.13	0.46	0.12	0.01	-0.08	0.13	-0.20	0.01	-0.32	0.02	-0.29	0.00	0.12	0.04	-0.41	0.02	0.22	0.02	0.16	0.01	0.23	0.01	0.24	0.00	0.12	0.05
RAD24	0.08	0.11	-0.51	0.00	-0.74	0.00	0.09	0.42	-0.54	0.00	0.05	0.54	0.01	0.96	-0.69	0.00	0.00	0.93	0.09	0.80	0.00	0.97	-0.13	0.04	-0.55	0.01	0.04	0.16	-0.26	0.17
RAD27	0.10	0.12	0.46	0.12	0.16	0.03	0.14	0.26	-0.08	0.22	-0.08	0.38	0.76	0.10	-0.06	0.28	0.02	0.60	-0.09	0.43	-0.41	0.01	-0.19	0.38	0.05	0.35	-0.26	0.00	0.00	0.99
RAD28	0.05	0.11	-0.05	0.14	-0.06	0.68	0.04	0.55	0.03	0.72	-0.03	0.29	-0.08	0.16	-0.10	0.10	-0.01	0.92	0.10	0.50	-0.02	0.76	-0.08	0.18	-0.01	0.95	-0.08	0.03	-0.28	0.16
RAD30	0.05	0.30	-0.19	0.01	-0.19	0.01	-0.07	0.05	-0.08	0.09	-0.10	0.25	-0.15	0.01	0.10	0.05	0.09	0.05	0.18	0.21	0.07	0.06	-0.07	0.39	0.03	0.48	0.00	0.85	0.06	0.38
RAD33	0.05	0.23	0.04	0.32	0.03	0.87	-0.03	0.61	0.08	0.33	-0.03	0.17	-0.15	0.02	0.01	0.91	0.15	0.19	0.04	0.59	-0.06	0.44	-0.07	0.77	0.02	0.92	-0.03	0.61	0.43	0.01
RAD34	0.05	0.45	0.20	0.27	0.10	0.59	0.07	0.26	0.14	0.32	0.15	0.01	0.14	0.21	0.09	0.36	0.06	0.33	0.08	0.53	0.05	0.34	0.02	0.50	0.01	0.83	-0.01	0.61	-0.10	0.13
RAD4	0.37	0.04	0.49	0.16	0.45	0.16	-0.17	0.75	0.07	0.87	0.51	0.54	1.92	0.27	0.90	0.41	0.48	0.59	1.62	0.32	0.29	0.30	0.77	0.20	0.88	0.13	0.21	0.13	-0.04	0.94
RAD5	0.12	0.02	0.02	0.85	-0.07	0.58	0.13	0.18	-0.35	0.01	-0.09	0.12	2.47	0.00	-0.07	0.21	-0.02	0.73	-0.39	0.52	-0.07	0.15	-0.15	0.52	-0.01	0.84	0.01	0.83	-0.33	0.17
RAD50	0.11	0.11	1.11	0.03	2.57	0.04	-0.06	0.32	-0.47	0.14	-0.02	0.64	1.33	0.17	2.09	0.51	-0.15	0.01	0.94	0.43	-0.19	0.01	1.58	0.09	4.61	0.00	-0.16	0.11	-0.15	0.43
RAD51	0.05	0.19	-0.56	0.03	-0.70	0.00	-0.12	0.20	-0.77	0.00	0.00	0.99	0.09	0.88	-0.12	0.80	-0.07	0.49	-0.24	0.67	-0.06	0.26	1.24	0.05	3.82	0.03	0.04	0.40	1.59	0.34
RAD52	0.13	0.07	0.05	0.90	-0.77	0.09	0.07	0.29	-0.44	0.38	0.09	0.68	4.05	0.01	1.94	0.08	0.03	0.75	-0.20	0.79	-0.26	0.01	1.33	0.32	0.03	0.96	0.00	0.85	0.75	0.03
RAD54	0.02	0.42	0.22	0.43	-0.32	0.49	-0.11	0.11	-0.28	0.06	0.08	0.19	1.82	0.05	0.12	0.74	0.00	0.98	-0.53	0.06	0.05	0.26	0.35	0.32	1.25	0.10	-0.11	0.00	-0.10	0.44
RAD55	0.04	0.27	0.08	0.46	-0.21	0.16	-0.06	0.40	-0.23	0.08	0.06	0.32	1.10	0.03	0.34	0.66	-0.06	0.30	-0.71	0.00	0.07	0.18	-0.05	0.91	-0.59	0.54	0.03	0.59	-0.25	0.28
RAD57	0.09	0.01	0.10	0.37	0.62	0.18	0.02	0.75	-0.23	0.33	0.31	0.31	-14.00	0.24	-21.65	0.02	0.12	0.67	-0.60	0.11	0.12	0.09	1.75	0.21	22.61	0.20	-0.06	0.08	0.62	0.28
RAD6	0.03	0.49	-0.03	0.10	-0.10	0.01	0.00	0.89	-0.10	0.18	0.08	0.05	0.09	0.01	0.10	0.06	0.11	0.05	-0.08	0.10	0.05	0.18	0.02	0.62	0.08	0.09	0.04	0.03	0.11	0.07
RAD61	-0.67	0.00	-0.51	0.01	-0.18	0.04	-0.94	0.00	-0.79	0.00	-0.94	0.00	-0.20	0.81	-0.42	0.49	-1.00	0.00	-1.00	0.00	-0.53	0.24	-0.05	0.94	0.00	1.00	-0.44	0.41	-0.13	0.87
RAD9	0.07	0.10	-0.59	0.00	-0.82	0.00	0.02	0.77	-0.42	0.06	0.03	0.55	-0.19	0.03	-0.58	0.00	0.02	0.76	-0.49	0.09	0.03	0.63	-0.43	0.00	-0.89	0.00	0.00	0.92	-0.12	0.49
RDH54	0.07	0.49	-0.63	0.00	-0.51	0.11	-0.17	0.13	-0.28	0.15	0.11	0.02	-0.12	0.54	-0.13	0.60	0.05	0.36	-0.12	0.74	-0.07	0.10	-0.26	0.07	-0.30	0.24	-0.11	0.07	-0.63	0.04
REV1	0.03	0.31	-0.39	0.13	-0.16	0.03	0.04	0.29	-0.31	0.01	0.07	0.24	-0.40	0.01	0.08	0.27	0.10	0.17	-0.18	0.27	-0.04	0.31	-0.55	0.00	-0.03	0.57	-0.02	0.31	0.00	1.00
REV3	0.04	0.27	-0.60	0.00	-0.19	0.01	0.02	0.76	-0.34	0.04	0.08	0.21	-0.31	0.01	0.10	0.09	0.04	0.46	-0.14	0.10	-0.01	0.76	-0.48	0.00	0.11	0.10	-0.01	0.74	-0.05	0.40
REV7	0.10	0.07	0.19	0.07	-0.14	0.01	-0.08	0.09	0.27	0.04	0.12	0.08	-0.19	0.07	0.05	0.48	-0.05	0.39	-0.64	0.02	-0.08	0.12	-0.15	0.12	-0.15	0.00	-0.13	0.03	0.13	0.04
REX3	-0.02	0.54	-0.01	0.87	0.17	0.60	-0.10	0.11	0.09	0.27	0.02	0.64	-0.08	0.01	-0.06	0.04	0.17	0.22	0.03	0.86	-0.15	0.05	-0.18	0.01	-0.12	0.37	-0.08	0.12	0.25	0.14
RFX1	-0.12	0.01	0.10	0.06	0.08	0.01	0.00	0.94	-0.02	0.80	-0.06	0.67	0.36	0.54	0.32	0.45	0.00	0.94	0.49	0.36	-0.20	0.04	-0.20	0.00	-0.12	0.07	-0.22	0.01	0.15	0.07

	SMC1										SCC1										SCC2									
	ND		MMS		CPT		BEN		BLE		ND		MMS		CPT		BEN		BLE		ND		MMS		CPT		BEN		BLE	
Gene	ec/c	pval	ec/c	pval	ec/c	pval	ec/c	pval	ec/c	pval	ec/c	pval	ec/c	pval	ec/c	pval	ec/c	pval	ec/c	pval	ec/c	pval	ec/c	pval	ec/c	pval	ec/c	pval	ec/c	pval
RGA2	0.10	0.28	-0.35	0.28	-0.38	0.05	-0.12	0.39	-0.17	0.44	0.18	0.06	0.06	0.48	0.20	0.12	0.00	0.94	-0.27	0.59	0.08	0.08	-0.11	0.58	-0.09	0.59	-0.01	0.92	-0.82	0.00
RLF2	0.13	0.05	-0.23	0.02	-0.15	0.18	0.28	0.00	-0.12	0.25	-0.23	0.46	0.66	0.64	0.34	0.71	-0.29	0.02	0.68	0.65	0.13	0.05	-0.18	0.09	0.05	0.65	0.05	0.24	-0.31	0.03
RMI1	0.10	0.14	-0.04	0.89	-0.40	0.02	0.10	0.15	-0.17	0.09	0.18	0.01	0.72	0.04	0.14	0.21	0.18	0.01	-0.04	0.87	-0.02	0.77	0.32	0.18	-0.08	0.08	0.01	0.77	-0.19	0.15
RNR1	0.25	0.01	0.56	0.00	0.75	0.00	0.54	0.00	0.55	0.01	0.50	0.00	-0.03	0.90	0.65	0.02	1.09	0.00	-0.61	0.36	0.12	0.55	0.00	0.98	0.76	0.04	0.63	0.00	0.27	0.53
RNR3	0.04	0.33	0.02	0.64	-0.01	0.88	0.04	0.47	0.05	0.44	0.02	0.83	-0.16	0.30	-0.08	0.48	-0.01	0.96	0.00	0.99	-0.13	0.09	0.10	0.67	0.35	0.54	-0.17	0.00	0.04	0.77
RNR4	0.28	0.03	0.54	0.06	0.75	0.09	0.95	0.00	-0.21	0.68	0.35	0.17	0.82	0.48	1.31	0.11	1.35	0.00	0.39	0.79	0.16	0.04	-0.12	0.44	0.99	0.00	0.40	0.00	2.68	0.02
RPA12	0.06	0.06	0.03	0.37	-0.21	0.02	0.11	0.18	-0.07	0.25	0.01	0.71	0.11	0.08	-0.16	0.00	0.03	0.39	-0.31	0.01	0.08	0.49	0.14	0.28	0.09	0.50	0.06	0.03	0.14	0.31
RPB9	0.07	0.30	-0.12	0.54	0.36	0.09	-0.24	0.13	-0.53	0.04	0.10	0.25	-0.64	0.00	-0.02	0.86	0.05	0.61	-0.77	0.13	0.01	0.80	-0.48	0.02	-0.19	0.01	-0.38	0.00	-0.25	0.43
RPD3	0.33	0.03	0.08	0.43	-0.31	0.00	0.83	0.00	0.32	0.06	-0.35	0.00	-0.07	0.81	-0.26	0.08	-0.09	0.20	-0.67	0.04	0.12	0.03	0.38	0.10	-0.05	0.52	0.23	0.00	0.51	0.19
RPH1	-0.06	0.06	-0.08	0.05	-0.10	0.03	-0.13	0.04	-0.10	0.02	0.04	0.10	0.01	0.69	0.01	0.88	0.10	0.23	-0.03	0.61	-0.19	0.00	-0.13	0.05	-0.15	0.05	-0.15	0.01	0.14	0.03
RPL13a	-0.03	0.49	0.13	0.03	0.12	0.18	0.09	0.16	-0.18	0.25	-0.02	0.74	0.20	0.00	0.09	0.16	-0.05	0.61	0.19	0.12	0.00	1.00	0.07	0.23	0.11	0.05	-0.02	0.64	-0.11	0.23
RPL2a	0.20	0.05	-0.03	0.51	0.03	0.73	0.37	0.01	-0.09	0.27	0.13	0.25	0.79	0.16	0.32	0.09	0.24	0.02	-0.06	0.72	0.24	0.01	0.25	0.06	0.40	0.00	0.17	0.01	0.26	0.14
RPL2b	0.04	0.47	0.06	0.21	-0.06	0.19	0.00	0.96	0.04	0.34	-1.00	0.37	-1.00	0.37	-1.00	0.37	-1.00	0.37	-1.00	0.37	-0.21	0.32	-0.04	0.73	0.04	0.72	-0.09	0.57	0.01	0.97
RPN10	0.01	0.78	0.03	0.55	-0.38	0.00	-0.25	0.00	-0.28	0.00	0.44	0.36	1.85	0.16	1.29	0.22	-0.33	0.00	0.96	0.38	0.19	0.01	0.21	0.02	-0.09	0.43	-0.41	0.00	-0.37	0.02
RPS9b	0.37	0.07	0.24	0.03	0.22	0.27	0.21	0.04	0.57	0.10	-0.24	0.00	-0.30	0.00	-0.16	0.00	-0.17	0.04	-0.68	0.01	0.15	0.54	0.37	0.37	0.80	0.30	0.01	0.87	0.44	0.31
RRD1	0.19	0.00	0.03	0.55	0.02	0.79	0.19	0.12	0.18	0.12	-0.01	0.83	0.18	0.36	0.25	0.07	-0.06	0.58	0.10	0.73	0.02	0.70	0.06	0.56	0.25	0.15	0.00	0.91	-0.23	0.31
RRI1	0.11	0.03	-0.04	0.27	0.02	0.89	0.04	0.33	0.02	0.69	0.10	0.19	-0.01	0.77	-0.04	0.45	-0.05	0.11	0.23	0.45	-0.08	0.03	-0.12	0.02	-0.12	0.26	-0.07	0.07	-0.34	0.02
RRM3	0.18	0.00	0.14	0.07	0.24	0.01	0.46	0.00	0.16	0.04	0.05	0.26	-0.03	0.76	0.15	0.04	0.21	0.03	0.05	0.72	0.04	0.33	0.08	0.61	0.28	0.31	0.12	0.04	0.16	0.08
RSC1	0.37	0.41	1.15	0.09	0.83	0.16	0.15	0.87	-0.14	0.84	1.50	0.32	4.52	0.18	1.84	0.28	0.87	0.50	1.72	0.46	0.10	0.43	1.16	0.00	1.51	0.00	0.91	0.11	0.93	0.01
RSC2	0.37	0.45	1.15	0.00	0.80	0.12	0.63	0.59	0.13	0.87	-0.69	0.12	-0.50	0.18	-0.69	0.03	-0.92	0.01	-0.92	0.05	0.44	0.00	1.27	0.00	1.85	0.00	0.52	0.05	0.79	0.00
RTC6	-0.05	0.18	-0.19	0.00	-0.25	0.00	-0.07	0.19	-0.06	0.50	0.09	0.16	0.08	0.34	0.24	0.01	0.19	0.01	-0.62	0.00	-0.01	0.83	0.04	0.52	0.21	0.00	0.06	0.08	-0.25	0.11
RTS1	0.03	0.84	0.34	0.38	0.26	0.54	0.17	0.64	-0.29	0.39	0.05	0.40	-0.08	0.34	-0.35	0.00	-0.29	0.00	-0.26	0.53	-0.32	0.00	-0.20	0.02	-0.33	0.09	-0.41	0.00	0.02	0.86
RTT101	0.21	0.12	1.48	0.47	2.06	0.48	0.06	0.41	-0.18	0.39	0.01	0.91	13.38	0.12	6.04	0.17	-0.07	0.16	-0.44	0.24	-0.08	0.22	-0.10	0.75	-0.38	0.23	-0.23	0.00	-0.52	0.02
RTT103	0.09	0.08	-0.12	0.03	-0.12	0.07	0.27	0.00	-0.14	0.17	0.28	0.00	-0.09	0.23	0.01	0.90	0.35	0.00	-0.05	0.71	-0.16	0.09	-0.19	0.06	-0.12	0.01	-0.12	0.00	-0.02	0.78
RTT107	0.12	0.01	-0.32	0.05	-0.56	0.00	0.19	0.03	-0.12	0.32	0.01	0.86	-0.38	0.11	-0.65	0.00	0.05	0.42	-0.77	0.00	0.02	0.18	-0.06	0.72	0.06	0.51	-0.01	0.79	-0.41	0.10
RTT109	0.02	0.66	-0.01	0.98	-0.38	0.47	-0.05	0.22	-0.32	0.03	0.20	0.69	1.60	0.51	1.97	0.53	-0.02	0.91	0.71	0.67	-0.30	0.01	-0.22	0.50	0.20	0.86	-0.11	0.11	-0.11	0.34
SAE2	0.06	0.12	-0.05	0.47	-0.62	0.00	0.13	0.07	-0.21	0.19	0.03	0.46	-0.12	0.33	-0.74	0.00	0.04	0.27	-0.08	0.45	-0.02	0.78	-0.04	0.88	-0.15	0.74	-0.05	0.58	0.27	0.12
SAP155	-0.06	0.03	-0.12	0.22	-0.08	0.10	-0.26	0.01	-0.29	0.03	-0.27	0.00	-0.32	0.00	-0.32	0.00	-0.41	0.00	-0.66	0.01	-0.22	0.01	-0.33	0.00	-0.40	0.00	-0.46	0.00	-0.58	0.02
SAP190	0.16	0.10	0.08	0.14	0.04	0.87	0.11	0.09	0.34	0.25	0.24	0.00	0.58	0.28	0.67	0.16	0.24	0.01	0.53	0.20	0.14	0.18	0.07	0.53	0.18	0.16	0.04	0.33	-0.11	0.34
SAP4	0.05	0.67	-0.44	0.01	-0.39	0.01	-0.14	0.26	0.05	0.76	0.03	0.60	-0.10	0.18	0.07	0.25	-0.04	0.37	-0.38	0.23	0.01	0.89	-0.16	0.03	-0.19	0.04	-0.05	0.34	-0.82	0.00

	SMC1										SCC1										SCC2									
	ND		MMS		CPT		BEN		BLE		ND		MMS		CPT		BEN		BLE		ND		MMS		CPT		BEN		BLE	
Gene	ec/c	pval	ec/c	pval	ec/c	pval	ec/c	pval	ec/c	pval	ec/c	pval	ec/c	pval	ec/c	pval	ec/c	pval	ec/c	pval	ec/c	pval	ec/c	pval	ec/c	pval	ec/c	pval	ec/c	pval
SAS2	0.40	0.83	0.01	0.99	0.14	0.93	0.51	0.79	0.13	0.93	0.32	0.74	2.24	0.30	0.99	0.45	0.07	0.96	-0.95	0.39	-0.20	0.77	-0.03	0.97	0.17	0.81	-0.04	0.96	-0.23	0.75
SAT4	0.16	0.06	0.15	0.14	-0.06	0.16	0.19	0.10	-0.65	0.00	-0.05	0.46	-0.25	0.00	-0.20	0.02	0.08	0.35	2.68	0.01	0.03	0.44	0.12	0.07	-0.04	0.59	0.13	0.09	0.33	0.43
SBA1	0.06	0.23	-0.08	0.03	-0.11	0.48	0.15	0.01	0.00	0.98	0.19	0.08	0.05	0.40	0.18	0.03	0.16	0.06	0.03	0.67	-0.03	0.43	-0.05	0.35	0.09	0.01	0.01	0.56	0.02	0.72
SEH1	0.18	0.02	0.16	0.42	0.10	0.77	-0.02	0.80	0.06	0.71	0.06	0.24	0.26	0.07	0.06	0.50	0.09	0.35	-0.17	0.17	-0.23	0.01	-0.21	0.01	-0.20	0.00	-0.19	0.00	-0.33	0.00
SEM1	0.02	0.66	-0.22	0.01	-0.19	0.02	0.14	0.03	-0.51	0.00	-0.19	0.02	0.13	0.11	-0.07	0.32	0.08	0.08	-0.65	0.01	0.10	0.04	-0.03	0.56	0.24	0.00	0.18	0.02	-0.43	0.07
SGF73	0.02	0.76	0.13	0.03	-0.36	0.00	0.29	0.01	-0.25	0.01	-0.32	0.02	-0.36	0.00	-0.37	0.02	-0.10	0.10	-0.74	0.00	0.06	0.04	-0.11	0.13	-0.05	0.21	0.12	0.02	-0.28	0.03
SGO1	0.00	0.99	0.22	0.31	0.22	0.47	-0.65	0.00	-0.02	0.97	-0.10	0.18	0.02	0.91	0.07	0.77	-0.45	0.01	-0.34	0.16	-0.50	0.00	-0.31	0.01	-0.33	0.00	-0.69	0.00	-0.33	0.01
SGS1	0.06	0.06	0.22	0.33	-0.17	0.27	0.05	0.40	-0.16	0.03	0.19	0.00	0.16	0.62	0.04	0.44	0.25	0.03	-0.26	0.12	-0.04	0.69	0.17	0.34	-0.06	0.40	0.04	0.20	-0.01	0.95
SHP1	0.46	0.00	0.81	0.12	0.16	0.52	0.22	0.02	0.02	0.82	-0.46	0.28	-0.73	0.02	-0.75	0.01	-0.88	0.01	N/A	NA	-0.34	0.00	-0.48	0.11	-0.25	0.03	-0.40	0.01	-0.55	0.36
SHU1	-0.01	0.78	-0.14	0.08	-0.33	0.02	0.03	0.58	-0.21	0.00	0.03	0.56	-0.34	0.01	-0.20	0.01	0.08	0.17	-0.16	0.02	0.02	0.70	-0.07	0.47	-0.13	0.05	0.01	0.83	0.01	0.93
SHU2	-0.01	0.65	-0.11	0.04	-0.32	0.00	0.00	0.98	-0.23	0.00	0.06	0.31	-0.15	0.10	-0.18	0.00	0.06	0.20	-0.13	0.01	0.07	0.09	-0.08	0.27	-0.08	0.10	-0.01	0.77	0.02	0.70
SIN3	0.27	0.01	0.21	0.17	-0.14	0.13	0.83	0.00	0.20	0.07	-0.03	0.72	0.16	0.72	-0.23	0.27	0.00	0.99	-0.79	0.25	0.06	0.64	0.08	0.35	-0.32	0.05	0.30	0.00	0.18	0.28
SIR2	N/A	NA	N/A	NA	N/A	NA	N/A	NA	N/A	NA	N/A	NA	N/A	NA	N/A	NA	N/A	NA	N/A	NA	N/A	NA	N/A	NA	N/A	NA	N/A	NA	N/A	NA
SIT4	0.50	0.21	0.52	0.30	-0.17	0.59	-0.67	0.14	-0.72	0.20	0.58	0.70	2.01	0.47	0.95	0.59	-0.25	0.69	1.30	0.62	0.62	0.13	1.56	0.15	-0.07	0.67	-0.28	0.51	-0.02	0.99
SKY1	0.13	0.02	0.17	0.06	-0.01	0.84	0.35	0.02	0.36	0.00	0.06	0.20	-0.10	0.18	-0.23	0.01	0.11	0.07	0.32	0.09	0.00	0.94	-0.25	0.02	-0.21	0.09	0.12	0.13	0.34	0.00
SLH1	-0.09	0.09	-0.02	0.66	-0.14	0.01	-0.07	0.10	0.04	0.27	0.04	0.33	0.05	0.16	0.05	0.13	0.18	0.03	-0.07	0.47	-0.13	0.03	-0.08	0.33	-0.25	0.01	-0.14	0.03	0.00	0.96
SLX1	0.08	0.12	-0.04	0.10	-0.21	0.00	0.08	0.09	-0.01	0.70	0.12	0.08	0.07	0.32	0.03	0.64	0.15	0.06	-0.09	0.08	0.06	0.27	0.08	0.50	0.15	0.29	0.07	0.33	0.06	0.38
SLX4	0.09	0.03	-0.05	0.91	-0.16	0.48	0.10	0.29	-0.16	0.29	-0.06	0.29	-0.14	0.81	-0.37	0.04	0.02	0.69	-0.47	0.01	0.13	0.07	0.24	0.60	0.28	0.38	0.08	0.15	-0.02	0.88
SLX5	0.31	0.39	0.08	0.85	0.26	0.66	0.03	0.86	0.25	0.69	0.43	0.53	1.36	0.34	0.92	0.32	-0.09	0.67	0.14	0.91	-0.15	0.14	0.21	0.76	0.34	0.67	-0.09	0.30	0.24	0.45
SLX8	0.14	0.34	-0.09	0.74	0.08	0.85	0.09	0.34	-0.20	0.29	-0.14	0.09	0.06	0.90	-0.21	0.19	-0.24	0.01	-0.65	0.01	0.20	0.39	0.66	0.47	0.64	0.51	-0.04	0.59	0.40	0.53
SNF12	1.27	0.16	1.35	0.08	1.28	0.39	0.05	0.82	6.49	0.35	0.70	0.01	0.93	0.05	0.18	0.60	0.43	0.05	0.75	0.12	0.23	0.08	0.70	0.01	0.64	0.14	0.04	0.71	0.47	0.03
SNF4	0.20	0.17	0.63	0.11	0.69	0.02	0.06	0.64	1.44	0.19	0.14	0.12	-0.06	0.59	-0.09	0.10	0.16	0.01	-0.84	0.00	-0.03	0.72	-0.10	0.45	0.03	0.93	-0.03	0.35	-0.61	0.02
SNF5	0.44	0.14	0.54	0.01	-0.03	0.87	0.01	0.98	-0.32	0.54	0.97	0.00	2.62	0.00	1.29	0.00	1.16	0.00	0.85	0.02	0.23	0.27	0.42	0.13	0.46	0.17	0.27	0.01	0.37	0.29
SNF6	0.26	0.01	0.12	0.02	-0.51	0.00	-0.47	0.00	-0.78	0.02	0.43	0.09	0.53	0.00	0.04	0.39	0.39	0.03	-0.62	0.17	0.09	0.13	0.14	0.13	0.34	0.23	-0.05	0.49	0.16	0.63
SNT309	0.02	0.49	0.06	0.75	0.12	0.52	-0.10	0.27	0.06	0.75	0.44	0.00	0.86	0.00	0.64	0.00	-0.24	0.06	0.78	0.02	0.26	0.00	0.33	0.20	0.67	0.00	-0.09	0.60	0.37	0.27
SNU66	0.04	0.44	-0.04	0.60	0.01	0.92	0.14	0.25	-0.07	0.32	0.12	0.01	0.07	0.13	0.11	0.15	-0.06	0.25	-0.19	0.01	0.02	0.59	0.02	0.76	0.19	0.07	0.04	0.41	-0.14	0.19
SOD1	0.11	0.18	-0.16	0.16	-0.36	0.00	0.01	0.95	-0.63	0.19	-0.11	0.89	1.00	0.60	0.16	0.87	-0.66	0.11	-0.30	0.75	-0.22	0.42	-0.34	0.42	-0.43	0.07	-0.19	0.60	0.59	0.77
SPO11	0.01	0.79	0.09	0.04	-0.20	0.00	0.03	0.72	-0.19	0.12	-0.02	0.73	-0.06	0.11	-0.11	0.03	0.05	0.58	-0.35	0.04	0.05	0.49	0.01	0.79	-0.15	0.01	0.02	0.76	-0.06	0.43
SPS1	0.02	0.60	0.08	0.40	0.31	0.38	-0.01	0.92	0.10	0.41	0.11	0.04	0.14	0.24	0.12	0.08	0.23	0.00	0.02	0.41	0.00	0.90	0.04	0.68	0.01	0.96	0.02	0.75	0.25	0.00
SPT4	0.32	0.01	0.33	0.04	0.25	0.25	0.65	0.00	0.26	0.01	0.64	0.00	2.02	0.00	1.16	0.01	0.82	0.00	1.37	0.00	0.45	0.41	1.13	0.17	1.61	0.17	0.30	0.14	0.75	0.24

	SMC1										SCC1										SCC2									
	ND		MMS		CPT		BEN		BLE		ND		MMS		CPT		BEN		BLE		ND		MMS		CPT		BEN		BLE	
Gene	ec/c	pval	ec/c	pval	ec/c	pval	ec/c	pval	ec/c	pval	ec/c	pval	ec/c	pval	ec/c	pval	ec/c	pval	ec/c	pval	ec/c	pval	ec/c	pval	ec/c	pval	ec/c	pval	ec/c	pval
SRP40	0.00	0.91	0.13	0.15	0.16	0.20	0.06	0.35	0.37	0.01	0.00	0.97	0.54	0.32	0.32	0.30	-0.04	0.55	0.40	0.11	0.12	0.01	0.12	0.36	0.34	0.04	0.15	0.00	-0.03	0.85
SRS2	-0.11	0.01	-0.58	0.00	-0.68	0.00	-0.18	0.02	-0.63	0.00	-0.20	0.02	-0.43	0.04	-0.74	0.00	-0.17	0.02	-0.62	0.00	-0.22	0.00	-0.26	0.17	-0.23	0.14	-0.16	0.04	-0.29	0.01
SRV2	-0.09	0.86	-0.23	0.02	0.59	0.27	-0.02	0.96	-0.25	0.63	0.09	0.91	0.38	0.70	0.43	0.66	-0.39	0.66	0.52	0.77	0.04	0.95	0.28	0.76	0.70	0.54	-0.20	0.72	0.47	0.64
SSF1	0.05	0.23	0.10	0.46	0.21	0.46	0.22	0.00	0.15	0.45	-0.06	0.21	0.02	0.33	0.18	0.02	0.16	0.01	-0.33	0.01	0.05	0.50	0.11	0.01	0.30	0.00	0.18	0.00	0.04	0.72
SSN3	0.83	0.30	2.88	0.02	1.74	0.06	6.42	0.33	1.67	0.37	-0.45	0.58	0.65	0.73	-0.01	1.00	-0.33	0.77	-0.76	0.25	-0.13	0.76	0.58	0.34	0.81	0.05	0.40	0.45	-0.22	0.62
SSN8	0.22	0.10	-0.23	0.72	0.73	0.05	0.68	0.02	0.48	0.78	-0.70	0.06	-0.83	0.09	-0.42	0.16	-0.65	0.02	N/A	NA	-0.35	0.34	0.46	0.54	1.21	0.22	-0.17	0.18	-0.88	0.17
SSZ1	-0.06	0.25	0.36	0.13	-0.41	0.04	0.04	0.74	-0.85	0.00	0.15	0.19	0.08	0.87	-0.52	0.18	0.10	0.21	-0.97	0.38	0.09	0.64	0.18	0.34	-0.28	0.41	0.17	0.30	-0.17	0.82
SWC5	0.48	0.25	1.07	0.03	1.19	0.12	-0.55	0.26	0.84	0.42	0.67	0.53	3.86	0.19	1.63	0.30	-0.07	0.94	0.20	0.86	0.56	0.00	1.20	0.00	1.76	0.00	0.79	0.01	0.76	0.00
SWI3	0.27	0.04	0.32	0.01	-0.38	0.08	-0.33	0.05	-0.80	0.14	1.62	0.08	4.09	0.16	1.65	0.30	0.15	0.76	16.48	0.33	0.09	0.04	0.11	0.27	0.05	0.44	0.05	0.08	-0.01	0.95
SWR1	-0.04	0.67	0.71	0.22	0.14	0.72	-0.38	0.19	-0.69	0.00	-0.07	0.81	0.79	0.60	0.28	0.73	-0.28	0.43	0.22	0.87	0.10	0.35	0.62	0.04	1.03	0.00	-0.16	0.47	0.46	0.02
SYF2	-0.01	0.84	-0.06	0.37	0.04	0.85	-0.19	0.01	-0.19	0.02	0.10	0.03	0.01	0.82	0.05	0.38	-0.05	0.43	-0.35	0.01	-0.01	0.91	-0.04	0.53	-0.06	0.18	-0.11	0.01	-0.25	0.04
TAF14	0.01	0.97	0.40	0.45	0.57	0.13	3.28	0.18	0.25	0.68	0.82	0.69	6.58	0.44	2.38	0.53	0.21	0.88	13.71	0.40	0.30	0.02	1.14	0.00	1.59	0.00	0.71	0.01	0.86	0.00
TDP1	0.09	0.31	-0.04	0.68	-0.25	0.01	0.02	0.69	-0.20	0.25	0.32	0.73	0.61	0.61	0.31	0.75	0.38	0.69	0.05	0.97	-0.72	0.05	-0.52	0.15	-0.49	0.17	-0.39	0.31	-0.86	0.01
TEL1	0.04	0.43	-0.30	0.00	-0.56	0.00	0.11	0.15	-0.12	0.14	-0.03	0.55	-0.27	0.02	-0.50	0.00	0.01	0.87	-0.30	0.26	0.05	0.28	-0.21	0.01	-0.41	0.00	-0.02	0.63	-0.37	0.03
TFB5	0.33	0.09	0.49	0.39	0.45	0.25	0.30	0.26	0.42	0.45	0.52	0.33	0.94	0.51	0.66	0.38	0.38	0.37	0.24	0.85	-0.06	0.50	-0.42	0.08	-0.11	0.40	-0.18	0.00	-0.35	0.13
THP1	0.09	0.81	0.54	0.39	0.03	0.94	1.15	0.01	-0.47	0.28	0.50	0.65	2.01	0.37	1.26	0.42	-0.21	0.61	1.55	0.57	-0.03	0.90	1.21	0.35	0.58	0.53	-0.18	0.05	0.91	0.09
TOF1	-0.67	0.00	-0.72	0.00	-0.41	0.01	-0.97	0.00	-0.65	0.09	-0.93	0.13	-1.00	0.12	-1.00	0.12	-1.00	0.12	-1.00	0.12	-0.99	0.00	0.12	0.92	0.49	0.71	-0.88	0.01	-1.00	0.19
TOP1	0.16	0.02	0.31	0.00	0.86	0.00	0.16	0.07	-0.07	0.34	0.07	0.20	0.15	0.06	0.77	0.00	0.25	0.04	-0.59	0.05	0.05	0.41	0.37	0.00	1.46	0.00	0.36	0.00	0.48	0.03
TOR1	0.03	0.32	-0.01	0.84	-0.17	0.03	-0.07	0.13	-0.12	0.11	0.22	0.12	0.69	0.22	0.34	0.21	0.09	0.25	1.48	0.06	0.00	0.95	-0.08	0.14	-0.12	0.00	-0.12	0.01	-0.24	0.18
TPP1	0.00	0.89	-0.10	0.01	-0.18	0.06	-0.10	0.36	-0.03	0.75	0.08	0.03	0.08	0.54	0.04	0.69	0.04	0.28	-0.08	0.65	0.01	0.88	0.02	0.88	-0.09	0.38	-0.05	0.01	-0.31	0.03
TRF5	-0.08	0.05	-0.03	0.40	-0.05	0.43	-0.11	0.28	-0.41	0.02	0.05	0.07	0.03	0.30	0.08	0.35	0.02	0.74	-0.64	0.00	0.02	0.87	0.25	0.46	0.41	0.40	0.10	0.02	0.22	0.63
TRM2	0.01	0.70	-0.03	0.29	-0.14	0.02	-0.06	0.22	0.04	0.52	0.17	0.30	0.38	0.30	0.34	0.35	0.02	0.73	0.58	0.26	0.01	0.77	0.07	0.16	0.12	0.02	0.01	0.86	-0.06	0.45
TSA1	0.11	0.24	-0.35	0.01	0.10	0.05	0.01	0.84	0.01	0.89	0.00	0.94	-0.23	0.06	0.02	0.89	0.17	0.08	-0.44	0.00	-0.05	0.57	-0.18	0.64	-0.08	0.64	-0.15	0.02	-0.47	0.02
TUB3	0.00	0.98	-0.08	0.01	-0.10	0.04	1.75	0.02	-0.12	0.03	-0.03	0.34	0.08	0.08	0.07	0.19	1.64	0.01	-0.36	0.00	-0.09	0.08	-0.15	0.05	-0.07	0.14	-0.43	0.03	-0.14	0.06
UBC12	0.09	0.13	0.01	0.73	-0.38	0.01	0.02	0.74	0.08	0.51	0.23	0.01	-0.02	0.62	-0.18	0.00	0.15	0.08	0.13	0.27	0.05	0.21	-0.15	0.18	-0.42	0.00	-0.02	0.36	-0.66	0.02
UBC13	0.15	0.00	0.27	0.18	0.05	0.72	0.38	0.03	-0.15	0.28	0.04	0.69	1.80	0.00	0.16	0.36	0.18	0.10	-0.64	0.01	0.15	0.01	0.99	0.40	0.34	0.00	0.11	0.04	0.33	0.30
UBP13	0.14	0.01	0.04	0.26	-0.07	0.20	-0.09	0.20	0.20	0.10	0.41	0.03	1.47	0.10	0.70	0.17	0.11	0.07	1.80	0.08	0.00	0.97	0.00	0.97	-0.04	0.82	-0.10	0.04	0.07	0.61
UBP9	0.05	0.53	0.00	1.00	0.00	1.00	0.08	0.52	-0.02	0.63	0.09	0.27	0.06	0.30	-0.01	0.82	0.00	0.94	-0.16	0.26	0.07	0.26	0.20	0.00	0.38	0.03	0.06	0.40	-0.16	0.13
UBR1	0.01	0.94	-0.20	0.50	-0.40	0.02	-0.37	0.04	-0.44	0.04	0.02	0.75	0.04	0.77	-0.07	0.69	0.09	0.31	-0.54	0.27	-0.33	0.00	-0.66	0.00	-0.85	0.00	-0.72	0.00	-0.92	0.00
ULS1	0.12	0.05	0.05	0.43	-0.03	0.80	0.29	0.00	0.00	0.97	-0.02	0.55	-0.10	0.17	0.03	0.44	0.05	0.31	-0.38	0.15	0.03	0.55	0.02	0.69	0.15	0.00	0.13	0.03	-0.16	0.02

	SMC1										SCC1										SCC2									
	ND		MMS		CPT		BEN		BLE		ND		MMS		CPT		BEN		BLE		ND		MMS		CPT		BEN		BLE	
Gene	ec/c	pval	ec/c	pval	ec/c	pval	ec/c	pval	ec/c	pval	ec/c	pval	ec/c	pval	ec/c	pval	ec/c	pval	ec/c	pval	ec/c	pval	ec/c	pval	ec/c	pval	ec/c	pval	ec/c	pval
UNG1	0.12	0.09	0.09	0.09	-0.06	0.52	0.28	0.08	-0.02	0.80	0.11	0.09	0.41	0.35	0.35	0.25	0.09	0.44	0.24	0.63	0.11	0.07	0.03	0.38	0.07	0.27	0.11	0.07	-0.23	0.19
VPS34	0.08	0.82	-0.14	0.31	-0.19	0.24	0.41	0.46	-0.71	0.14	4.36	0.39	9.25	0.31	4.09	0.37	4.25	0.35	N/A	0.37	-0.73	0.00	-0.62	0.02	-0.85	0.00	-0.80	0.02	-1.00	0.02
VPS75	-0.09	0.08	0.01	0.73	-0.05	0.37	-0.08	0.06	-0.25	0.00	0.04	0.51	0.14	0.01	0.10	0.03	0.09	0.24	-0.09	0.19	-0.04	0.61	0.20	0.06	0.17	0.01	0.08	0.18	0.31	0.00
XRS2	0.06	0.23	2.04	0.06	0.94	0.30	-0.21	0.04	0.04	0.75	-0.16	0.02	0.08	0.84	-0.25	0.68	-0.15	0.12	0.68	0.13	-0.20	0.03	1.07	0.20	7.93	0.38	-0.16	0.02	0.54	0.22
YAF9	0.69	0.09	0.78	0.28	1.00	0.04	1.18	0.31	1.17	0.33	-0.98	0.11	-1.00	0.12	-0.97	0.08	-1.00	0.12	-1.00	0.12	0.14	0.74	0.72	0.37	1.38	0.09	0.27	0.67	0.26	0.71
YEN1	0.07	0.10	0.05	0.24	-0.17	0.00	0.05	0.38	-0.08	0.17	0.13	0.03	0.17	0.03	0.11	0.11	0.15	0.02	0.11	0.14	0.05	0.11	0.00	0.92	0.06	0.19	0.01	0.81	0.08	0.04
YKU70	0.02	0.69	-0.07	0.52	0.13	0.51	0.06	0.31	0.09	0.35	0.04	0.09	-0.18	0.21	0.07	0.19	0.03	0.42	-0.41	0.05	-0.11	0.12	-0.12	0.19	-0.07	0.75	-0.11	0.21	-0.01	0.83
YKU80	0.41	0.09	0.68	0.15	0.68	0.12	-0.27	0.66	-0.16	0.73	0.29	0.75	1.81	0.45	0.92	0.49	0.12	0.89	0.49	0.62	0.05	0.83	0.72	0.17	0.91	0.19	0.20	0.61	-0.25	0.57
YTA7	0.04	0.49	-0.09	0.07	-0.07	0.04	-0.27	0.01	-0.32	0.00	0.00	0.99	0.36	0.59	0.33	0.58	-0.22	0.03	0.08	0.93	0.06	0.57	0.15	0.47	0.25	0.20	-0.14	0.06	-0.18	0.05
ZUO1	0.08	0.42	0.30	0.07	0.12	0.73	0.07	0.53	1.71	0.00	0.22	0.10	0.09	0.74	-0.01	0.97	0.08	0.30	-0.66	0.56	0.21	0.13	0.44	0.07	0.29	0.04	0.31	0.01	0.74	0.06

Table 3-1. Primary SGA screen results using the three cohesin queries.

Green indicates hits with a score greater than 0.2 (i.e. PS hits). Red indicates hits with a score lower than -0.2 (i.e. SL or SC hits).

Yellow filling indicates hits with p-value <0.05 (significant).

The number of initial genetic interactions, per query and per condition, are indicated in Figure 3-2.

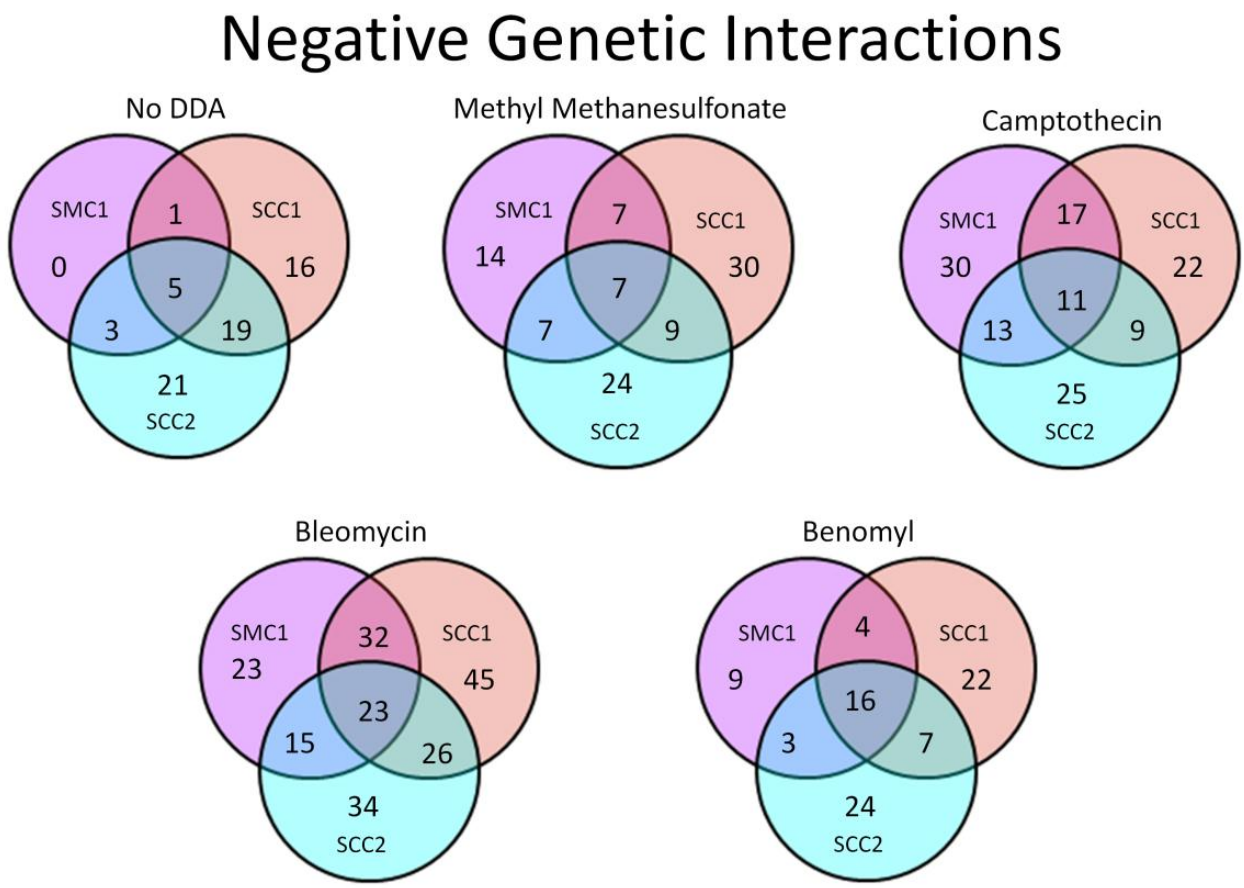

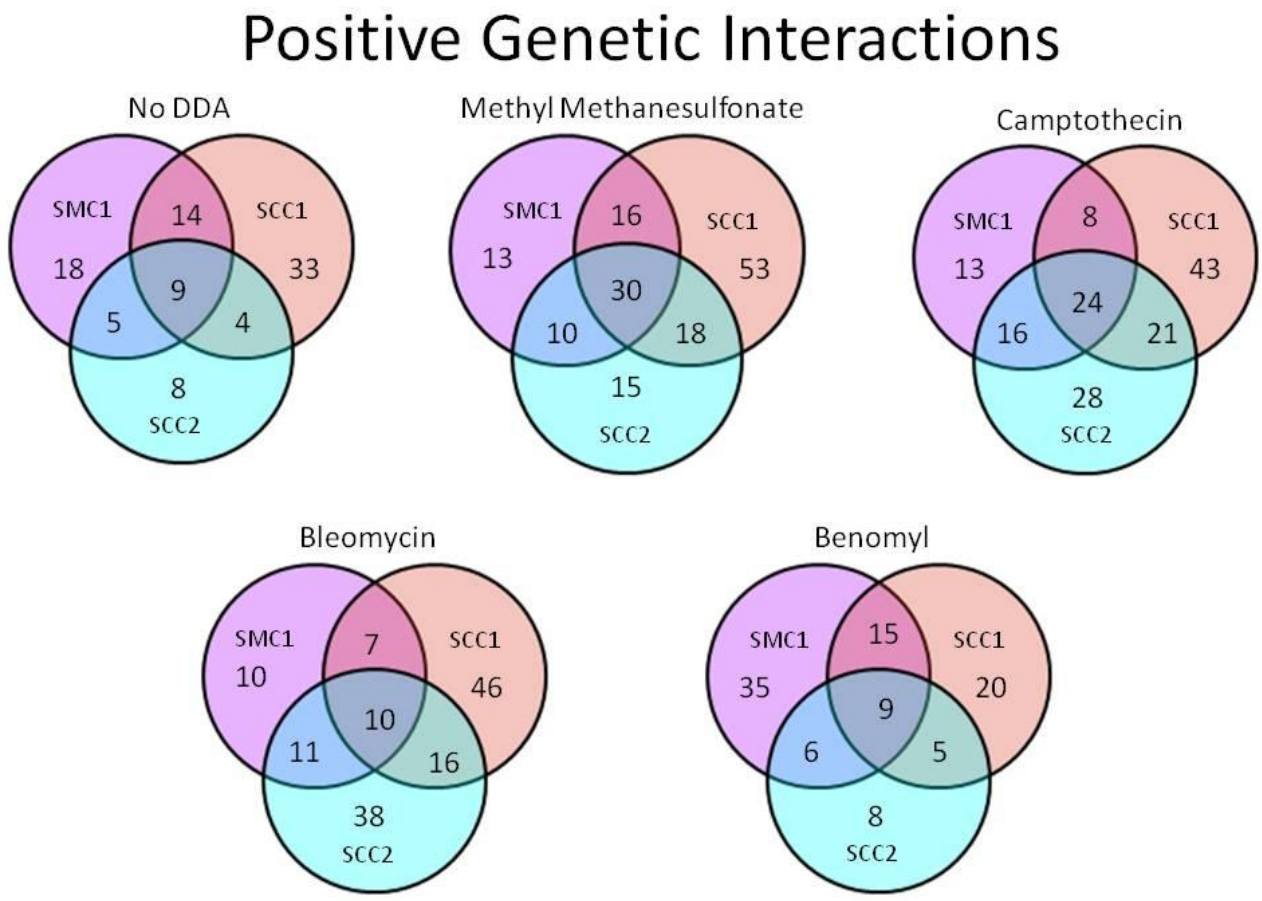

Figure 3-2. Venn diagrams representing the number of initial hits per cohesin query.

Diagrams are based on the raw data from the SGA analysis.

3.1.1 SL and SC genetic interaction networks

In order to reduce false positives, interactions observed in at least two out of the three independent cohesin SGA screens were prioritized for further analysis. As a consequence, mutated genes that interacted with only one of the mutated cohesin query genes were excluded at this stage.

Out of 4,650 possible genetic interactions, 124 genes that scored as negative interaction in two of three screens were identified, participating in 234 interactions across all five

conditions. Many hits belonged to other cellular pathways and processes, in addition to the DDR pathway, such as cell cycle progression, chromatin organization, transcription, translation and pathways in other organelles (e.g. mitochondria, endoplasmic reticulum, etc.).

Using Cytoscape software, genetic interaction maps for the three SGA screens were created (Figure 3-3 to 3-7). Seven genes that are known to be false positives were filtered out from these maps. These false positive interactions appear in all screens to date (H. Li, personal communication), regardless of the condition and may be due to sporulation or meiosis defects associated with these particular array genes.

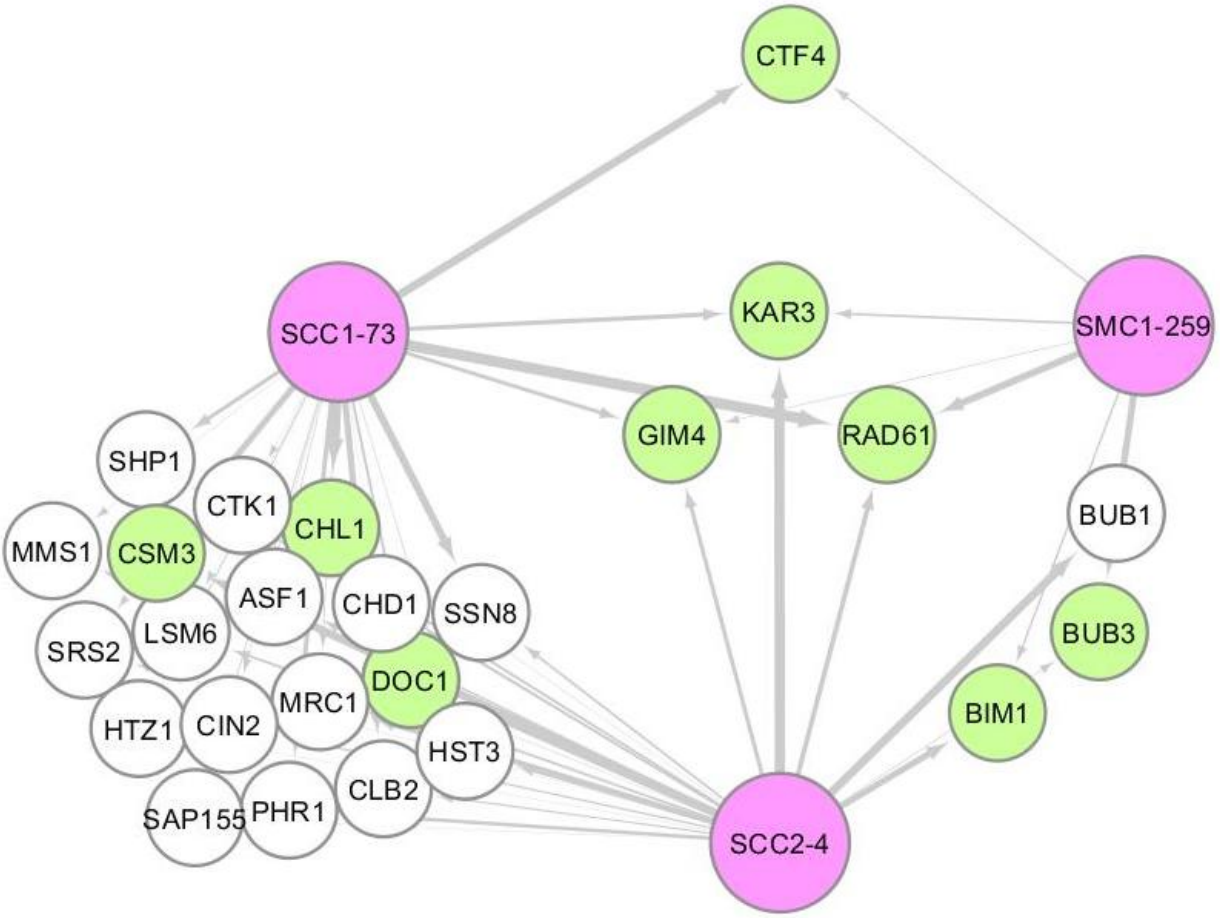

Figure 3-3. Synthetic Lethal initial hits network.

Network in the absence of a DNA-damaging agent. Pink indicates cohesin query genes. Width of connecting arrows indicates the magnitude of the genetic interaction (the wider the arrow-the stronger the interaction). In this network map, three hits (center) are shared between all cohesin queries. Three genes are shared between *smc1-259* and *scc2-4*, while 18 are shared between *scc1-73* and *scc2-4* and one gene between *scc1-73* and *smc1-259*. Green indicates previously validated SL hits[76]. Out of the core subunits. *scc1-73* SGA screen recapitulated 7 previously validated SL hits, compared to 6 for *smc1-259*. The cohesin loader, *scc2-4*, recapitulated 8 previously validated SL hits.

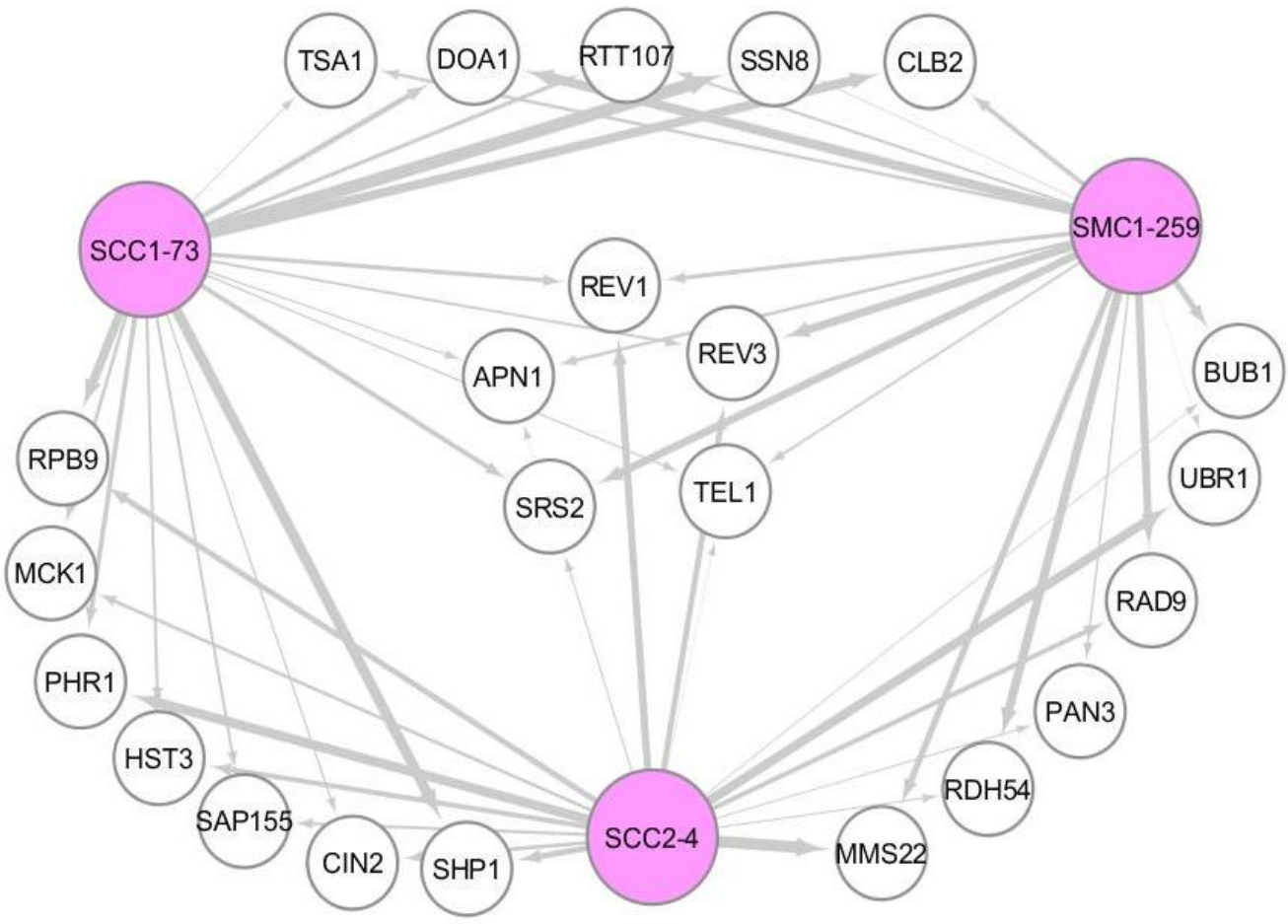

Figure 3-4. Synthetic Cytotoxic initial hits network with MMS.

Network in the presence of the DDA methyl methanesulfonate (MMS). Pink indicates cohesin query genes. Width of connecting arrows indicates the magnitude of the genetic interaction (the wider the arrow-the stronger the interaction). In this network map, five hits (center) are shared between all three cohesin queries. Six genes are shared between *smc1-259* and *scc2-4*, while seven are shared between *scc1-73* and *scc2-4* and five genes between *scc1-73* and *smc1-259*. The concentration of MMS used in the SGA (high concentration) is indicated in the **MATERIALS AND M** chapter.

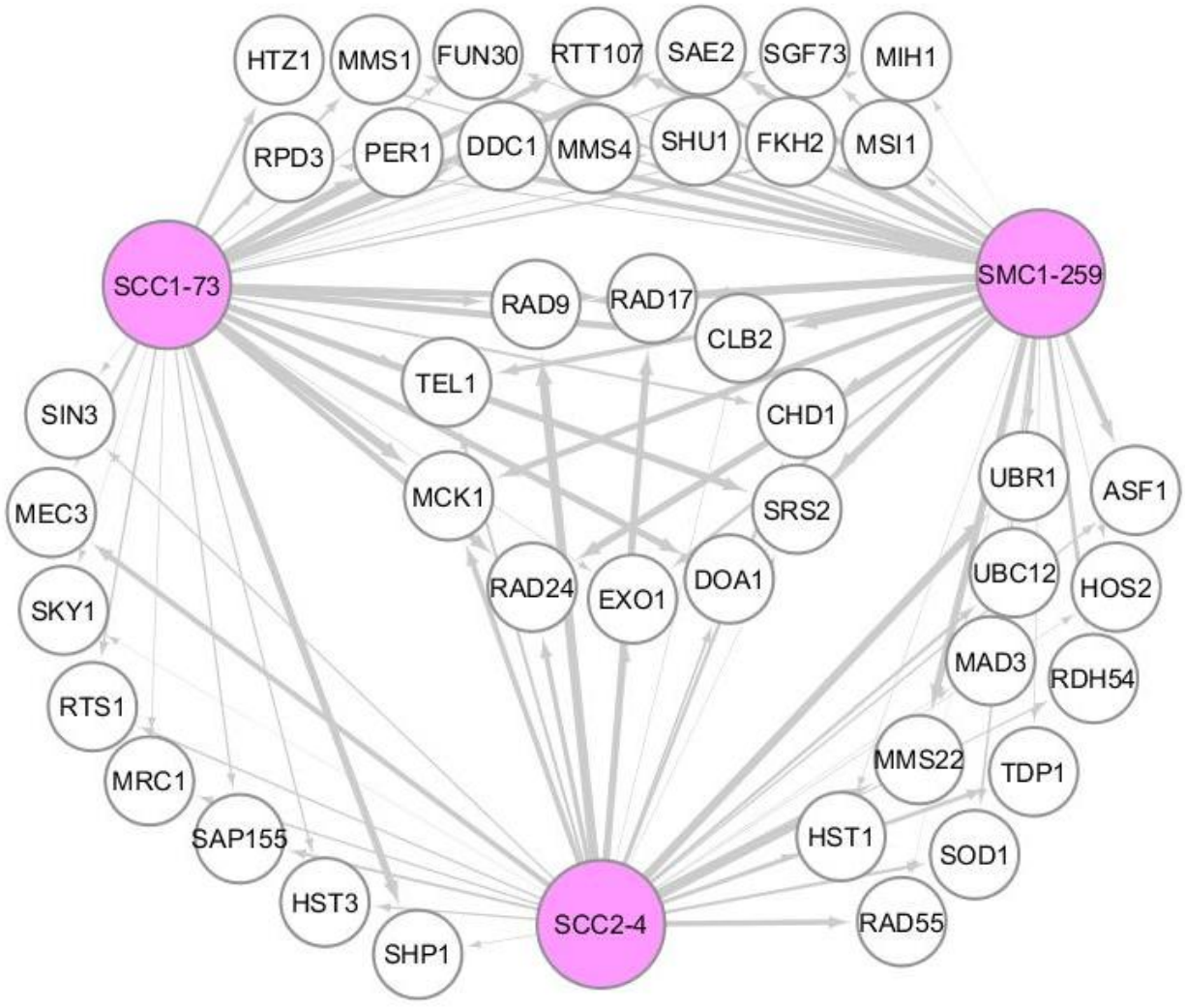

Figure 3-5. Synthetic Cytotoxic initial hits network with CPT.

Network in the presence of the DDA camptothecin (CPT). Pink indicates cohesin query genes. Width of connecting arrows indicates the magnitude of the genetic interaction (the wider the arrow-the stronger the interaction). In this network map, 10 hits (center) are shared between all three cohesin queries. The *smc1-259* and *scc2-4* screens share 11 gene hits, while eight are shared between *scc1-73* and *scc2-4* and 14 genes between *scc1-73* and *smc1-259*. The concentration of CPT used in the SGA (high concentration) is indicated in the **MATERIALS AND M** chapter.

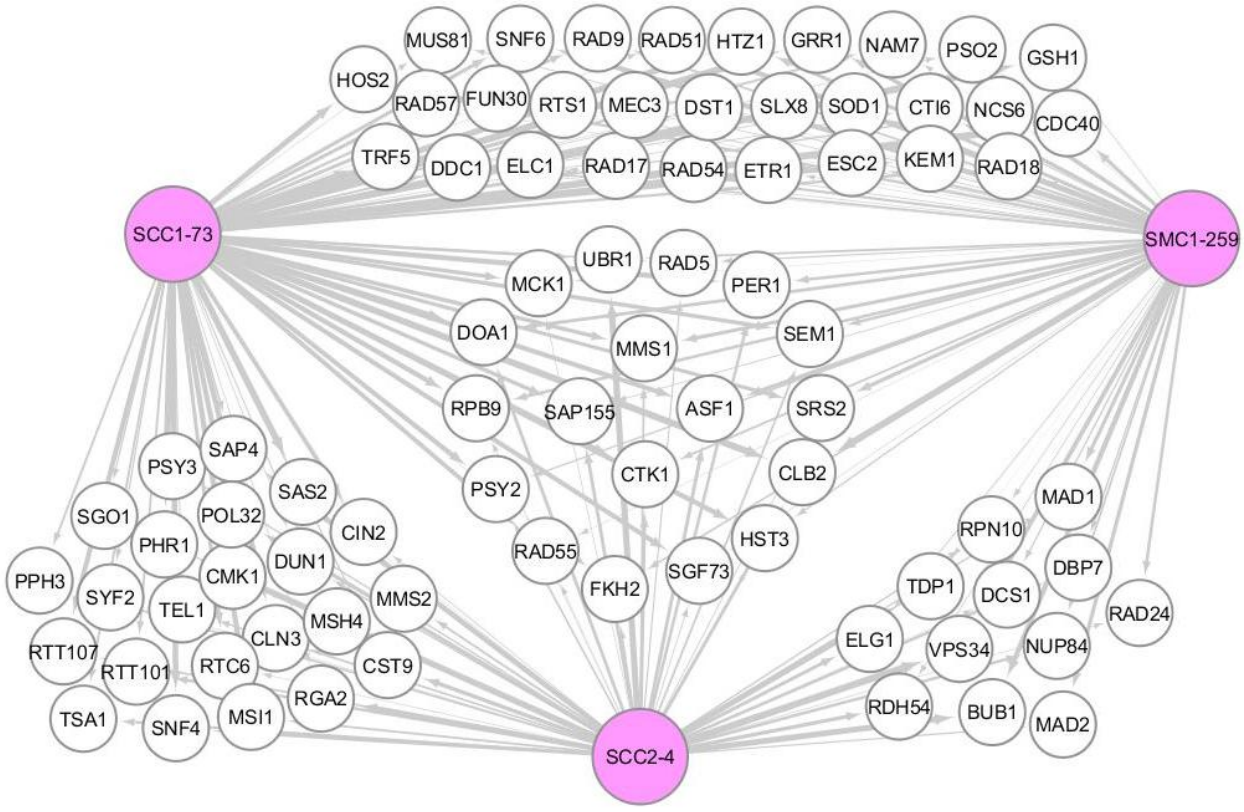

Figure 3-6. Synthetic Cytotoxic initial hits network with bleomycin.

Network in the presence of the DDA bleomycin. Pink indicates cohesin query genes. Width of connecting arrows indicates the magnitude of the genetic interaction (the wider the arrow-the stronger the interaction). In this network map, 18 hits (center) are shared between all three cohesin queries. The *smc1-259* and *scc2-4* screens share 12 gene hits, while 23 are shared between *scc1-73* and *scc2-4* and 29 genes between *scc1-73* and *smc1-259*. The concentration of bleomycin used in the SGA (high concentration) is indicated in the **MATERIALS AND M** chapter. The large number of gene interactions in the presence of bleomycin might be due to low fitness values for the single array mutants in the presence of the bleomycin concentration used.

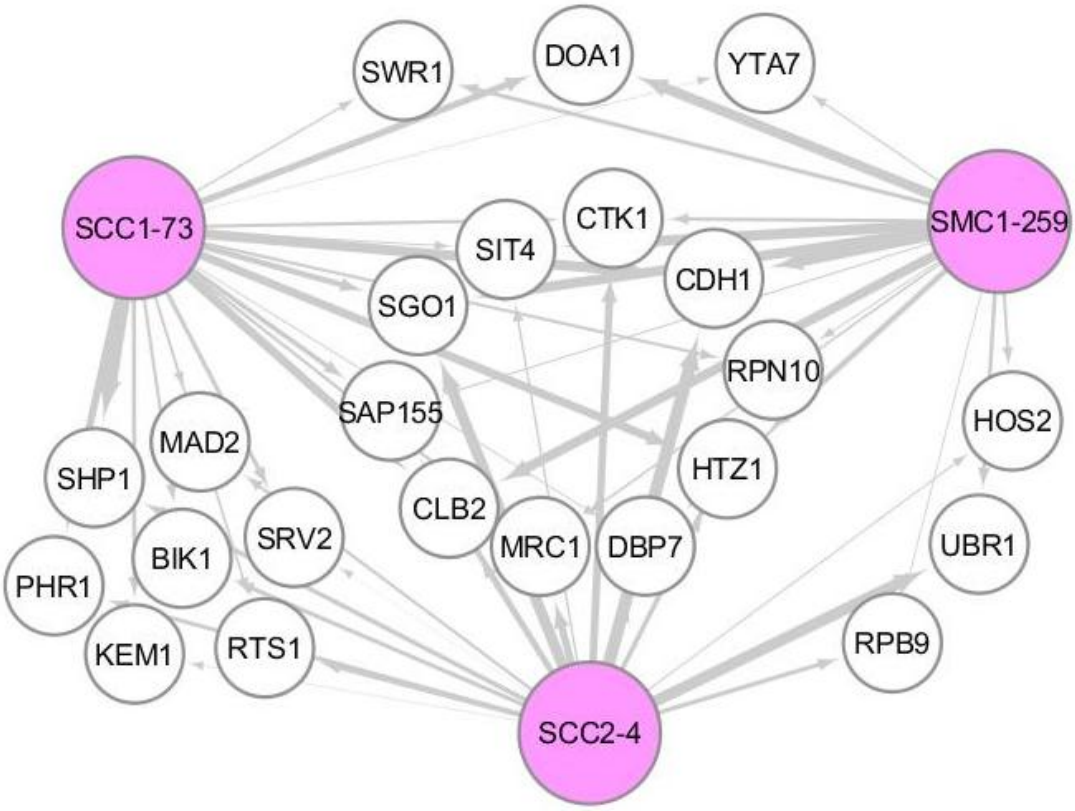

Figure 3-7. Synthetic Cytotoxic initial hits network with benomyl.

Network in the presence of the DDA benomyl. Pink indicates cohesin query genes. Width of connecting arrows indicates the magnitude of the genetic interaction (the wider the arrow-the stronger the interaction). In this network map, 10 hits (center) are shared between all three cohesin queries. The *smc1-259* and *scc2-4* screens share three gene hits, while seven are shared between *scc1-73* and *scc2-4* and three genes between *scc1-73* and *smc1-259*. The concentration of benomyl used in the SGA (high concentration) is indicated in the **MATERIALS AND M** chapter.

3.1.2 PS genetic interactions

A positive genetic interaction is defined by better than expected growth of the double mutant as predicted by the growth of the individual single mutants. Out of 4,650 possible genetic interactions, 111 genes representing positive interaction hits were identified, participating in 254 interactions across all five conditions and shared between at least two out of the three cohesin queries (Figure 3-8 to 3-12).

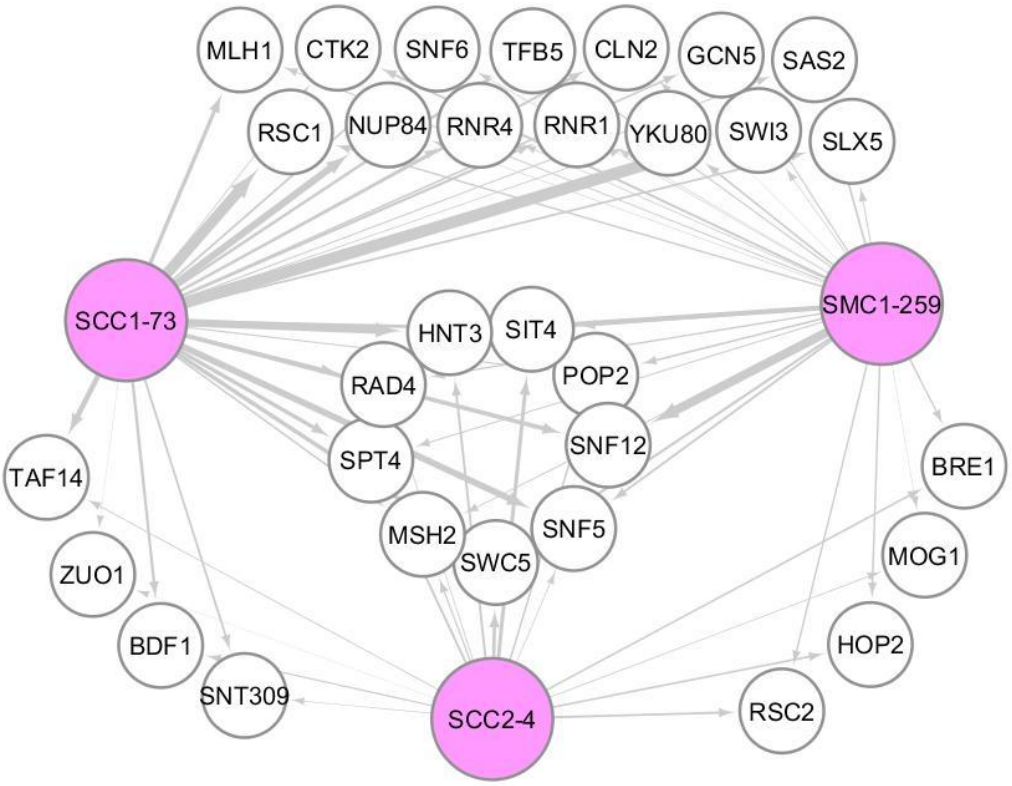

Figure 3-8. Phenotypic Suppression initial hits network without a DDA.

Network in the absence of a DNA-damaging agent. Pink indicates cohesin query genes. Width of connecting arrows indicates the magnitude of the genetic interaction (the wider the arrow-the stronger the interaction). In this network map, nine hits (center) are shared between all cohesin queries. Four genes are shared between *smc1-259* and *scc2-4*, while four are shared between *scc1-73* and *scc2-4* and 14 gene2 between *scc1-73* and *smc1-259*.

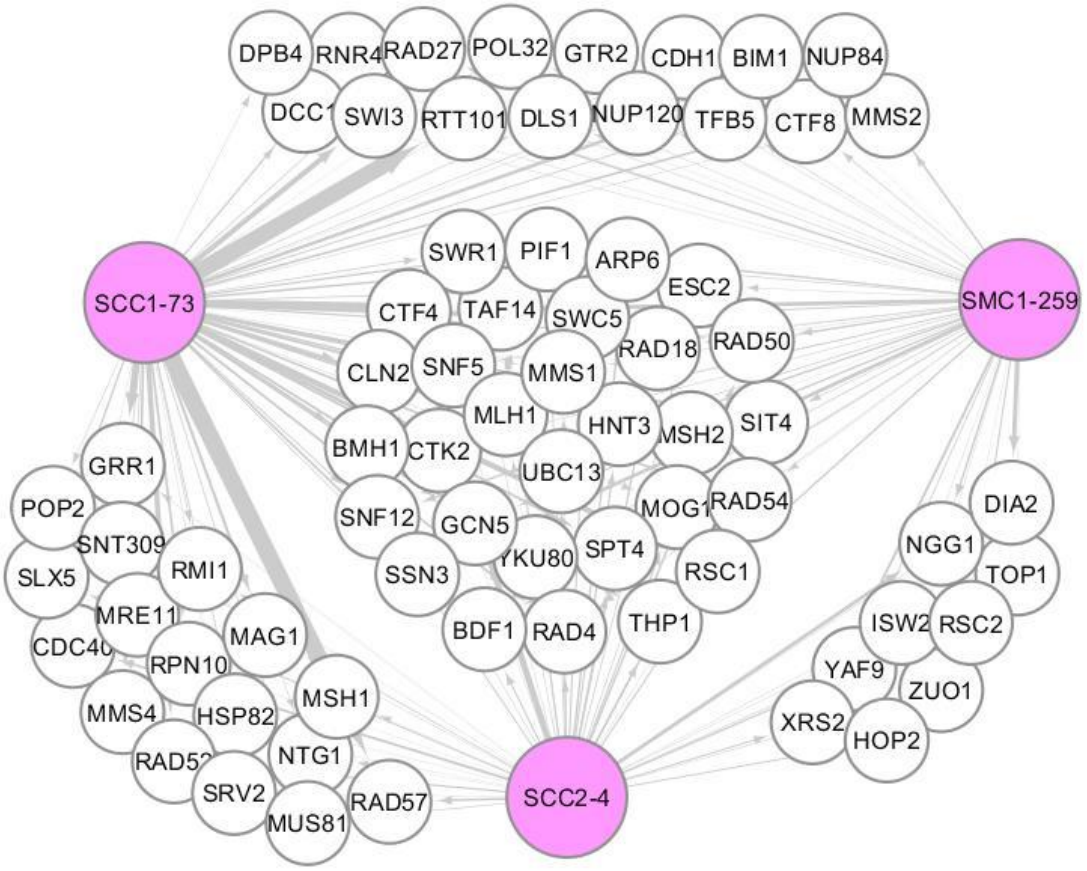

Figure 3-9. Phenotypic Suppression initial hits network with MMS.

Network in the presence of the DDA methyl methanesulfonate (MMS). Pink indicates cohesin query genes. Width of connecting arrows indicates the magnitude of the genetic interaction (the wider the arrow-the stronger the interaction). In this network map, 30 hits (center) are shared between all three cohesin queries. Nine genes are shared between *smc1-259* and *scc2-4*, while 17 are shared between *scc1-73* and *scc2-4* and 16 genes between *scc1-73* and *smc1-259*. The concentration of MMS used in the SGA (high concentration) is indicated in the **MATERIALS AND M** chapter.

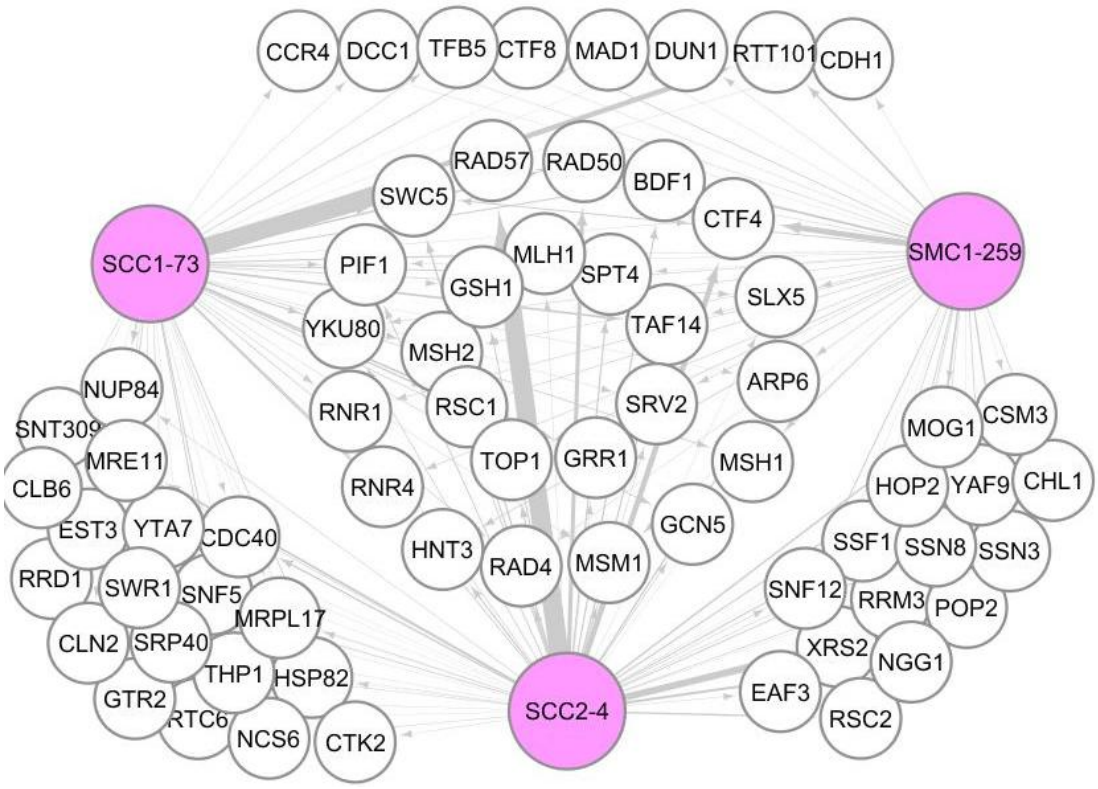

Figure 3-10. Phenotypic Suppression initial hits network with CPT.

Network in the presence of the DDA camptothecin (CPT). Pink indicates cohesin query genes. Width of connecting arrows indicates the magnitude of the genetic interaction (the wider the arrow-the stronger the interaction). In this network map, 25 hits (center) are shared between all three cohesin queries. The *smc1-259* and *scc2-4* screens share 15 gene hits, while 19 are shared between *scc1-73* and *scc2-4* and eight genes between *scc1-73* and *smc1-259*. The concentration of CPT used in the SGA (high concentration) is indicated in the **MATERIALS AND M** chapter.

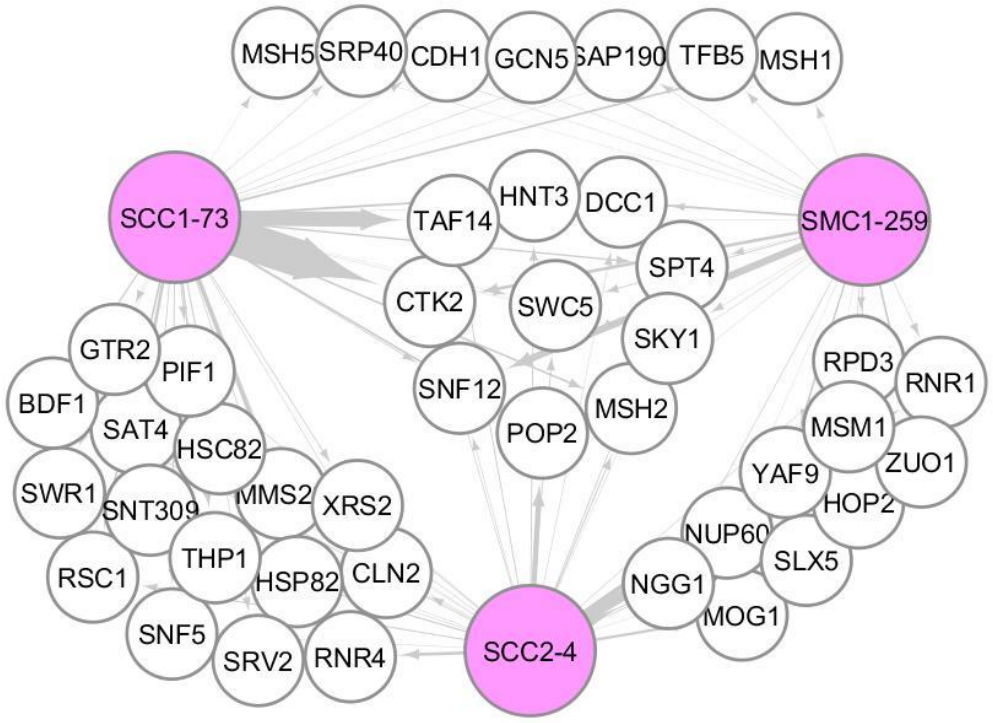

Figure 3-11. Phenotypic Suppression initial hits network with bleomycin.

Network in the presence of the DDA bleomycin. Pink indicates cohesin query genes. Width of connecting arrows indicates the magnitude of the genetic interaction (the wider the arrow-the stronger the interaction). In this network map, 10 hits (center) are shared between all three cohesin queries. The *smc1-259* and *scc2-4* screens share 10 gene hits, while 16 are shared between *scc1-73* and *scc2-4* and seven genes between *scc1-73* and *smc1-259*. The concentration of bleomycin used in the SGA (high concentration) is indicated in the MATERIALS AND M chapter.

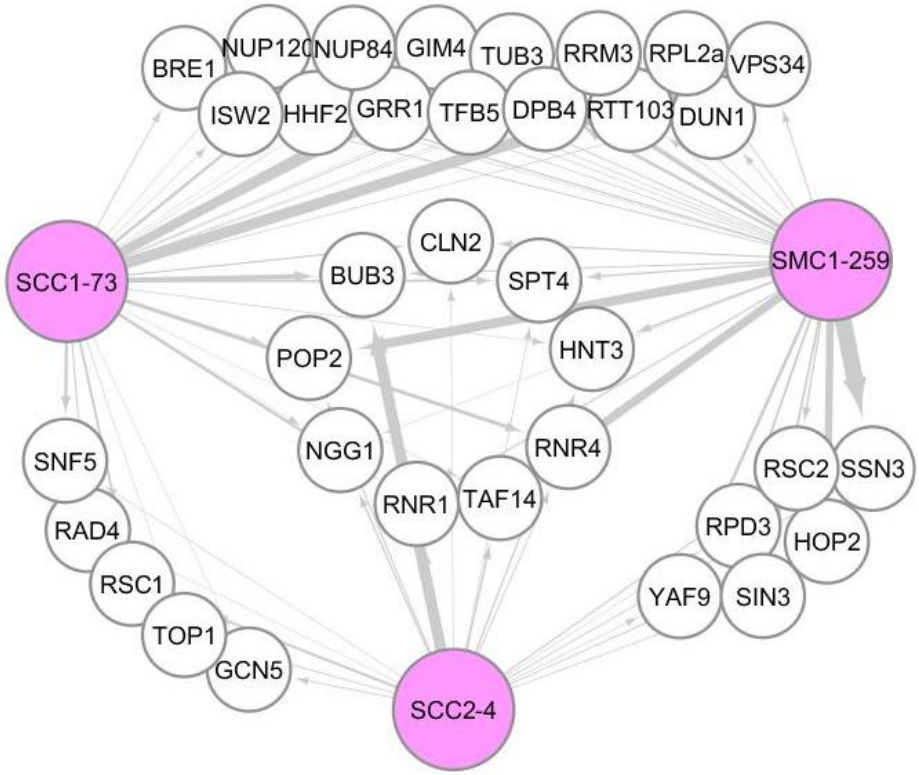

Figure 3-12. Phenotypic Suppression initial hits network with benomyl.

Network in the presence of the DDA benomyl. Pink indicates cohesin query genes. Width of connecting arrows indicates the magnitude of the genetic interaction (the wider the arrow-the stronger the interaction). In this network map, nine hits (center) are shared between all three cohesin queries. The *smc1-259* and *scc2-4* screens share six gene hits, while five are shared between *scc1-73* and *scc2-4* and 15 genes between *scc1-73* and *smc1-259*. The concentration of benomyl used in the SGA (high concentration) is indicated in the **MATERIALS AND M** chapter.

3.2 Validation of hits- retesting in ScanLag and Tecan

Double mutants from the *scc1-73* SGA screen were chosen for further analysis and validation. Validation was performed with *scc1-73*, as it is a core cohesin and exhibits better fitness compared to *smc1-259* [76].

A new growth measurement method named ScanLag[87,89] was used to validate interactions identified in SGA screens. Previously, validation was performed in liquid growth assays using a

Tecan M1000 plate reader. ScanLag measures colony growth on solid media plates to generate growth curves. One advantage of ScanLag is that the same conditions used in the SGA screen can be applied (media, concentration of DDAs, incubator, and temperature fluctuation). Tecan, on the other hand, might require adjustments to find an appropriate DDA concentration that is comparable to the concentrations in SGA plates. In addition, ScanLag is more efficient in terms of the quantity of plates that can be analyzed at the same time (up to five plates, as opposed to one 96 well plate in the Tecan). ScanLag enables the validation of 12 genetic interactions on all four DDAs and in the absence of a DDA (control) at the same time, whereas Tecan can only assess two genetic interactions under all five conditions. Furthermore, ScanLag provides the opportunity to test 4-5 different drug concentrations simultaneously to find a therapeutic window. This means that in a single experiment, the concentration range for a strong negative effect on the fitness of the double mutant without killing the single mutant can be determined. Preparation of liquid cultures of strains being analyzed, however, is the same for both methods. Thus, ScanLag is beneficial for retesting SGA screen hits, as an efficient and adjustable follow-up method.

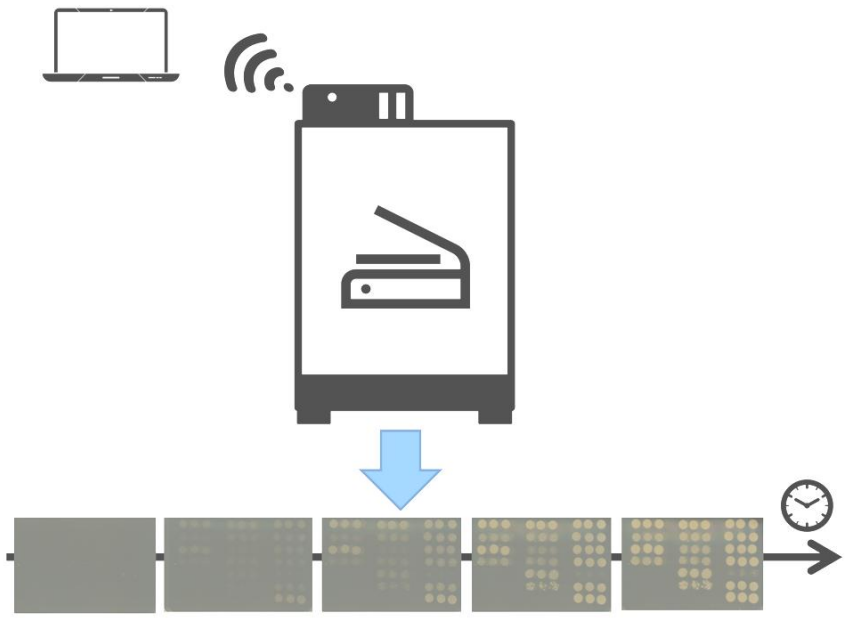

Figure 3-13. ScanLag method components.

The ScanLag software installed on the designated computer communicates with the scanner inside the incubator to acquire images of the plates over time. Running the program and accessing the stored images can be done through any computer via TeamViewer software.

The ScanLag system was set up by placing a scanner inside a 30^0C incubator, and connecting it to a designated computer located outside of the incubator. This computer has several programs installed on it, including ScanLag[87,89], to enable the recognition and communication between the two devices (i.e. scanner and computer). The activity of the scanner was monitored to ensure that it did not affect the temperature inside the incubator by placing thermometers inside the incubator and near the scanner, and comparing the results to the temperature-indicating screen on the incubator's exterior door.

The ScanLag script was programmed to instruct the scanner to acquire images every two hours, for a period of 48 hours. The computer connected to the scanner, stores the periodic scans

and can be accessed by both lab and personal computers through a remote control/access software named TeamViewer.

In order to compare ScanLag to Tecan, a parallel experiment using the same yeast cultures for both methods was performed. At least three replicates for each strain were present for each experiment, and included a WT strain, a positive control in the presence of a DDA (*rad52Δ*), the double mutant hit from the *scc1-73* screen, *rev1Δscc1-73*, and the respective single mutants, *scc1-73* and *rev1Δ*. Strains were grown overnight in YPD, diluted to an OD of ~0.1 by adding 100µl of the culture to a new tube containing 5 ml of fresh YPD media, and allowed to grow for 3 hours while rotating at 25^{o}C. After 3 hours, cultures were diluted precisely to an OD600 of 0.1 in a single 96-well plate filled with YPD. Since the double mutant was putative SC in the presence of MMS, strains were tested in the absence of a DDA by plating them on YPD plates or inoculating into YPD liquid media, and in the presence of a DDA by plating on YPD+MMS plates or inoculating into YPD+MMS liquid media. Both experiments were performed at 30^{o}C for 48 hours for ScanLag and 24 hours for Tecan. All strains were analyzed as described in MATERIALS AND M, to calculate the AUC and generate growth curves.

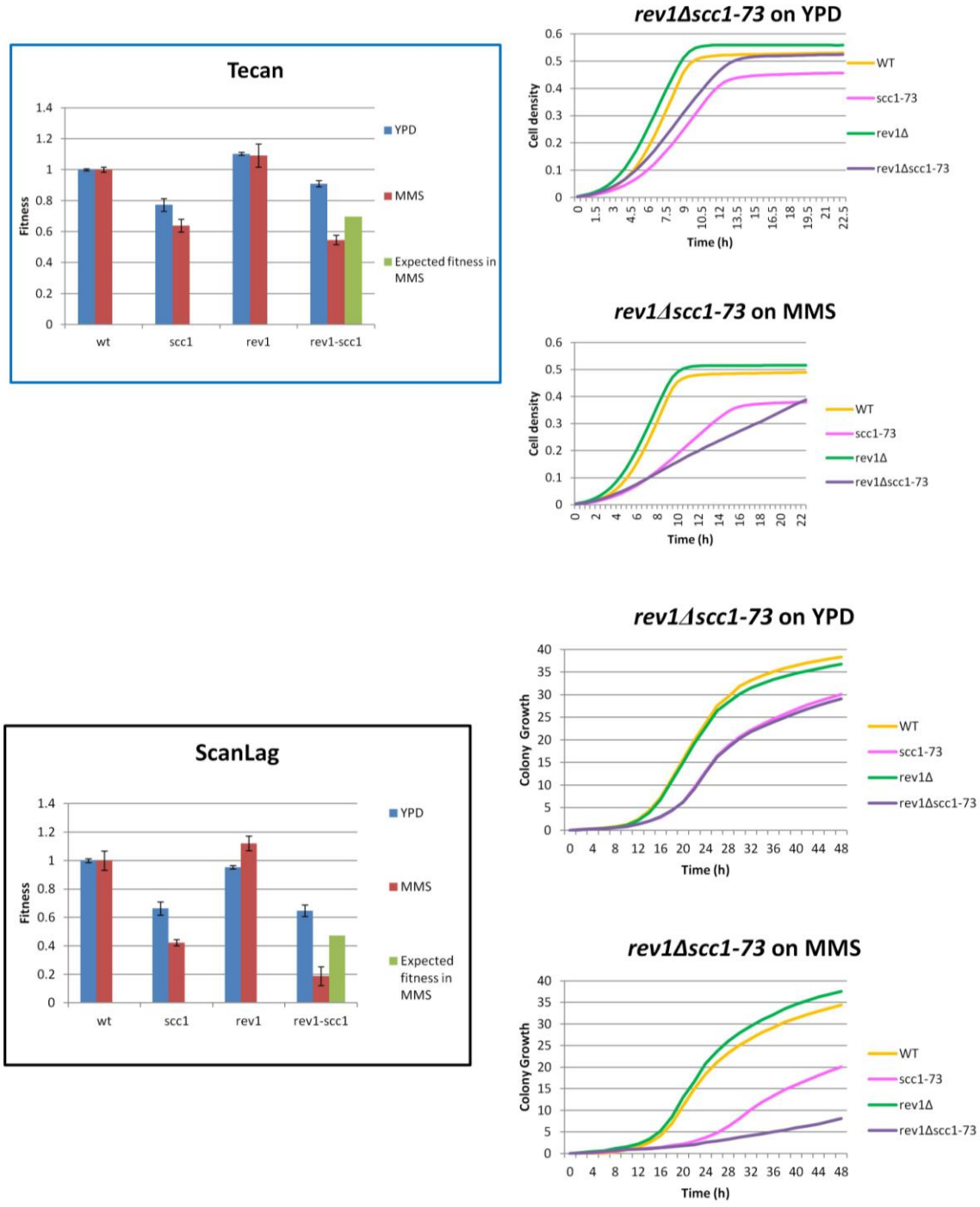

Figure 3-14. Tecan (top) vs. ScanLag (bottom) parallel experiments.

The analysis of the *rev1Δscc1-73* double mutant demonstrated a larger growth differential when assessed using ScanLag compared to Tecan under the DDA concentration used. The effect

on the fitness of the strains was measured by using an observed-predicted calculation (o-p for short), which is generated by calculating the predicted (i.e. multiplying the fitness of both single mutants under a specific condition) growth rate from the observed double mutant growth to assess any growth defect. The growth differential between the two methods used for double mutants that originated from the same colony (and overnight culture), might be attributed to a lower effective MMS concentration and different exposure of the cells to it in liquid compared to solid media.

Given that ScanLag resulted in similar results to the Tecan measurements, especially after a 24 hours analysis, and given that ScanLag allowed for more interactions to be tested in the same amount of time and allowed us to use the same drug concentration as in the SGA screen, ScanLag was used for further validation of genetic interactions identified in the SGA experiments.

3.2.1 Validation of genetic interactions using ScanLag

ScanLag was used to retest digenic interactions from the SGA data. Initially, 24 double mutants from the SGA plates were isolated for validation assays. These double mutant strains exhibited inconsistent phenotypes, most likely due to the gain of additional modifying mutations during extended storage of the plates at 4^{o}C. New double mutants were therefore isolated via resporulation of the original *scc1-73* DMA double heterozygous diploids. We then tested 28 new double mutants, and their respective singles, and found 6 double mutant strains exhibiting different phenotypes than predicted by SGA. Since the origin of the double mutants was from sporulated strains and a single round of haploid selection, we were concerned that one round of selection was not sufficient to eliminate diploids and that the phenotypic differences we observed

might be due to the presence of heterozygous diploid strains. Indeed, testing for haploidy using a mating type test revealed that the majority of strains were actually diploids.

A new set of double mutants was generated after two rounds of haploid selection. To test whether the selected double mutants were haploid, 51 strains (*rev1Δscc1-73* and *ctk1Δscc1-73* were not retested as they had recapitulated the genetic interaction) were tested for haploidy using a mating-type test. Fifty verified double mutant haploid strains were then carried on for validation. One strain, *clb2Δscc1-73* was found to be a heterozygous diploid and was removed from the list.

Twenty-five SL interactions were chosen for validation (Figure 3-7). These SL interactions include gene pairs that were previously tested and validated for the SL phenotype using the same cohesin queries[76], and new interactions that were not previously identified. Each SL double mutant was tested under all five conditions (no-DDA, termed ND, and on all 4 DDAs), using ScanLag (MATERIALS AND M).

For the validation of the SC network, genetic interactions that were observed for all three cohesin queries were prioritized. Each SC interaction was retested in all conditions for two reasons: 1) to assess whether a SC interaction seen initially under a particular DDA was true positive and 2) to assess whether SC interactions with other DDA were missed (i.e. false negative) in the SGA screen. As a consequence, some interactions that appeared in only two out of the three SGA screens in the presence of a certain DDA, were retested under those conditions. This expanded the number of genetic interactions being tested for validation.

Growth of 25 SL interaction double mutants, 43 SC interaction double mutants (including 5 on MMS, 10 on CPT, 18 on Bleomycin and 10 on Benomyl) and 4 chosen PS interaction double mutants, were measured using ScanLag. Overall, 48 negative interaction gene pairs and 4

positive interaction gene pairs were tested in all 5 conditions (YPD, MMS, CPT, Bleomycin and Benomyl) using the *scc1* query mutant (MATERIALS AND M).

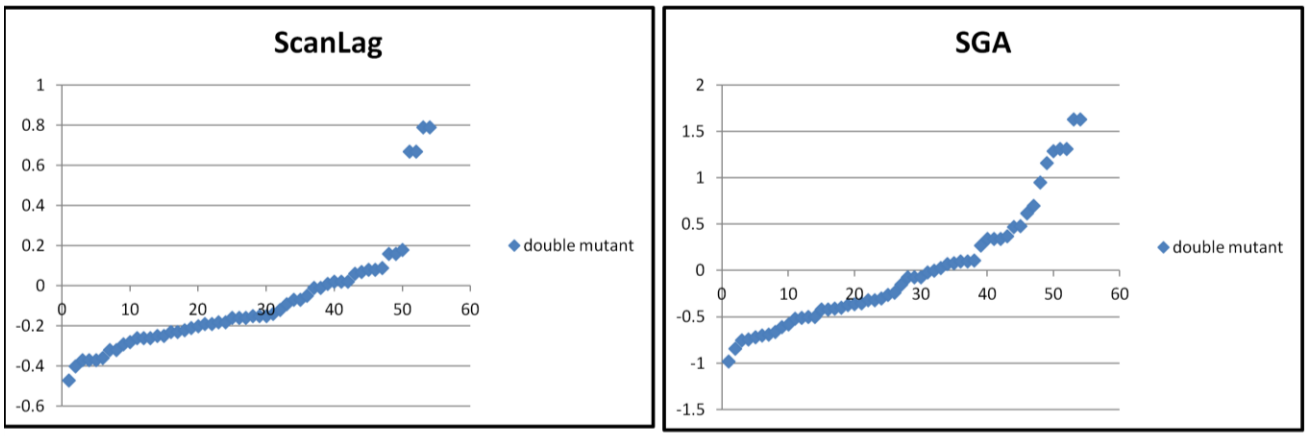

Figure 3-15. Double-mutant hits score distribution under CPT, ScanLag vs. SGA.

Each dot represents a single strain. ScanLag score is calculated as o-p (observed - predicted). SGA score is calculated as e-c/c.

Genetic interactions were assessed by analyzing the growth of the spotted cell cultures using ScanLag over time, which were then used to calculate the fitness of the mutant strains. Growth was quantified by calculating the AUC. Genetic interaction scores were normalized to the WT strain growth on the same plate. These AUC values were used to calculate o-p scores. In this method, **o** is the observed fitness relative to WT and **p** is the calculated predicted fitness of the double mutant, based on the combined growth of the two single mutants (i.e. multiplying their observed fitness) relative to WT. Since the ScanLag method (specifically ImageJ software) provides arbitrary units for measuring of colony size over time, we wished to determine the correlation of growth measurement between the two methods (i.e. SGA and ScanLag). To compare ScanLag and SGA, observed minus predicted (o-p) growth scores were calculated using ScanLag and compared to the e-c/c SGA scores.

The numerical range of growth values from ScanLag (o-p) and SGA (e-c/c) were quite different, with the SGA scores having a larger range than ScanLag values. In order to adjust the ScanLag window to make it more comparable to SGA scores, a different cutoff was needed to identify interactions. Since *scc1-73* is a slow grower that is highly sensitive to induced DNA-damage, different cutoff values were determined for each condition, a stricter cutoff in their absence (no-DDA, ND), and a less stringent cutoff in the presence of DDAs.

Double mutants tested without a DDA (SS/SL) that showed a negative growth greater than expected, were considered 'validated' if the o-p $\leq$-0.20. Double mutants tested with a DDA (SC) that showed a negative growth greater than expected, were considered 'validated' if the o-p $\leq$-0.1. Double mutants that showed growth greater than expected with or without a DDA (PS), were considered 'validated' if the o-p $\geq$0.20. For the 52 *scc1-73* DMA double mutants tested, we found 25 double mutant strains that were validated as having either SL or SC interactions and five double mutant strains that were validated as having PS interactions with a mutated cohesin, under the condition used.

Gene Hit	Type of predicted GI	YPD ScanLag	MMS ScanLag	CPT ScanLag	Bleomycin ScanLag	Benomyl ScanLag
CTF4	SL	0.08	0.1	0.02	0.02	-0.19
GIM4	SL	-0.32	-0.09	-0.29	-0.06	0.2?
KAR3	SL	-0.17	-0.16	-0.32	-0.06	-0.22
RAD61	SL	-0.21	0.16	0.08	0.02	0.39
BUB3	SL	0.2	0.1	0.18	-0.05	-0.01
BIM1	SL	-0.17	-0.18	-0.22	-0.07	-0.26
CHL1	SL	-0.14	-0.01	0.08	0.13	0.1
DOC1	SL	-0.3	-0.13	-0.19	-0.07	-0.24
CSM3	SL	-0.32	-0.16	-0.18	0	0.01
BUB1	SL	0.65	0.61	0.67	0.47	0.25
SHP1	SL	0.13	0.08	0.02	-0.08	0.1
MMS1	SL	-0.33	0	-0.01	-0.77	0.05
SRS2	SL	-0.38	-0.18	-0.28	DG	x
HTZ1	SL	-0.26	-0.25	-0.16	-0.06	0.17
SAP155	SL	-0.25	-0.26	-0.19	-0.97	-0.1
LSM6	SL	-0.2	-0.08	-0.15	-0.07	-0.16
CIN2	SL	-0.27	-0.13	-0.15	DG	x
PHR1	SL	-0.12	0.02	-0.16	DG	x
ASF1	SL	-0.01	0.11	0.16	-0.05	0.05
MRC1	SL	-0.36	-0.21	-0.26	-0.08	-0.47
CHD1	SL	-0.1	-0.31	-0.2	DG	x
SSN8	SL	-0.15	0	-0.05	DG	x
HST3	SL	-0.18	-0.14	-0.18	DG	x
CTK1	SL	-0.34	-0.18	-0.23	x	-0.08
REV1	SC (mms)	0.02	-0.29	0.06	x	x
REV3	SC (mms)	-0.13	-0.18	-0.15	-0.3	0.07
APN1	SC (mms)	-0.3	-0.28	-0.26	DG	x
TEL1	SC (mms, cpt)	-0.37	-0.29	-0.37	DG	x
MCK1	SC (cpt, bleo)	-0.26	-0.38	-0.25	DG	x
RAD17	SC (cpt)	-0.04	0.03	-0.07	x	x
RAD24	SC (cpt)	-0.17	-0.16	-0.14	-0.43	-0.17

Gene Hit	Type of predicted GI	YPD ScanLag	MMS ScanLag	CPT ScanLag	Bleomycin ScanLag	Benomyl ScanLag
RAD9	SC (cpt)	-0.17	-0.04	-0.12	-0.1	-0.03
DOA1	SC (cpt, bleo)	-0.26	-0.25	-0.26	0.13	-0.33
EXO1	SC (cpt)	-0.39	-0.45	-0.47	DG	x
UBR1	SC (bleo)	-0.28	-0.19	-0.09	x	x
RAD5	SC (bleo)	-0.2	0.05	-0.16	-0.69	0.03
PER1	SC (bleo)	-0.12	-0.11	0.01	x	x
SEM1	SC (bleo)	-0.1	-0.03	-0.01	0.02	0.17
SGF73	SC (bleo)	-0.17	-0.11	-0.07	-0.85	0
FKH2	SC (bleo)	-0.29	-0.21	-0.21	-0.52	-0.02
RAD55	SC (bleo)	-0.17	0.01	0.02	0.01	-0.02
PSY2	SC (bleo)	-0.19	-0.11	-0.25	x	x
RPB9	SC (bleo)	-0.06	0.05	0.07	0.03	-0.05
SIT4	SC (beno)	-0.27	-0.15	-0.37	-0.14	-0.33
CDH1	SC (beno)	-0.13	-0.17	-0.37	-0.02	-0.22
RPN10	SC (beno)	-0.25	-0.06	-0.23	-0.25	-0.07
DBP7	SC (beno)	-0.24	-0.22	-0.36	-0.12	-0.05
SGO1	SC (beno)	-0.29	-0.38	-0.4	-0.02	-0.32
SPT4	PS	0.18	0.11	0.16	x	x
RNR4	PS	-0.2	-0.24	-0.32	-0.12	-0.35
SWC5	PS	0.54	0.61	0.79	0.35	-0.07
CLN2	PS	0.26	-0.04	0.09	x	x

Table 3-2. Results of retested initial SGA scc1 hits.

Gene name filled in yellow indicated previously validated negative interaction hits using the cohesin query[76]. Gene name filled in blue were verified for haploidy. Red filled scores are negative interaction that passed the specific cutoff (i.e. validated). Green filled scores are phenotypic suppressors (PS) validated hits. GI stands for genetic interaction as predicted by SGA primary data. The 'x' symbolizes that the experiment has not been done. DG indicates an experiment in which *scc1* query mutant did not grow.

Several strong genetic interactions were validated. The *rev3Δscc1-73* interaction was a good example in which the genetic interaction of the double mutant is stronger in the presence of a DDA, specifically MMS, compared to in the absence of a DDA. Thus, we validated *rev3Δ* as an SC interaction with a mutated cohesin complex. The o-p score (normalized to the WT strain under the same condition) of the double mutant on YPD was -0.13, compared to -0.18 on MMS. While the predicted growth defect was 0.25 on MMS, the observed fitness of the double mutant was 0.08.

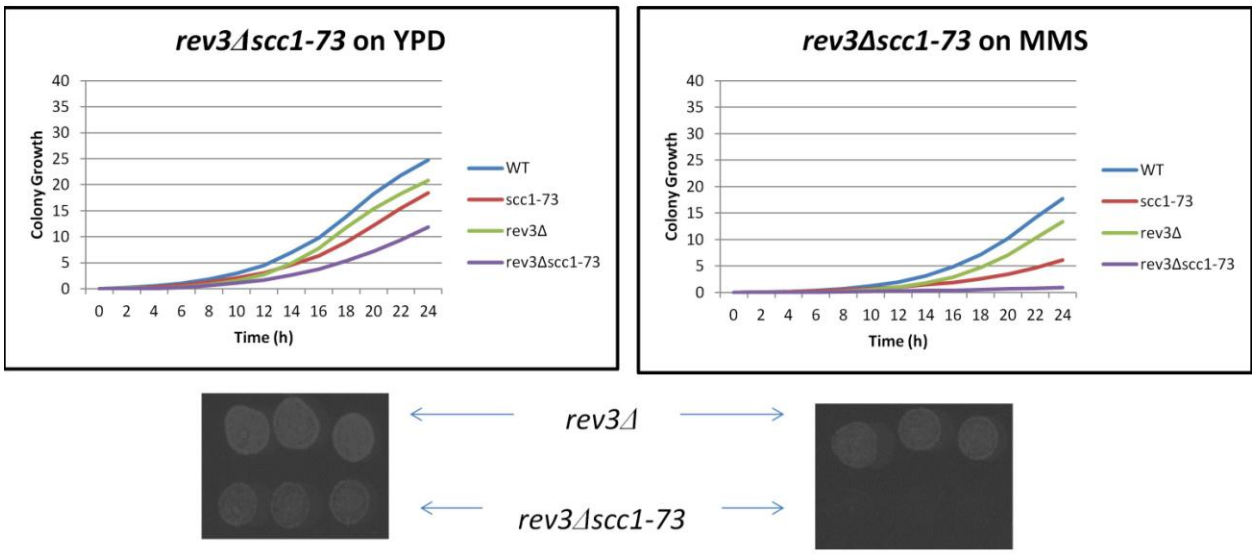

Figure 3-16. Growth curves of SC interaction on MMS.

The double mutant *rev3Δscc1-73* without a DDA (left) and with MMS (right), respective to a WT strain and the two single mutants. Growth curves were generated after 24 hours. Images from scanned plates were taken after 24 hours, presenting the single mutant *rev3Δ* (top) and the double mutant *rev3Δscc1-73* (bottom) under each condition.

Another validated SC interaction was *cdh1Δscc1-73* on CPT, where the differential in fitness of the double mutant, both with and without CPT, was substantial. The o-p score (normalized to the WT strain under the same condition) of the double mutant was -0.13 on YPD

compared to -0.37 on CPT. While the predicted growth defect was -0.39 on CPT, the observed fitness of the double mutant was 0.02.

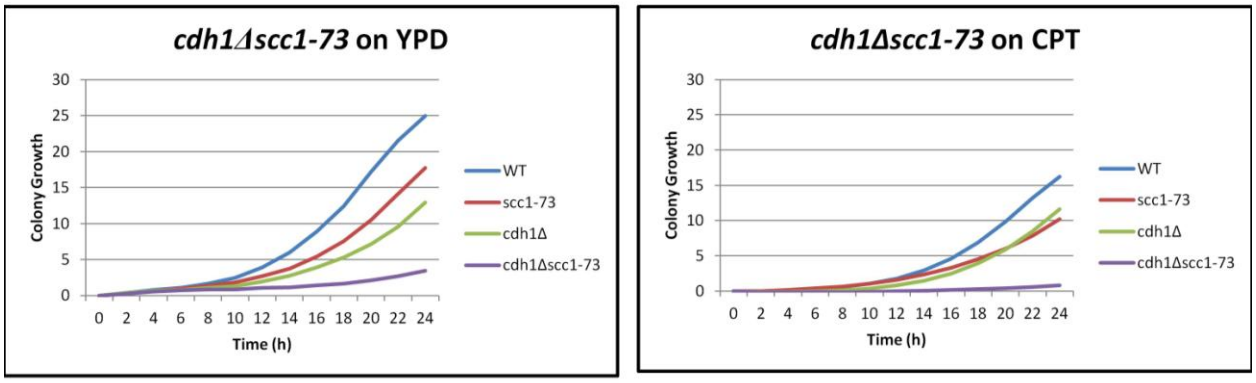

Figure 3-17. Growth curves of SC interaction on CPT.

The double mutant *cdh1Δscc1-73* without a DDA (left) and with CPT(right), respective to a WT strain and the two single mutants. Growth curves were generated after 24 hours.

A strong SC interaction with *scc1* was observed on benomyl for both *sit4Δ* and *sgo1Δ*. The o-p score (normalized to the WT strain under the same condition) of *sit4Δscc1-73* double mutant was -0.27 on YPD and -0.33 on benomyl. While the predicted growth defect was -0.41 on benomyl, the observed fitness of the double mutant was 0.08. The o-p score of *sgo1Δscc1-73* was -0.29 on YPD and -0.32 on benomyl. While the predicted growth defect was 0.4 on benomyl, the observed fitness of the double mutant was 0.08. These interactions are good examples of weak interactions that occur in the absence of a DDA, while exhibiting a strong SC interaction with the addition of a DDA.

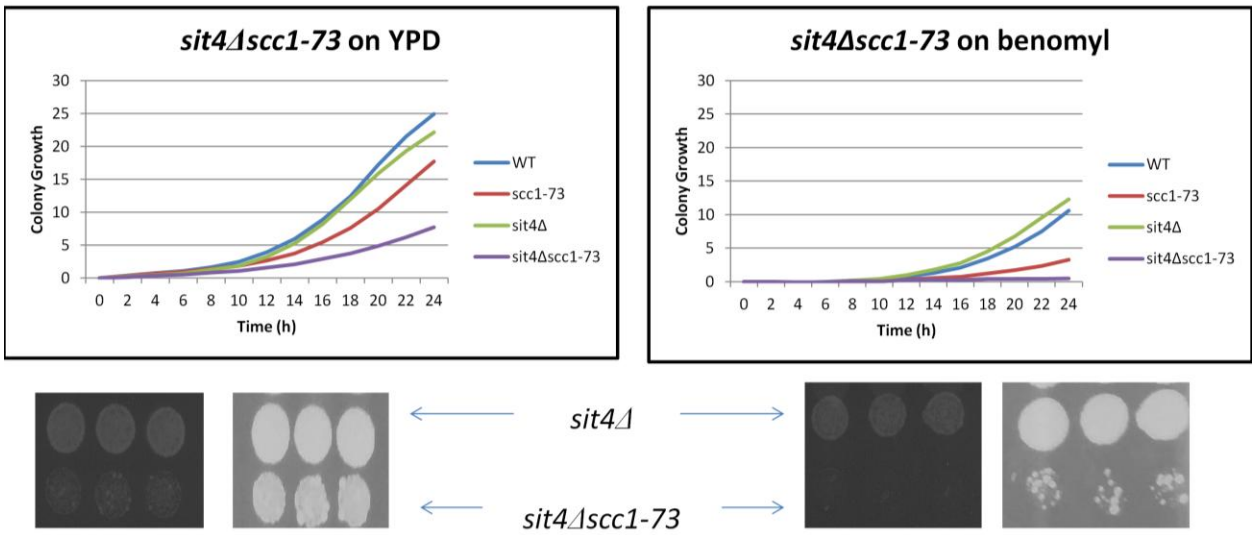

Figure 3-18. Growth curves of SC interaction on benomyl.

The double mutant *sit4Δscc1-73* without a DDA (left) and with benomyl (right), respective to a WT strain and the two single mutants. Growth curves were generated after 24 hours. Images from scanned plates (left) were taken after 24 hours, presenting the single mutant *sit4Δ* (top) and the double mutant *sit4Δscc1-73* (bottom) under each condition. Images from scanned plates (right) were taken after 72 hours (three days).

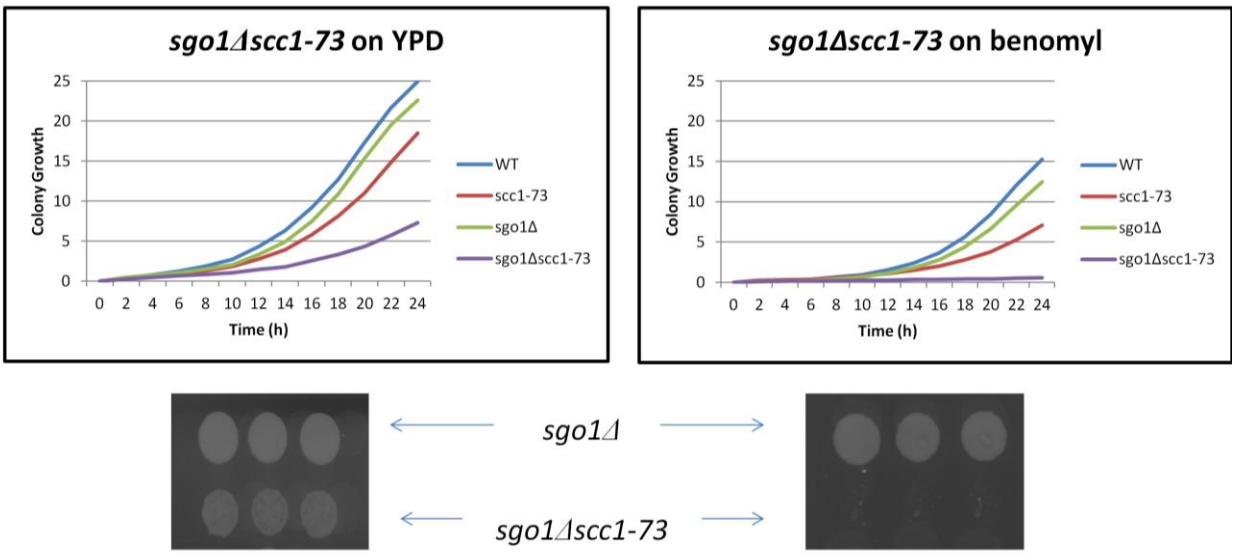

Figure 3-19. Growth curves of SC interaction on benomyl.

The double mutant *sgo1Δscc1-73* without a DDA (left) and with benomyl (right), respective to a WT strain and the two single mutants. Growth curves were generated after 24 hours. Images from scanned plates were taken after 48 hours, presenting the single mutant *sgo1Δ* (top) and the double mutant *sgo1Δscc1-73* (bottom).

As for the reassessment of SL hits, we found several validated hits, including examples that were previously validated (e.g. *gim4Δscc1-73*), as well as novel genetic interactions (e.g. *rpn10Δscc1-73*, *lsm6Δscc1-73*). For all of these examples, the lethal interaction was maintained with the addition of the DDAs.

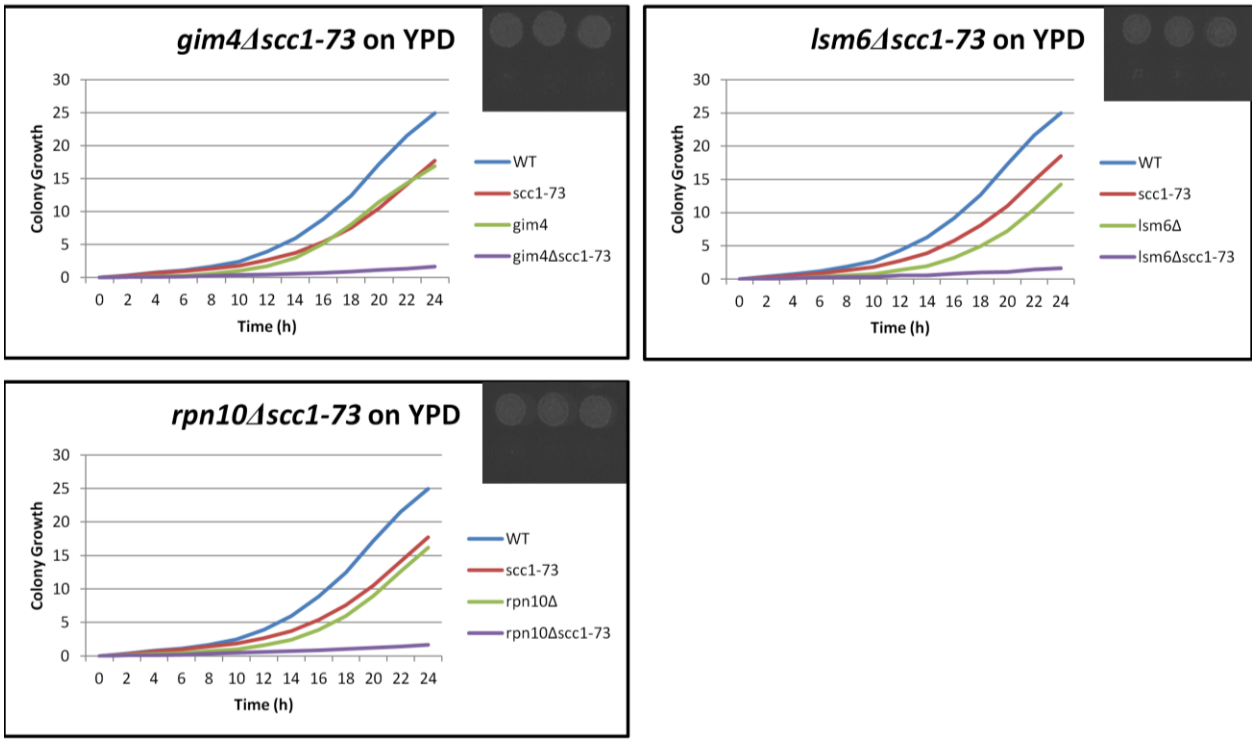

Figure 3-20. Growth curves of SL interaction.

The double mutants *gim4Δscc1-73*, *rpn10Δscc1-73*, *lsm6Δscc1-73*, without a DDA, respective to a WT strain and the two single mutants. Growth curves were generated after 24 hours. Images from scanned plates were taken after 24 hours, presenting the single mutant (top) and the double mutant (bottom).

A strong PS genetic interaction was observed between *scc1* and *swc5Δ* across four out of the five conditions. The predicted fitness was 0.35 (normalized to the WT strain on YPD), while the observed fitness of the double mutant was 0.88.

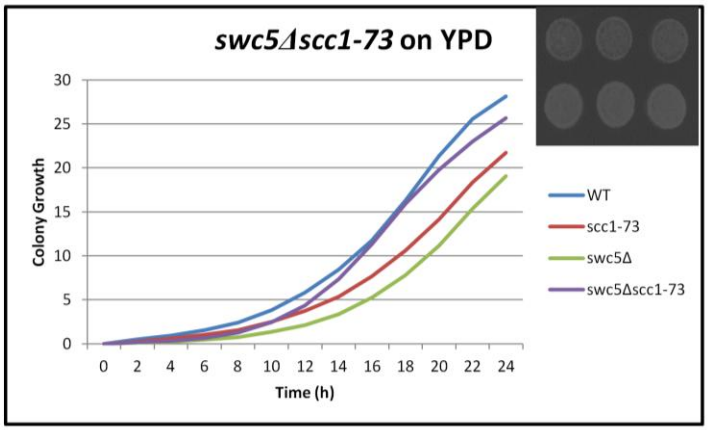

Figure 3-21. Growth curves of PS interaction.

The double mutants *swc5Δscc1-73* without a DDA, relative to a WT strain and the two single mutants. Growth curves were generated after 24 hours. The image from scanned plates was taken after 24 hours, and present in the upper right corner with the single mutant (top) and the double mutant (bottom).

Data obtained from the bleomycin experiments were highly variable. This was due, in part, to the high sensitivity of the query strain to bleomycin. Growth of single and double mutants was tested under different concentrations of bleomycin in order to find the optimum concentration to maximize the effect on double mutant strains without strongly affect the growth of the query, *scc1*. However, such optimal concentration was not found, suggesting that the concentration range of bleomycin for *scc1* was narrow.

Chapter 4: DISCUSSION

4.1 Summary of findings

4.1.1 Overview

Aim #1- Identifying synthetic cytotoxic interactions with cohesin

The aim of my thesis was to identify genetic interactions with cohesin mutations that result in synthetic cytotoxicity (SC) to DNA damaging agents (DDAs) . SC interactions with cohesin mutations could be used to leverage the high frequency of cohesin mutations in cancer to improve the efficacy, safety and selectivity of current anti-cancer treatments. Four DDAs, representing common classes of traditional anti-cancer cytotoxic agents, were used to discover new DDA-associated genetic interactions, thereby expanding on previous genetic screens for genetic interactions with cohesin mutations[76,81]. To achieve this aim, I performed high-throughput SGA screens, using three different cohesin mutations as query genes with a curated array of 310 DNA-associated mutations, in the presence and absence of four distinctive DDAs (five conditions overall).

Determining interactions + SGA limitations

In order to determine initial SGA interactions, an e-c/c score threshold was chosen that identified hundreds of genetic interactions, both negative (i.e. SL, SC) and positive (i.e. PS), with the cohesin-mutated queries (carrying ts-mutations in the core-subunits SMC1 and SCC1, and in the loader SCC2). For each screen an average of 46 negative genetic interactions and 65 positive genetic interactions were obtained. As with any large-scale genetic screen, such as SGA, one must consider false positive and false negative results. Despite using a relatively small, recently confirmed yeast array (see MATERIALS AND M) that contains many functionally related genes

which would be expected to interact with the query, false positive and false negative results are inevitable. False results can be due to technical pinning errors (i.e. missing spots), the emergence of suppressor mutations, variation in media stocks and condition, and temperature fluctuations that can affect the phenotype of temperature sensitive query mutations.

We expected that overlapping the three preliminary data sets would enrich for robust biologically-meaningful interactions and potentially minimize the false positive rate. As predicted, a subset of genetic interactions, both negative and positive, was shared among the different cohesin mutations. A total of 124 negative interaction (NI) and 111 positive interaction (PI) mutated genes were found that were shared between at least two out of the three cohesin query mutations. These interactions spanned a number of biological processes in addition to DDR (which is enriched for in our array), including transcription, translation, protein modification, folding and degradation, cell cycle progression, chromatin modification and metabolism.

Cohesin mutations have been previously screened by SGA for genetic interactions in both large[81] and small scale[76] efforts. The interactions found in these studies can be used to compare against the results from the three SGA experiments I performed using the DDR-MA in the absence of DDA. A comparison between the large genetic interaction database[81] (known as The CellMap) using the three cohesin queries and my SGA results was made. By using the cutoff used in the database for determining hits (<-0.08, and using the e-c formula instead of e-c/c used in this study), and filtering for shared genetic interactions between at least 2 out of the 3 cohesin queries, I found 23 shared negative genetic interactions out of 41 genes that are on the DDR-MA, with CellMap hit genes (including 2 false positives). For example, *csm3Δscc1-73*, *mrc1Δscc1-73* , *chl1Δscc1-73* and *kar3Δscc1-73* were shared negative genetic interactions. Out of 32 PS genetic

interactions identified in my SGA screen data (in the absence of DDAs and shared between at least 2 out of the 3 queries), no shared interactions (that passed CellMap cutoff of >0.08) were found. This may be due to the fact that while NI tend to occur between genes with clear functional relationships, a feature represented in our selective small array, PI often map to more general pathways such as cellular proteostasis and cell cycle progression that might be underrepresented in the array[81]. In addition, PIs can also occur due to spontaneous suppressor mutations that correct the fitness defects of the strain carrying a deletion or hypomorphic mutant allele. It is also possible, that the combination of the two mutations in these identified interactions increases mutation rate and contributes to the appearance of new mutations that can improve the growth defect of the double mutant.

Aim #2- Development of ScanLag as a tool for validation of genetic interactions

The second goal of my thesis was to use and assess ScanLag as a technique to validate the genetic interactions identified in the large-scale SGA screen. After filtering out seven genetic interactions that are known to be false positives, initial genetic interaction network maps were created, in the absence and presence of the four distinctive DDAs, from which the interactions for validation were chosen. Given that many genetic interactions profoundly affect growth, double mutant selection must be rigorous to prevent the selection of heterozygous diploids. During the process of our early validation attempts, it was apparent that SGA strains need two haploid-selection rounds to avoid diploid double heterozygous mutants that escaped selection due to strong selection against haploid double-mutants with strong fitness defects.

The utility of ScanLag lies in its ability to combine the advantages of two well-known yeast techniques, quantitative growth curves and qualitative spot assays, which have been extensively used to validate the identified genetic interactions following an SGA screen.

ScanLag was originally designed by the Balaban lab to measure in parallel the delay in growth (Lag time) and growth rate (i.e. the speed at which the number of cells in the population increases) of bacteria cells[87,89]. Using an optical scanner to measure bacterial colony size over time, ScanLag software is able to identify and quantify different parameters, such as the time of appearance and growth time of each colony. I repurposed ScanLag to quantify the effect on the growth rate of yeast double mutants, compared to the parental single mutant strains, on a variety of conditions per single experiment, using a different bioinformatic analysis tool (i.e. ImageJ instead of MATLAB). Using solid agar plates containing the same conditions as in the SGA screen, ScanLag allows for a fast retesting process of many genetic interactions simultaneously. The major advantage of ScanLag over Tecan is its ability to retest ~6-fold more genetic interactions in one round of experiment, in the absence and presence of DDAs, and thus is suitable for retesting the hundreds of genetic interactions that can be identified in an SGA screen. This use of ScanLag for measuring yeast growth has not been published.

In order to validate genetic interactions, a growth differential threshold needed to be assigned. ScanLag uses different measurements for growth, therefore, it is important to understand how ScanLag growth curves correlate with SGA. In order to choose a threshold for ScanLag, observed - predicted (o-p) scores for the tested interactions were plotted and the distributions of the overall double mutant scores were compared to values determined by SGA. The distribution of scores in ScanLag were approximately half those observed for SGA. For example, on camptothecin (CPT), double-mutant e-c/c values range from -0.98 to 1.63 with SGA, while ScanLag values ranged from -0.47 to 0.8 using (Figure 4-1).

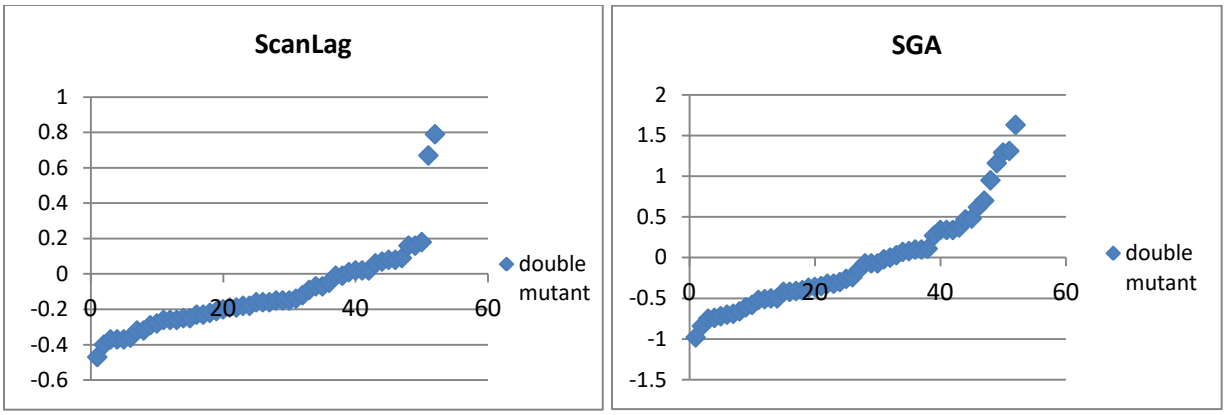

Figure 4-1. Distribution of double-mutant in ScanLag vs. SGA

Double-mutant scores distribution, ScanLag vs. SGA, under CPT. ScanLag scores are calculated using o-p formula, while e-c/c formula for SGA.

Selecting two different thresholds for the absence and presence of a DDA, was based on the observation that the chosen query strain, carrying the *scc1-73* allele, was sensitive to DDAs resulting in a lesser maximum growth value. Therefore, a different cutoff was needed in order to capture these interactions. Furthermore, it was found that some interactions required longer growth periods to maximize the differential between single mutants and double mutants. ScanLag experiments were analyzed after 24 hours in order to maximize the number of genetic interactions that could be tested in a given time period. However, it is possible to run a ScanLag experiment for longer time periods. However, if WT is used as the reference, analyzing at a time point less than 48 hours is ideal, as WT will reach saturation in less than 48 hours. Ideally, growth over longer periods would allow for a wider range over which to screen for growth differentials when using sensitive or slow-growing mutant strains. Due to the fact that the single *scc1-73* is a slow-growing and a DDA-sensitive strain, the growth window for identifying SC interactions is small within a 24 hours period. The small growth window could be expanded by lowering the DDA concentration, and/or extending growth periods, to increase the differential

between the double mutant and single mutants in the presence of the DDA. For some genetic interactions, it may be necessary to perform multiple ScanLag assays to identify ideal growth periods and DDA concentrations to determine if interactions are additive or SC. In some cases, it might be difficult to discern additive genetic interactions in the presence of a DDA from true SC interactions, due to the fact that *scc1-73* is sensitive to many DDAs and frequently exhibits SS interactions with many different array gene mutations even in the absence of DDA. However, even if the effect on the fitness of the double mutant is additive, it still might be of interest to pursue in human cancer cell lines as an additive cytotoxic interaction results in a greater cytotoxic effect than either single mutant with DDA or the double mutant without DDA.

Fifty-two double mutants were retested by ScanLag. Genetic interactions with bleomycin resulted in variable responses and were, therefore, removed from further analysis. By considering only interactions that passed the specific cutoff for the absence and presence of a DDA, 30 of 44 (not including bleomycin) genetic interactions recapitulated the genetic interaction (negative or positive) observed by SGA and were deemed validated (Table 4-3). These 44 expected genetic interactions included 24 SL interactions, 16 SC interactions and 4 PS interactions. Validated interactions that were recapitulated as predicted by SGA were, for example, *csm3Δscc1-73*, *doc1Δscc1-73* and *gim4Δscc1-73* as SL interactions. The strong SC interaction *rev3Δscc1-73* on MMS was also recapitulated. These results demonstrate that ScanLag is a viable approach for retesting genetic interactions following a large-scale genetic screen.

Some genetic interactions that were not recapitulated upon retesting with ScanLag, included five double mutants that were previously validated as SL genetic interactions[76], such as *ctf4Δscc1-7* and *bub3Δscc1-73*. Seven other double mutants initially identified to be SLs in my

SGA screen data, also failed to validate, with three of them being SCs (*phr1Δscc1-73*, *chd1Δscc1-73, hst3Δscc1-73*). In addition, two PS interactions, *spt4Δscc1-73* and *rnr4Δscc1-73*, also failed to validate using ScanLag and in the case of the latter double mutant, changed to a SL/SS across all conditions (Table 3-2). A possible explanation could be that the *rnr4Δscc1-73* double mutant exhibits a negative genetic interaction but gained a suppressor mutation in the course of the SGA, leading to its spread throughout the strain spot on the plate. Fifteen double mutants predicted to be SC on MMS, CPT and/or benomyl, showed 30 new genetic interactions by ScanLag which differed from the one seen by SGA, on these DDAs (Table 4-4). Out of 9 double mutants expected to be SC on only bleomycin, 6 demonstrated new genetic interactions on other conditions (Table 4-4). These new (not observed by SGA) genetic interactions include 2 new SCs on benomyl, 10 new SCs on CPT, 13 new SCs on MMS and 19 genetic interactions that were observed as SC by SGA but SL/SS by ScanLag.

SC interactions that were found to be SL/SS upon retesting with ScanLag, were probably SLs that were missed initially in the course of the SGA, suggesting that these SL genetic interactions were false negatives in the SGA screen. Since in the course of a ScanLag experiment, strains that originated from single colonies are tested, rather than from a mixed population as on the SGA plates, the effect of the interaction can be detected without being masked by colonies with suppressor mutations that could take over the spot. Examples that were predicted to be SCs and were found to have a strong genetic interaction in the absence of a DDA (SS) are *tel1Δscc1-73,* and *ubr1Δscc1-73,* which was a previously observed strong negative interaction [81]. Other double mutants that exhibited reduced fitness in the absence of DDA that was increased to lethality in the presence of DDAs (SC) were *rev3Δscc1-73* on MMS, *cdh1Δscc1-73* on CPT*, sit4Δscc1-73* and *sgo1Δscc1-73* on benomyl.

In the set of validated genetic interactions were some new and unexpected interactions. Cohesin interacts directly with SGO1 to retain SGO1 at the inner centromeres[90,91]. This interaction can suppress CIN by stabilizing kinetochore-microtubule attachment, and by protecting centromeric Scc1/Rad21 from prophase dissociation during M-phase. The validated SC interaction of *sgo1Δscc1-73* with benomyl is new but not unexpected, as mutations affecting spindle checkpoint genes such as *SGO1* might be expected to be sensitive to the spindle poison benomyl and to defective cohesin function. This is because both stabilized kinetochore-microtubule attachment and functioning cohesin complex are important in ensuring faithful chromosome tethering and separation during cell division[92]. Another new yet not unexpected SL interaction is *rpn10Δscc1-73*. The *RPN10* gene functions as a non-ATPase base subunit of the 26S proteasome in yeast[93–96]. It was found that proteasome activity is necessary to complete cell division in human cells, independent of cohesin cleavage[97], therefore, it is possible that a combination of both a deficient cohesin and a deficient proteasome activity results in cell death due to inability to complete cell division.

I also found that loss of the translesion synthesis (TLS) polymerases REV1 or REV3 in cohesin mutated strains resulted in SC genetic interactions with MMS. The DNA repair gene *REV1* is a deoxycytidyl transferase that is involved in TLS[98–101]. REV1 functions in an error-prone translesion pathway, recruiting the DNA polymerase zeta complex (that includes REV3 and REV7 as subunits) to sites of damaged DNA[102,103]. A null mutation in either *REV1* or *REV3* results in sensitivity to the alkylating agent MMS[104]. It has been suggested, that upon induced DNA damage by a DDA such as MMS during S phase, REV1 is needed to switch to TLS polymerase and bypass the damaged site. Since cohesin also functions in DNA repair via mediating homologous recombination (HR) between two sister chromatids to repair double-

strand breaks (DSBs), this might serve as an alternate model to bypass the DNA damage caused by MMS in the absence of the REV proteins. However, a combination of a null *REV1* or *REV3* and a compromised cohesin, might lead to cellular death in the presence of MMS due to unrepaired damage. This model can be further supported by the observations that HR is impaired in Drosophila lacking DNA polymerase zeta[105] and that REV1−/− vertebrate cells exhibit a decreased level of immunoglobulin gene conversion which is mediated by HR[106], suggesting participation of REV1 in the recombination-based pathway.

Positive interactions (i.e. PS), could confer an advantage to cohesin-mutated cells, and therefore, could be relevant to some cases of resistance to chemotherapeutic agents. The genetic interaction *swc5Δscc1-73,* for example, was recapitulated and validated as a positive genetic interaction in the course of this study. The null mutation in *SWC5* (*CFDP1* gene in humans), which affects histone exchange and chromatin remodeling, together with a cohesin mutation, resulted in a better than expected growth relative to either single mutant under all conditions except benomyl. The *SWC5* gene is a component of the SWR1 complex, which exchanges histone variant Htz1p (homolog of human *H2AZ*) for chromatin-bound histone H2A[98,107–110]. This dynamic exchange of histones can affect transcription, epigenetic silencing, DNA damage repair and chromosome segregation[111]. In the absence of SWC5, the complex is able to bind to the chromatin but the replacement of histones is abolished[111]. The PS may be due, in part, to a change in transcription profile that stimulates other pathways or proteins that overcome the cellular stress. Other subunits of the complex in yeast also include SWR1 and YAF9, which were both present on the DDR-MA and were PS hits based on the preliminary SGA data. The observed PS, which is observed in the presence of all four DDAs except benomyl, will need further studies in order to understand its mechanism.

In summary, the aim of this study was to identify SC interactions with a compromised cohesin complex, in the presence of DDAs that represent different chemotherapeutic classes. Strong candidates, both with negative and positive genetic interactions with a mutated cohesin, were identified and validated. Synthetic sick (SS) interactions were found to be highly prevalent in this study, as most of the gene deletion mutations on the DDR-MA, as well as the query mutation, *scc1*, cause CIN and/or sensitivity to DDAs, thus resulting in a narrow window for more accurate analysis with the condition used in this study. Further investigation will be required to determine if these interactions are due to general or specific synergistic defects and if they are conserved in human cell lines as well.

4.2 Significance of findings

In this work, I exploited the SGA method available in yeast, which enables rapid screening of thousands of possible double mutant combinations on one plate, to identify SL, SC and PS genetic interactions with a mutated cohesin complex. Previous studies had identified SL interactions with cohesin mutations. My work extended the range of genetic interactions with cohesin mutations by introducing DNA damaging agents, demonstrating the potential of exploiting SC to broaden the spectrum of potential anticancer drug targets. Given that the array used was curated to represent DDR and CIN genes that are highly conserved between yeast and human, the identified genetic interactions in this study can thereby translate into a potential therapeutic candidates for inhibition while exploiting existing traditional cytotoxic agents. In addition to identifying potential anticancer drug targets, the genetic interactions I found also have the potential to shed light on the biological mechanisms underlying the role of cohesin in cancer and genome stability.

ScanLag was found to be a useful method for validating genetic interactions identified in high throughput SGA screens. ScanLag was previously used to measure bacterial growth rate and lag time. My work demonstrates that it is a powerful tool for measuring yeast growth as well. This method is efficient and enabled the validation of many genetic interactions. ScanLag could be incorporated into SGA workflows to validate genetic interactions found in high-throughput screens.

4.3 Future directions

The interesting SC interactions, such as *rev3Δscc1-73* and *rev1Δscc1-73* with MMS, and the positive genetic interaction *swc5Δscc1-73*, can be characterized and tested with other mutated cohesin alleles to confirm a consistent effect on growth fitness. Understanding the biological mechanism behind these interactions could provide further valuable insights on the function of cohesin under different cellular stresses. While the smaller-scale mutant-array used in this study is a proof of principle, SGA can also be expanded to test whole genome. This will enable to broaden the number of potential interactions that can be identified, as well as to discover novel genetic interactions that otherwise might not have been expected to interact with a compromised cohesin. Similarly, other DDAs could be used in additional cohesin SGA screens, such as antimetabolites, which represent another class of chemotherapeutic agents used in the clinic and induce DNA-damage by, for example, inhibiting one or more enzymes that are critical for DNA synthesis (such as needed for DNA repair)[112], and UV radiation, which introduces a specific type of damage and represents a highly common environmental factor. The genes identified as validated SC interaction partners with cohesin mutations can also be used as SGA queries themselves to determine if these genes are highly connected SL/SC hubs that might be relevant to other cancer associated mutations.

ScanLag can be further exploited as a follow-up method for SGA. However, determining an optimal time and condition for analysis to enable for better separation between growth curves will be needed when using query strains with strong fitness defects, as seen in this work with cohesin query mutations.

The query gene array was selected to represent important genes and processes that are conserved between yeast and human. The validated genetic interactions identified in this study can be tested for conservation in cohesin-mutated mammalian cell line studies to translate these findings into a pre-clinical human model system.

Bibliography

1. Kandoth, C. *et al.* Mutational landscape and significance across 12 major cancer types. *Nature* **502,** 333–339 (2013).
2. Hanahan, D. & Weinberg, R. A. Hallmarks of Cancer: The Next Generation. *Cell* **144,** 646–674 (2011).
3. Solomon, D. A., Kim, J.-S. & Waldman, T. Cohesin gene mutations in tumorigenesis: from discovery to clinical significance. *BMB Rep.* **47,** 299–310 (2014).
4. Hartwell, L. H., Szankasi, P., Roberts, C. J., Murray, A. W. & Friend, S. H. Integrating genetic approaches into the discovery of anticancer drugs. *Science* **278,** 1064–8 (1997).
5. Kaelin, W. G. The Concept of Synthetic Lethality in the Context of Anticancer Therapy. *Nat. Rev. Cancer* **5,** 689–698 (2005).
6. Li, X., O'Neil, N. J., Moshgabadi, N. & Hieter, P. Synthetic Cytotoxicity: Digenic Interactions with TEL1/ATM Mutations Reveal Sensitivity to Low Doses of Camptothecin. *Genetics* **197,** 611–623 (2014).
7. Botstein, D. & Fink, G. R. Yeast: an experimental organism for 21st Century biology. *Genetics* **189,** 695–704 (2011).
8. Heinicke, S. *et al.* The Princeton Protein Orthology Database (P-POD): A Comparative Genomics Analysis Tool for Biologists. *PLoS One* **2,** e766 (2007).
9. WHO | Cancer. *WHO* (2017).
10. Sjöblom, T. *et al.* The consensus coding sequences of human breast and colorectal cancers. *Science* **314,** 268–74 (2006).
11. Vogelstein, B. *et al.* Cancer genome landscapes. *Science* **339,** 1546–58 (2013).
12. Stratton, M. R., Campbell, P. J. & Futreal, P. A. The cancer genome. *Nature* **458,** 719–24

(2009).

13. Ponder, B. A. J. Cancer genetics. *Nature* **411,** 336–341 (2001).

14. Sudhakar, A. History of Cancer, Ancient and Modern Treatment Methods. *J. Cancer Sci. Ther.* **1,** 1–4 (2009).

15. Shewach, D. S. & Kuchta, R. D. Introduction to cancer chemotherapeutics. *Chem. Rev.* **109,** 2859–61 (2009).

16. Hyman, D. M. *et al.* Implementing Genome-Driven Oncology. *Cell* **168,** 584–599 (2017).

17. Baker, S. J. & Reddy, E. P. Targeted inhibition of kinases in cancer therapy. *Mt. Sinai J. Med.* **77,** 573–86 (2010).

18. Mellman, I., Coukos, G. & Dranoff, G. Cancer immunotherapy comes of age. *Nature* **480,** 480–489 (2011).

19. Dai, X. *et al.* Breast cancer intrinsic subtype classification, clinical use and future trends. *Am. J. Cancer Res.* **5,** 2929–43 (2015).

20. Di Cosimo, S. & Baselga, J. Management of breast cancer with targeted agents: importance of heterogenicity. *Nat. Rev. Clin. Oncol.* **7,** 139–147 (2010).

21. Wahba, H. A. & El-Hadaad, H. A. Current approaches in treatment of triple-negative breast cancer. *Cancer Biol. Med.* **12,** 106–16 (2015).

22. Zeichner, S. B., Stanislaw, C. & Meisel, J. L. Prevention and Screening in Hereditary Breast and Ovarian Cancer. *Oncology (Williston Park).* **30,** (2016).

23. Lord, C. J. & Ashworth, A. BRCAness revisited. *Nat. Rev. Cancer* **16,** 110–120 (2016).

24. Laskin, J. *et al.* Lessons learned from the application of whole-genome analysis to the treatment of patients with advanced cancers. *Cold Spring Harb. Mol. case Stud.* **1,** a000570 (2015).

25. Pagliarini, R., Shao, W. & Sellers, W. R. Oncogene addiction: pathways of therapeutic response, resistance, and road maps toward a cure. *EMBO Rep.* **16,** 280–296 (2015).

26. Druker, B. J. *et al.* Five-Year Follow-up of Patients Receiving Imatinib for Chronic Myeloid Leukemia. *N. Engl. J. Med.* **355,** 2408–2417 (2006).

27. Salesse, S. & Verfaillie, C. M. BCR/ABL: from molecular mechanisms of leukemia induction to treatment of chronic myelogenous leukemia. *Oncogene* **21,** 8547–8559 (2002).

28. Bower, H. *et al.* Life Expectancy of Patients With Chronic Myeloid Leukemia Approaches the Life Expectancy of the General Population. *J. Clin. Oncol.* **34,** 2851–7 (2016).

29. DOBZHANSKY, T. Genetics of natural populations; recombination and variability in populations of Drosophila pseudoobscura. *Genetics* **31,** 269–90 (1946).

30. Lucchesi, J. C. Synthetic lethality and semi-lethality among functionally related mutants of Drosophila melanfgaster. *Genetics* **59,** 37–44 (1968).

31. Kaiser, C. A. & Schekman, R. Distinct sets of SEC genes govern transport vesicle formation and fusion early in the secretory pathway. *Cell* **61,** 723–33 (1990).

32. Hennessy, K. M., Lee, A., Chen, E. & Botstein, D. A group of interacting yeast DNA replication genes. *Genes Dev.* **5,** 958–69 (1991).

33. Bender, A. & Pringle, J. R. Use of a screen for synthetic lethal and multicopy suppressee mutants to identify two new genes involved in morphogenesis in Saccharomyces cerevisiae. *Mol. Cell. Biol.* **11,** 1295–305 (1991).

34. Nagel, R., Semenova, E. A. & Berns, A. Drugging the addict: non-oncogene addiction as a target for cancer therapy. *EMBO Rep.* **17,** 1516–1531 (2016).

35. Helleday, T. The underlying mechanism for the PARP and BRCA synthetic lethality: Clearing up the misunderstandings. *Mol. Oncol.* **5,** 387–393 (2011).

36. Powell, S. N. & Kachnic, L. A. Roles of BRCA1 and BRCA2 in homologous recombination, DNA replication fidelity and the cellular response to ionizing radiation. *Oncogene* **22,** 5784–5791 (2003).

37. Bryant, H. E. *et al.* Specific killing of BRCA2-deficient tumours with inhibitors of poly(ADP-ribose) polymerase. *Nature* **434,** 913–917 (2005).

38. Farmer, H. *et al.* Targeting the DNA repair defect in BRCA mutant cells as a therapeutic strategy. *Nature* **434,** 917–921 (2005).

39. Audeh, M. W. *et al.* Oral poly(ADP-ribose) polymerase inhibitor olaparib in patients with BRCA1 or BRCA2 mutations and recurrent ovarian cancer: a proof-of-concept trial. *Lancet* **376,** 245–251 (2010).

40. Tutt, A. *et al.* Oral poly(ADP-ribose) polymerase inhibitor olaparib in patients with BRCA1 or BRCA2 mutations and advanced breast cancer: a proof-of-concept trial. *Lancet* **376,** 235–244 (2010).

41. Guénolé, A. *et al.* Dissection of DNA Damage Responses Using Multiconditional Genetic Interaction Maps. *Mol. Cell* **49,** 346–358 (2013).

42. Bandyopadhyay, S. *et al.* Rewiring of Genetic Networks in Response to DNA Damage. *Science (80-.).* **330,** 1385–1389 (2010).

43. Bailey, M. L. *et al.* Glioblastoma Cells Containing Mutations in the Cohesin Component STAG2 Are Sensitive to PARP Inhibition. *Mol. Cancer Ther.* **13,** 724–732 (2014).

44. Losada, A. Cohesin in cancer: chromosome segregation and beyond. *Nat. Rev. Cancer* **14,** 389–393 (2014).

45. Wood, A. J., Severson, A. F. & Meyer, B. J. Condensin and cohesin complexity: the expanding repertoire of functions. *Nat. Rev. Genet.* **11,** 391–404 (2010).

46. Nasmyth, K. & Haering, C. H. Cohesin: Its Roles and Mechanisms. *Annu. Rev. Genet.* **43,** 525–558 (2009).

47. Brooker, A. S. & Berkowitz, K. M. The roles of cohesins in mitosis, meiosis, and human health and disease. *Methods Mol. Biol.* **1170,** 229–66 (2014).

48. Kon, A. *et al.* Recurrent mutations in multiple components of the cohesin complex in myeloid neoplasms. *Nat. Genet.* **45,** 1232–1237 (2013).

49. Sun, Q.-Y. *et al.* Ordering of mutations in acute myeloid leukemia with partial tandem duplication of MLL (MLL-PTD). *Leukemia* **31,** 1–10 (2017).

50. Villanueva, M. T. Genetics: Acute myeloid leukaemia: driving the driver. *Nat. Rev. Cancer* **16,** 479–479 (2016).

51. Garg, M. *et al.* Profiling of somatic mutations in acute myeloid leukemia with FLT3-ITD at diagnosis and relapse. *Blood* **126,** 2491–2501 (2015).

52. Alexandrov, L. B. *et al.* Signatures of mutational processes in human cancer. *Nature* **500,** 415–421 (2013).

53. Taylor, C. F., Platt, F. M., Hurst, C. D., Thygesen, H. H. & Knowles, M. A. Frequent inactivating mutations of STAG2 in bladder cancer are associated with low tumour grade and stage and inversely related to chromosomal copy number changes. *Hum. Mol. Genet.* **23,** 1964–1974 (2014).

54. Guo, G. *et al.* Whole-genome and whole-exome sequencing of bladder cancer identifies frequent alterations in genes involved in sister chromatid cohesion and segregation. *Nat. Genet.* **45,** 1459–1463 (2013).

55. Balbás-Martínez, C. *et al.* Recurrent inactivation of STAG2 in bladder cancer is not associated with aneuploidy. *Nat. Genet.* **45,** 1464–1469 (2013).

56. Liu, J. & Krantz, I. Cornelia de Lange syndrome, cohesin, and beyond. *Clin. Genet.* **76,** 303–314 (2009).

57. Skibbens, R. V. *et al.* Cohesinopathies of a Feather Flock Together. *PLoS Genet.* **9,** e1004036 (2013).

58. Remeseiro, S., Cuadrado, A. & Losada, A. Cohesin in development and disease. *Development* **140,** (2013).

59. Le Quesne Stabej, P. *et al.* STAG3 truncating variant as the cause of primary ovarian insufficiency. *Eur. J. Hum. Genet.* **24,** 135–138 (2016).

60. Caburet, S. *et al.* Mutant Cohesin in Premature Ovarian Failure. *N. Engl. J. Med.* **370,** 943–949 (2014).

61. Zakari, M., Yuen, K. & Gerton, J. L. Etiology and pathogenesis of the cohesinopathies. *Wiley Interdiscip. Rev. Dev. Biol.* **4,** 489–504 (2015).

62. Schrier, S. A. *et al.* Causes of death and autopsy findings in a large study cohort of individuals with Cornelia de Lange syndrome and review of the literature. *Am. J. Med. Genet. Part A* **155,** 3007–3024 (2011).

63. Maruiwa, M. *et al.* Cornelia de Lange syndrome associated with Wilms' tumour and infantile haemangioendothelioma of the liver: report of two autopsy cases. *Virchows Arch. A. Pathol. Anat. Histopathol.* **413,** 463–8 (1988).

64. Mulla, W., Zhu, J. & Li, R. Yeast: a simple model system to study complex phenomena of aneuploidy. *FEMS Microbiol. Rev.* **38,** 201–212 (2014).

65. Guaragnella, N. *et al.* The expanding role of yeast in cancer research and diagnosis:

insights into the function of the oncosuppressors p53 and BRCA1/2. *FEMS Yeast Res.* **14,** 2–16 (2014).

66. Pfau, S. J. & Amon, A. Chromosomal instability and aneuploidy in cancer: from yeast to man. *EMBO Rep.* **13,** 515–527 (2012).

67. Haber, J. E. Bisexual mating behavior in a diploid of Saccharomyces cerevisiae: evidence for genetically controlled non-random chromosome loss during vegetative growth. *Genetics* **78,** 843–58 (1974).

68. Hartwell, L. H. & Smith, D. Altered fidelity of mitotic chromosome transmission in cell cycle mutants of S. cerevisiae. *Genetics* **110,** 381–95 (1985).

69. Spencer, F. *et al.* Chromosomal aneuploidy in Saccharomyces cerevisiae. *Prog. Clin. Biol. Res.* **318,** 293–306 (1989).

70. Yuen, K. W. Y. *et al.* Systematic genome instability screens in yeast and their potential relevance to cancer. *Proc. Natl. Acad. Sci.* **104,** 3925–3930 (2007).

71. Stirling, P. C. *et al.* The Complete Spectrum of Yeast Chromosome Instability Genes Identifies Candidate CIN Cancer Genes and Functional Roles for ASTRA Complex Components. *PLoS Genet.* **7,** e1002057 (2011).

72. Michaelis, C., Ciosk, R. & Nasmyth, K. Cohesins: chromosomal proteins that prevent premature separation of sister chromatids. *Cell* **91,** 35–45 (1997).

73. Guacci, V., Koshland, D. & Strunnikov, A. A direct link between sister chromatid cohesion and chromosome condensation revealed through the analysis of MCD1 in S. cerevisiae. *Cell* **91,** 47–57 (1997).

74. Barber, T. D. *et al.* Chromatid cohesion defects may underlie chromosome instability in human colorectal cancers. *Proc. Natl. Acad. Sci. U. S. A.* **105,** 3443–8 (2008).

75. Rajagopalan, H., Nowak, M. A., Vogelstein, B. & Lengauer, C. The significance of unstable chromosomes in colorectal cancer. *Nat. Rev. Cancer* **3,** 695–701 (2003).

76. McLellan, J. L. *et al.* Synthetic Lethality of Cohesins with PARPs and Replication Fork Mediators. *PLoS Genet.* **8,** e1002574 (2012).

77. Tong, A. H. Y. *et al.* Systematic Genetic Analysis with Ordered Arrays of Yeast Deletion Mutants. *Science (80-.).* **294,** 2364–2368 (2001).

78. Boone, C., Bussey, H. & Andrews, B. J. Exploring genetic interactions and networks with yeast. *Nat. Rev. Genet.* **8,** 437–449 (2007).

79. Tong, A. H. Y. & Boone, C. Synthetic genetic array analysis in Saccharomyces cerevisiae. *Methods Mol. Biol.* **313,** 171–92 (2006).

80. Costanzo, M. *et al.* The Genetic Landscape of a Cell. *Science (80-.).* **327,** 425–431 (2010).

81. Costanzo, M. *et al.* A global genetic interaction network maps a wiring diagram of cellular function. *Science (80-.).* **353,** aaf1420-aaf1420 (2016).

82. Baker Brachmann, C. *et al.* Designer deletion strains derived fromSaccharomyces cerevisiae S288C: A useful set of strains and plasmids for PCR-mediated gene disruption and other applications. *Yeast* **14,** 115–132 (1998).

83. Ben-Aroya, S. *et al.* Toward a Comprehensive Temperature-Sensitive Mutant Repository of the Essential Genes of Saccharomyces cerevisiae. *Mol. Cell* **30,** 248–258 (2008).

84. Giaever, G. *et al.* Functional profiling of the Saccharomyces cerevisiae genome. *Nature* **418,** 387–391 (2002).

85. Pan, X. *et al.* A Robust Toolkit for Functional Profiling of the Yeast Genome. *Mol. Cell* **16,** 487–496 (2004).

86. Young, B. P. & Loewen, C. J. Balony: a software package for analysis of data generated by synthetic genetic array experiments. *BMC Bioinformatics* **14,** 354 (2013).

87. Levin-Reisman, I. *et al.* Automated imaging with ScanLag reveals previously undetectable bacterial growth phenotypes. *Nat. Methods* **7,** 737–739 (2010).

88. Schneider, C. A., Rasband, W. S. & Eliceiri, K. W. NIH Image to ImageJ: 25 years of image analysis. *Nat. Methods* **9,** 671–675 (2012).

89. Levin-Reisman, I., Fridman, O. & Balaban, N. Q. ScanLag: High-throughput Quantification of Colony Growth and Lag Time. *J. Vis. Exp.* e51456–e51456 (2014). doi:10.3791/51456

90. Yamagishi, Y., Sakuno, T., Shimura, M. & Watanabe, Y. Heterochromatin links to centromeric protection by recruiting shugoshin. *Nature* **455,** 251–255 (2008).

91. Liu, H., Jia, L. & Yu, H. Phospho-H2A and Cohesin Specify Distinct Tension-Regulated Sgo1 Pools at Kinetochores and Inner Centromeres. *Curr. Biol.* **23,** 1927–1933 (2013).

92. Tanno, Y. *et al.* The inner centromere-shugoshin network prevents chromosomal instability. *Science (80-.).* **349,** 1237–1240 (2015).

93. Finley, D. *et al.* Unified nomenclature for subunits of the Saccharomyces cerevisiae proteasome regulatory particle. *Trends Biochem. Sci.* **23,** 244–5 (1998).

94. Deveraux, Q., Ustrell, V., Pickart, C. & Rechsteiner, M. A 26 S protease subunit that binds ubiquitin conjugates. *J. Biol. Chem.* **269,** 7059–61 (1994).

95. Glickman, M. H. *et al.* A subcomplex of the proteasome regulatory particle required for ubiquitin-conjugate degradation and related to the COP9-signalosome and eIF3. *Cell* **94,** 615–23 (1998).

96. Elsasser, S. *et al.* Proteasome subunit Rpn1 binds ubiquitin-like protein domains. *Nat. Cell*

Biol. **4,** 725–730 (2002).

97. Gimenez-Abian, J. F., Díaz-Martínez, L. A., Wirth, K. G., Torre, C. de la & Clarke, D. J. Proteasome Activity is Required for Centromere Separation Independently of Securin Degradation in Human Cells. *Cell Cycle* **4,** 1558–1560 (2005).

98. Tkach, J. M. *et al.* Dissecting DNA damage response pathways by analysing protein localization and abundance changes during DNA replication stress. *Nat. Cell Biol.* **14,** 966–976 (2012).

99. Haracska, L. *et al.* Roles of yeast DNA polymerases delta and zeta and of Rev1 in the bypass of abasic sites. *Genes Dev.* **15,** 945–954 (2001).

100. Nelson, J. R., Lawrence, C. W. & Hinkle, D. C. Deoxycytidyl transferase activity of yeast REV1 protein. *Nature* **382,** 729–731 (1996).

101. Larimer, F. W., Perry, J. R. & Hardigree, A. A. The REV1 gene of Saccharomyces cerevisiae: isolation, sequence, and functional analysis. *J. Bacteriol.* **171,** 230–7 (1989).

102. Murakumo, Y. *et al.* Interactions in the error-prone postreplication repair proteins hREV1, hREV3, and hREV7. *J. Biol. Chem.* **276,** 35644–51 (2001).

103. Ohashi, E. *et al.* Interaction of hREV1 with three human Y-family DNA polymerases. *Genes to Cells* **9,** 523–531 (2004).

104. Hanway, D. *et al.* Previously uncharacterized genes in the UV- and MMS-induced DNA damage response in yeast. *Proc. Natl. Acad. Sci.* **99,** 10605–10610 (2002).

105. Kane, D. P., Shusterman, M., Rong, Y., McVey, M. & Phillis, R. Competition between Replicative and Translesion Polymerases during Homologous Recombination Repair in Drosophila. *PLoS Genet.* **8,** e1002659 (2012).

106. Okada, T. *et al.* Multiple roles of vertebrate REV genes in DNA repair and recombination.

Mol. Cell. Biol. **25,** 6103–11 (2005).

107. Krogan, N. J. *et al.* A Snf2 family ATPase complex required for recruitment of the histone H2A variant Htz1. *Mol. Cell* **12,** 1565–76 (2003).

108. Dastidar, R. *et al.* The nuclear localization of SWI/SNF proteins is subjected to oxygen regulation. *Cell Biosci.* **2,** 30 (2012).

109. Mizuguchi, G. *et al.* ATP-Driven Exchange of Histone H2AZ Variant Catalyzed by SWR1 Chromatin Remodeling Complex. *Science (80-.).* **303,** 343–348 (2004).

110. Huh, W.-K. *et al.* Global analysis of protein localization in budding yeast. *Nature* **425,** 686–691 (2003).

111. Morillo-Huesca, M., Clemente-Ruiz, M., Andújar, E. & Prado, F. The SWR1 Histone Replacement Complex Causes Genetic Instability and Genome-Wide Transcription Misregulation in the Absence of H2A.Z. *PLoS One* **5,** e12143 (2010).

112. Parker, W. B. Enzymology of purine and pyrimidine antimetabolites used in the treatment of cancer. *Chem. Rev.* **109,** 2880–93 (2009).

Appendices

Appendix A

A.1 List of yeast strains

ORF	GENE	Function	Human	pathway	fitness
YGR163W	GTR2	EGO and GSE complexes	RagB,RagC,RagD	activates transcription	decreased
YLR085C	ARP6	SWR1 complex	ARP6	ATP-dependent histone exchange	decreased
YML021C	UNG1	mtDNA	UNG,UNG2	BER	decreased
YOL115W	PAP2	TRAMP complex	TRF4-1,POLK	BER	increased
YAL015C	NTG1	DNA N-glycosylase, AP lyase	NTHL1	BER(mitochondria),SSR	increased
YER142C	MAG1	3-methyl-adenine DNA glycosylase	Aag	BER,DR	increased
YKL113C	RAD27	5' to 3' exonuclease, 5' flap endonuclease	Fen1	BER,NHEJ	decreased
YBL019W	APN2	AP lyase 2	HAP1	BER,SSR	normal
YKL114C	APN1	AP lyase 1	APEX1, APEX2	BER,SSR	decreased
YML060W	OGG1		OGG1	BER,SSR	increased
YOL043C	NTG2	DNA N-glycosylase, AP lyase	NTHL1	BER,SSR	increased
YOR258W	HNT3	DNA 5' AMP hydrolase	Aprataxin,PNKP	BER,SSR	decreased
YMR156C	TPP1		PNKP	BER,SSR,NHEJ	viable

ORF	GENE	Function	Human	pathway	fitness
YPR135W	CTF4		AND-1	BIR,sister chromatid cohesion	decreased
YGR270W	YTA7		ATAD2B	chromatin	viable
YKL117W	SBA1		PTGES3	chromatin	viable
YLR418C	CDC73		CDC73	chromatin	viable
YBL002W	HTB2	Histone H2B, H2A-H2B heterodimer	Histone	chromatin assemble	viable
YBL003C	HTA2	Histone H2A, H2A-H2B heterodimer	Histone	chromatin assemble	normal
YBR009C	HHF1	Histone H4, H3-H4 heterodimer	Histone	chromatin assemble	decreased
YBR010W	HHT1	Histone H3, H3-H4 heterodimer	H3.3	chromatin assemble	decreased
YBR195C	MSI1	CAF-1 complex	RbAp48,RbAp46	chromatin assemble	decreased
YDL070W	BDF2		Brd2,BAZ1B	chromatin assemble	decreased
YDR225W	HTA1	Histone H2A, H2A-H2B heterodimer	Histone	chromatin assemble	Decreased
YJR082C	EAF6	NuA4 HAT complex	FLJ11730	chromatin assemble	Decreased
YLR399C	BDF1		Brd2	chromatin assemble	Decreased
YML102W	CAC2	CAF-1 complex	Cac2	chromatin assemble	Decreased
YNL030W	HHF2	Histone H4, H3-H4 heterodimer	Histone	chromatin assemble	Decreased
YNL031C	HHT2	Histone H3, H3-H4 heterodimer	Histone	chromatin assemble	Decreased
YNL107W	YAF9	NuA4 HAT complex	AF9,ENL,GAS41	chromatin assemble	Decreased

ORF	GENE	Function	Human	pathway	fitness
YNL136W	EAF7	NuA4 HAT complex	MRGBP	chromatin assemble	Decreased
YOR191W	ULS1		TTF2	chromatin assemble	Decreased
YPR018W	RLF2	CAF-1 complex	p150,CHAF1A	chromatin assemble	Decreased
YPR023C	EAF3	NuA4 HAT complex	MORF4,MRG15/X	chromatin assemble	Decreased
YAL019W	FUN30		SMARCAD1	chromatin remodeling	Decreased
YDR334W	SWR1	SWR1 complex	SRCAP	chromatin remodeling	Decreased
YNL330C	RPD3	Histone deacetylase	hda2	chromatin remodeling	Viable
YOR304W	ISW2	ATP-dependent DNA translocase	SMARCA1	chromatin remodeling	Decreased
YBR245C	ISW1		SMARCA5	Chromatin remodelling	Viable
YBR289W	SNF5	SWI/SNF chromatin remodeling complex	Snf5(SMARCB1), BAF47/INI1	Chromatin remodelling	Decreased
YGR056W	RSC1	RSC chromatin remodeling complex	BAF180,PBRM1	Chromatin remodelling	Decreased
YJL065C	DLS1	ISW2/yCHRAC chromatin accessibility complex	CHRAC1	Chromatin remodelling	Viable
YJL176C	SWI3	SWI/SNF chromatin remodeling complex	SMARCC1	Chromatin remodelling	Decreased
YLR357W	RSC2	RSC chromatin remodeling complex	BAF180	Chromatin remodelling	Decreased
YNR023W	SNF12	RSC chromatin remodeling complex	SMARCD1	Chromatin remodelling	Viable
YNL068C	FKH2	Forkhead family transcription factor	FOXF2	chromatin silencing	Increased

ORF	GENE	Function	Human	pathway	fitness
YBL058W	SHP1		NSFL1C	chromosome segregation	Viable
YEL061C	CIN8		KIF11	chromosome segregation	Viable
YER016W	BIM1		MAPRE1	chromosome segregation	Viable
YER177W	BMH1		YWHAE	chromosome segregation	Viable
YGL003C	CDH1		FZR1	chromosome segregation	Viable
YGL240W	DOC1		ANAPC10	chromosome segregation	Viable
YML124C	TUB3		TUBA1A	chromosome segregation	Viable
YOR014W	RTS1		PPP2R5C	chromosome segregation	Viable
YGR285C	ZUO1		DNAJC2	cin	Viable
YHR064C	SSZ1		HSPA8	cin	Viable
YGL194C	HOS2	Set3 complex	HDAC11	Covalent modifications of histones	Decreased
YIL112W	HOS4	Set3 complex	ANKRD50	Covalent modifications of histones	Decreased
YNL021W	HDA1	class II histone deacetylase complex	HDAC5	Covalent modifications of histones	Decreased
YAL021C	CCR4		CNOT6	ddc	Viable
YAL040C	CLN3		CCNB1	DDC	Viable
YBL046W	PSY4	phosphatase PP4 complex	R2	DDC	Viable
YBR158W	AMN1		AMN1	ddc	Viable

ORF	GENE	Function	Human	pathway	fitness
YBR186W	PCH2	pachytene checkpoint	TRIP13	DDC	Increased
YBR274W	CHK1		Chk1	DDC	Increased
YCL029C	BIK1		KIF13B	ddc	Viable
YCL061C	MRC1		Claspin	DDC	Decreased
YCR008W	SAT4		CHEK1	ddc	Viable
YCR044C	PER1		PER1	DDC	Viable
YDL155W	CLB3	B-type cyclin	CCNA1	DDC	Viable
YDR364C	CDC40		CDC40	DDC	Viable
YDR379W	RGA2		C5orf4	DDC	Increased
YGL086W	MAD1	Mad1p-Mad2p complex	MAD1L1	DDC	Increased
YGR108W	CLB1	B-type cyclin	CCNA1	DDC	Decreased
YGR109C	CLB6	B-type cyclin	CCNA1	DDC	Viable
YGR188C	BUB1	spindle checkpoint	Bub1	DDC	Decreased
YGR252W	GCN5		KAT2A	DDC	Viable
YHR082C	KSP1		Chk2	DDC	Viable
YJL013C	MAD3	spindle checkpoint	BubR1	DDC	Decreased
YJL030W	MAD2	Mad1p-Mad2p complex	MAD2L1,MAD2L2	DDC	Decreased

ORF	GENE	Function	Human	pathway	fitness
YLR210W	CLB4	B-type cyclin	CCNA1	DDC	Viable
YMR036C	MIH1		CDC25B	DDC	Viable
YMR199W	CLN1	G1 cyclin	CCNB1	DDC	Viable
YNL201C	PSY2	phosphatase PP4 complex	R3	DDC	Viable
YOR026W	BUB3	spindle checkpoint	BUB3	DDC	Decreased
YOR073W	SGO1	spindle checkpoint	SGOL1	DDC	Decreased
YPL256C	CLN2		CCNB1	DDC	Viable
YPR119W	CLB2	B-type cyclin	CCNA1	DDC	Decreased
YLR288C	MEC3	Rad17p-Mec3p-Ddc1p	Hus1	DDC,BER	Decreased
YNL273W	TOF1	Tof1p-Mrc1p-Csm3p	Tof1,TIMELESS	DDC,DNA repair	Viable
YMR048W	CSM3	Replication fork associated factor	TIPIN	DDC,DNA replication	Decreased
YBL088C	TEL1		ATM	DDC,DSB	Decreased
YOR368W	RAD17	Rad17p-Mec3p-Ddc1p	Rad1	DDC,DSB,BER	Decreased
YPL194W	DDC1	Rad17p-Mec3p-Ddc1p	RAD9	DDC,HR,BER	Decreased
YDL101C	DUN1		Chk2	DDC,PRR	Decreased
YJR090C	GRR1	SCF ubiquitin-ligase complex	FBXL20	divalent cation transport	Decreased
YER169W	RPH1		JMJD2A	DNA damage-response	Decreased

ORF	GENE	Function	Human	pathway	fitness
YMR173W	DDR48		DSPP	DNA damage-response	Increased
YDL013W	SLX5	Slx5-Slx8 STUbL complex	RNF4,TTF2	DNA repair	Decreased
YDL116W	NUP84	Nup84 subcomplex	Nup107	DNA repair	Decreased
YDR263C	DIN7	homolog of the RAD2 and RAD27	EXO1	DNA repair	Normal
YER116C	SLX8	Slx5-Slx8 STUbL complex	RNF4	DNA repair	Decreased
YGL100W	SEH1	Nup84 subcomplex	SEH1	DNA repair	Viable
YGR129W	SYF2	nineteen complex	Prp19/CDC5	DNA repair	Decreased
YHR200W	RPN10		19S subunit S5a	DNA repair	Decreased
YIL153W	RRD1		PTPA	DNA repair	Decreased
YKL057C	NUP120	Nup84 subcomplex	Nup160	DNA repair	Decreased
YNL218W	MGS1		WHIP	DNA repair	Decreased
YOR386W	PHR1		CRY1/2	DNA repair	Increased
YPR052C	NHP6A		HMGB1,HMGB2	DNA repair	Viable
YPR101W	SNT309	nineteen complex	Prp19/CDC5	DNA repair	Decreased
YBR223C	TDP1		Tdp1	DNA repair,BER,SSR	Decreased
YOL006C	TOP1	Topoisomerase I	TOPI	DNA replication	Decreased
YOR080W	DIA2	SCF ubiquitin ligase complex	AC069113.1	DNA replication	Decreased

ORF	GENE	Function	Human	pathway	fitness
YHR031C	RRM3	5′-3′DNA helicase	PIF1	DNA replication,(HR)	Decreased
YML061C	PIF1	5′-3′DNA helicase	PIF1	DNA replication,mtDNA repair,(HR)	Decreased
YKL017C	HCS1	Hexameric DNA polymerase alpha-associated DNA helicase A	AQR,IGHMBP2	DNA synthesis	Increased
YJR043C	POL32	DNA polymerase δ	Cdc27,Polδ,POLD3	DNA synthesis,BER,NER,MMR,PRR	Decreased
YDR121W	DPB4	DNA polymerase ε/II	Polε,POLE	DNA synthesis,BER,SSR	Increased
YBR278W	DPB3	DNA polymerase ε/II	Polε,POLE	DNA synthesis,HR,BER,NER,MMR	Decreased
YDL200C	MGT1		MGMT	DR	Increased
YAR002W	NUP60	nuclear pore complex (NPC)	Nup153	DSB	Decreased
YDL047W	SIT4		PPP6C	DSB	Viable
YEL056W	HAT2	Hat1p-Hat2p HAT complex	RbAp48,RbAp46	DSB	Decreased
YFR040W	SAP155		PPP6R	DSB	Viable
YGL229C	SAP4		PPP6R	DSB	Viable
YHR154W	RTT107		MDC1	DSB	Decreased
YKR028W	SAP190		PPP6R	DSB	Viable
YKR056W	TRM2		TRMT2A	DSB	Increased
YMR127C	SAS2		KAT5	DSB	Viable

ORF	GENE	Function	Human	pathway	fitness
YPL001W	HAT1	Hat1p-Hat2p HAT complex	HAT1	DSB	Decreased
YLR320W	MMS22	Mms1-Mms22 complex	MMS22L	DSB,HR	Decreased
YBL067C	UBP13		USP1	DSR,FA	Viable
YER098W	UBP9		USP1	DSR,FA	Viable
YFR034C	PHO4		HES1,STRA13	DSR,FA	Viable
YOL087C	DUF1		WDR48	DSR,FA	Viable
YPL183W-A	RTC6		BRIP1	DSR,FA	Viable
YBR026C	ETR1		cin	Fatty acid biogenesis	Viable
YPL008W	CHL1		FANCJ,RTEL1	genome integrity,(HR)	Decreased
YOL012C	HTZ1		H2AFZ	Histone variant	Viable
YOR025W	HST3		cin	Histones and Chromatin	Viable
YBR073W	RDH54		RAD54B	HR	Decreased
YDR004W	RAD57	Rad55p-Rad57p heterodimer	Rad51B,Rad51C,Rad51D,XRCC 2,XRCC3	HR	Decreased
YDR076W	RAD55	Rad55p-Rad57p heterodimer	Rad51B,Rad51C,Rad51D,XRCC 2,XRCC3	HR	Decreased
YDR078C	SHU2	Shu1-Psy3-Shu2-Csm2	Xrcc2-Rad51D-Sws1	HR	Decreased

ORF	GENE	Function	Human	pathway	fitness
YER041W	YEN1	Holliday junction resolvase	GEN1	HR	Decreased
YGL175C	SAE2	Endonuclease	CtIP	HR	Decreased
YHL006C	SHU1	Shu1-Psy3-Shu2-Csm2	Xrcc2-Rad51D-Sws0	HR	Increased
YIL132C	CSM2	Shu1-Psy3-Shu2-Csm2	Xrcc2-Rad51D-Sws2	HR	Decreased
YIR002C	MPH1		FANCM	HR	Decreased
YJL047C	RTT101		Cul4	HR	Decreased
YLR376C	PSY3	Shu1-Psy3-Shu2-Csm2	Xrcc2-Rad51D-Sws1	HR	Increased
YOR144C	ELG1	alternative replication factor C complex	Rfc1	HR	Decreased
YPR164W	MMS1	Mms1-Mms22 complex	DDB1	HR	Decreased
YDL074C	BRE1		Bre1,RFWD3	HR,DDC	Decreased
YDR075W	PPH3	phosphatase PP4 complex	Ppp4c	HR,DDC	Increased
YBR228W	SLX1	Slx1-Slx4	SLX1A	HR,DSBR	Increased
YPL024W	RMI1	Sgs1-TopIII-Rmi1	BLAP75/Rmi1	HR,DSBR	Decreased
YMR190C	SGS1	Sgs1-TopIII-Rmi1,3'-5'DNA helicase	RecQL,RecQ4,RecQ5,BLM,WRN,RTS	HR,DSBR,BER,SSR	Decreased
YML032C	RAD52		Rad52,Rad52B	HR,DSBR,SDSA,SSA,BIR,PRR	Decreased
YOR033C	EXO1	5'-3' exonuclease and flap-endonuclease	Exo1,Hex1	HR,MMR	Increased

ORF	GENE	Function	Human	pathway	fitness
YDR369C	XRS2	MRX complex	NBS1	HR,NHEJ	Decreased
YMR137C	PSO2		Artemis,DCLRE1C	HR,NHEJ	Decreased
YMR224C	MRE11	MRX complex	Mre11	HR,NHEJ	Decreased
YNL250W	RAD50	MRX complex	Rad50	HR,NHEJ	Decreased
YER095W	RAD51		Rad51B,Rad51C,Rad51D,XRCC 2,XRCC3	HR,SDSA	Decreased
YJL092W	SRS2	3'-5'DNA helicase	Fbh1	HR,SDSA	Decreased
YGL163C	RAD54		RAD54	HR,SDSA,NHEJ	Decreased
YBR098W	MMS4	Mms4p-Mus81p endonuclease	Eme1,Eme2	meiotic HR	Decreased
YDR386W	MUS81	Mms4p-Mus81p endonuclease	Mus81	meiotic HR	Decreased
YER179W	DMC1	recombinase	Dmc1	meiotic HR	Decreased
YGL033W	HOP2		Hop2,GT198	meiotic HR	Viable
YGL251C	HFM1	3'-5'DNA helicase	HFM1	meiotic HR	Decreased
YHL022C	SPO11		SPO11	meiotic HR	Decreased
YHR086W	NAM8		PABP-1	meiotic HR	Decreased
YOR351C	MEK1		Chk2	meiotic HR	Normal
YHR120W	MSH1		MSH1	mitochondrial repair, MMR	Decreased

ORF	GENE	Function	Human	pathway	fitness
YBR272C	HSM3		19S subunit S5b	MMR	Decreased
YCR092C	MSH3	Msh2p-Msh3p heterodimer	MSH3	MMR	Decreased
YDL154W	MSH5	Msh4p-Msh5p heterodimer	MSH5	MMR	Decreased
YDR097C	MSH6	Msh2p-Msh6p heterodimer	MSH6,GTBP	MMR	Decreased
YFL003C	MSH4	Msh4p-Msh5p heterodimer	MSH4	MMR	Normal
YLR035C	MLH2		PMS1	MMR	Increased
YOL090W	MSH2	Msh2p-Msh6p heterodimer, Msh2p-Msh3p heterodimer	MSH2	MMR	Decreased
YMR167W	MLH1	Pms1p-Mlh1p dimer	MLH1	MMR,meiotic HR	Decreased
YNL082W	PMS1	Pms1p-Mlh1p dimer	PMS2	MMR,meiotic HR	Decreased
YPL164C	MLH3	Mlh1–Mlh3 complex	MLH1	MMR,meiotic HR	Increased
YER070W	RNR1		RRM1	Modulation of nucleotide pools	Viable
YGR180C	RNR4		RRM2	Modulation of nucleotide pools	Viable
YIL066C	RNR3		RRM1	Modulation of nucleotide pools	Viable
YLR270W	DCS1	hydrolase	DcpS	mRNA decapping	Decreased
YGL173C	KEM1	5'-3' exonuclease	XRN1	mRNA decay	Decreased
YDR378C	LSM6		cin	mRNA decay (LSM)	Viable

ORF	GENE	Function	Human	pathway	fitness
YDR030C	RAD28		CSA,CKN1,ERCC8	NER	Normal
YDR079C-A	TFB5		GTF2H5	NER	Decreased
YDR314C	RAD34		XPC	NER	Decreased
YEL037C	RAD23	NEF2	HR23a,HR23b	NER	Increased
YER162C	RAD4	NEF2	XPC	NER	Decreased
YGL070C	RPB9	RNA polymerase II	POLR3	NER	Viable
YGR003W	CUL3	Ubiquitin-protein ligase	CUL3	NER	Viable
YGR258C	RAD2		XPG,ERCC5	NER	Viable
YHL025W	SNF6	SWI/SNF chromatin remodeling complex	SWI/SNF	NER	Decreased
YIL128W	MET18		MMS19	NER	Decreased
YML011C	RAD33	Rad4-Rad23 complex	HR23B	NER	Decreased
YMR201C	RAD14	NEF1(Rad1p-Rad10p-Rad14p)	XPA	NER	Increased
YNL230C	ELA1		elongin C,TCEB2	NER	Viable
YPL046C	ELC1		elongin A,TCEB3	NER	Increased
YPL096W	PNG1	PNGASE-HR23 complex	PNG	NER	Increased
YER173W	RAD24	Rad24-RFC, Rad17p-Mec3p-Ddc1p	Rad17,RS1	NER,DDC	Increased
YDR217C	RAD9		53BP1	NER,DDC,(NHEJ)	Decreased

ORF	GENE	Function	Human	pathway	fitness
YPL022W	RAD1	NEF1(Rad1p-Rad10p-Rad14p)	XPF,ERCC4	NER,DSB,HR,ICLR,SSA	Decreased
YDL042C	SIR2	NAD+-dependent deacetylase	SIRT1,SIR2L1,Sir2α	NHEJ	Viable
YGL090W	LIF1		XRCC4	NHEJ	Increased
YJR066W	TOR1		PRKDC	NHEJ	Viable
YKL213C	DOA1		PLAA	NHEJ	Decreased
YLL002W	RTT109	Rtt109/Vps75 complex	p300	NHEJ	Decreased
YLR265C	NEJ1		XLF/Cernunnos	NHEJ	Increased
YMR106C	YKU80	telomeric Ku complex (Yku70p-Yku80p)	Ku80	NHEJ	Increased
YNL116W	DMA2	E3	RNF8	NHEJ	Viable
YNL246W	VPS75	Rtt109/Vps75 complex	SET	NHEJ	Decreased
YNL307C	MCK1		GSK3A/B	NHEJ	Decreased
YOL004W	SIN3	Sin3p-Rpd3p histone deacetylase complex	SIN3b	NHEJ	Decreased
YOR005C	DNL4	DNA ligase IV	Lig4	NHEJ	Decreased
YCR014C	POL4	DNA polymerase IV	POLL,POLB,Polλ	NHEJ,BER,SSR	Decreased
YMR284W	YKU70	telomeric Ku complex (Yku70p-Yku80p)	Ku70	NHEJ,telomere functions	Decreased
YNL299W	TRF5	TRAMP complex	PAPD5,POLK	nuclear RNA degradation	Decreased
YJR074W	MOG1		cin	Nucleocytoplasmic transport	Viable

ORF	GENE	Function	Human	pathway	fitness
YML028W	TSA1		cin	Oxidative Stress	Viable
YMR186W	HSC82		HSP90	pheromone signaling	Decreased
YPL240C	HSP82		HSP90	pheromone signaling	Decreased
YKR092C	SRP40		NHN1	preribosome assembly or transport	Decreased
YGR184C	UBR1		cin	Proteasome	Viable
YLR306W	UBC12		UBE2F	protein degradation	Decreased
YDL230W	PTP1		PTPn9	protein dephosphorylation	Decreased
YCR066W	RAD18	E2,RAD6-RAD18 heterodimer	Rad18	PRR	Decreased
YDR092W	UBC13	Mms2-Ubc13 ubiquitin	UBE2N,UBE2T	PRR	Increased
YGL087C	MMS2	Mms2-Ubc13 ubiquitin	MMS2,CROC1	PRR	Decreased
YGL094C	PAN2	Pan2p-Pan3p poly(A)-ribonuclease complex	PAN2	PRR	Increased
YKL025C	PAN3	Pan2p-Pan3p poly(A)-ribonuclease complex	PAN3	PRR	Increased
YDR419W	RAD30	DNA polymerase ζ	POLH,Rad30	PRR,BER,SSR	Decreased
YLR032W	RAD5		HLTF,SHPRH	PRR,DSB	Decreased
YIL139C	REV7	DNA polymerase ζ	REV7/MAD2B	PRR,DSB,ICL	Increased

ORF	GENE	Function	Human	pathway	fitness
YOR346W	REV1	DNA polymerase ζ	Rev1	PRR,DSB,ICL,BER,SSR	Decreased
YPL167C	REV3	DNA polymerase ζ	REV3L,Polζ,POLD1	PRR,DSB,ICL,BER,SSR	Increased
YGL058W	RAD6	E2,RAD6-RAD18 heterodimer	HHR6A,HHR6B	PRR,HR	Decreased
YIR019C	MUC1		NOLC1	pseudohyphal formation	Increased
YER164W	CHD1	SAGA and SLIK complexes	CHD8	regulate transcription	Decreased
YGR063C	SPT4		SPT4	regulate transcription	Decreased
YCR065W	HCM1	Forkhead transcription factor	FOXB1	regulates the late S-phase specific expression of genes	Decreased
YNL138W	SRV2	adenylyl cyclase complex	CAP1	regulation of actin	Decreased
YBR189W	RPS9B		cin	Ribosomal core component	Viable
YDL082W	RPL13A		cin	Ribosomal core component	Viable
YHR066W	SSF1		cin	Ribosome Biogenesis	Viable
YKR024C	DBP7		cin	Ribosome Biogenesis	Viable
YFR031C-A	RPL2A	large (60S) ribosomal subunit	RPL8	Ribosomes	Decreased
YIL018W	RPL2B	large (60S) ribosomal subunit	RPL8	Ribosomes	Decreased
YDR289C	RTT103		RPRD1B	RNA processing	Viable
YOL072W	THP1		PCID2	RNA processing	Viable

ORF	GENE	Function	Human	pathway	fitness
YMR216C	SKY1	SR protein kinase (SRPK)	CLK3	RNA metabolism	Decreased
YJL006C	CTK2		cin	RNA polymerase and TFIIs	Viable
YJR063W	RPA12		cin	RNA polymerase and TFIIs	Viable
YKL139W	CTK1		CDK11B	RNA processing	Decreased
YLR107W	REX3	RNA exonuclease	REXO1	RNA processing	Normal
YDR363W-A	SEM1	subunit of 26S proteasome	DSS1	RNA processing,(HR)	Viable
YGL066W	SGF73		cin	SAGA complex	Viable
YLR240W	VPS34		PIK3C2A	signal transduction	Viable
YCL016C	DCC1	Ctf18p complex	DSCC1	sister chromatid cohesion	Decreased
YHR191C	CTF8	Ctf18p complex	CTF8	sister chromatid cohesion	Decreased
YPR141C	KAR3		cin	Spindle	Viable
YOR308C	SNU66		cin	Spliceosome	Viable
YDR523C	SPS1	Putative protein serine/threonine kinase	TAO1	spore wall synthesis	Decreased
YLR135W	SLX4	5'flap endonuclease	BTBD12	SSA	Decreased
YFR014C	CMK1	Calmodulin-dependent protein kinase	CAMK1	stress response	Increased
YKL190W	CNB1	calcineurin	CIB1/2	stress response	Decreased

ORF	GENE	Function	Human	pathway	fitness
YDR363W	ESC2		NIP45,SUMO1	SUMO	Decreased
YLR394W	CST9	SUMO E3 ligase	RNF212	synaptonemal complex formation	Decreased
YIL009C-A	EST3	TERT	TERT	Telomere maintenance	Viable
YLR233C	EST1	TERT	TERT	Telomere maintenance	Viable
YLR318W	EST2	TERT	TERT	Telomere maintenance	Viable
YNL025C	SSN8	RNA polymerase II holoenzyme	CCNK	telomere maintenance	Decreased
YOL068C	HST1	Sum1p/Rfm1p/Hst1p complex	SIRT4	telomere maintenance	Decreased
YPL129W	TAF14		cin	TFIID	Viable
YPL181W	CTI6		MLL5	transcriptional activation	Increased
YPL042C	SSN3	RNA polymerase II holoenzyme	CDK8	transcriptional control	Decreased
YGL115W	SNF4	AMP-activated Snf1p kinase complex	PRKAG2	Transcriptional regulation	Decreased
YGR171C	MSM1		cin	Translation	Viable
YJR047C	ANB1		cin	Translation	Viable
YNL252C	MRPL17		cin	Translation	Viable
YGR271W	SLH1	Putative RNA helicase	POLH,ASCC3,HELQ	translation regulation,BER,SSR	Decreased
YGL211W	NCS6		CTU1	tRNA binding	Decreased
YEL003W	GIM4		cin	Tubulin folding	Viable

ORF	GENE	Function	Human	pathway	fitness
YPL241C	CIN2		cin	Tubulin folding	Viable
YDL216C	RRI1	COP9 signalosome (CSN) complex	COPS5	Ubiquitin response	Viable
YBR034C	HMT1		PRMT6	unknown	Viable
YBR231C	SWC5	SWR1 complex	CFDP1	unknown	Decreased
YDR176W	NGG1		TADA3	unknown	Viable
YER045C	ACA1		ATF2	unknown	Viable
YER051W	JHD1		FBXL10	unknown	Decreased
YER176W	ECM32		UPF1	unknown	Viable
YGL043W	DST1		TCEA1	unknown	Viable
YJL101C	GSH1		GCLC	unknown	Viable
YJL115W	ASF1		ASF1A	unknown	Viable
YJR104C	SOD1		SOD1	unknown	Viable
YLL019C	KNS1		CLK2	unknown	Decreased
YLR176C	RFX1		RFX	unknown	Viable
YLR247C	IRC20		SHPRH	unknown	Viable
YMR080C	NAM7		UPF1	unknown	Viable
YNR052C	POP2		CNOT7	unknown	Viable

ORF	GENE	Function	Human	pathway	fitness
YOR156C	NFI1		PIAS1	unknown	Viable

Table 4-1. List of array yeast strains and human homologous.

A.2 List of initial hit strains and frequency of significance.

ND			MMS			CPT			Bleomycin			Benomyl		
Gene	Number of shared screens	Significance frequency	Gene	Number of shared screens	Significance frequency	Gene	Number of shared screens	Significance frequency	Gene	Number of shared screens	Significance frequency	Gene	Number of shared screens	Significance frequency
ASF1	2	*	APN1	3	**	ASF1	2	***	ASF1	3		BIK1	2	*
BIM1	2	*	BUB1	2	*	BIM1	2		BIM1	2	***	BIM1	3	**
BUB1	2	**	BUB3	2	*	BUB3	2		BUB1	2		CDH1	3	
BUB3	2	*	CIN2	2		CHD1	3	*	BUB3	2	*	CIN8	3	**
CHD1	2	**	CIN8	3		CIN8	2	**	CDC40	2	*	CLB2	3	
CHL1	2	*	CLB2	2	***	CLB2	3	*	CHL1	2	*	CTF4	2	
CIN2	2	***	DOA1	2	*	DDC1	2	*	CIN2	2	*	CTK1	3	**
CIN8	3	***	DOC1	2		DOA1	3	*	CIN8	3		DBP7	3	
CLB2	2	***	GIM4	2		EXO1	3	***	CLB2	3		DOA1	2	
CSM3	2	**	HST3	2		FKH2	2	*	CLN3	2	*	DOC1	3	**
CTF4	2	**	KAR3	3	*	FUN30	2		CMK1	2	*	HOS2	2	*
CTK1	2	**	MCK1	2	*	GIM4	2		CSM3	2		HTZ1	3	*
DOC1	2	**	MMS22	2		HOS2	2	**	CST9	2	*	KAR3	3	*
GIM4	3	***	PAN3	2	*	HST1	2	**	CTF4	2	*	KEM1	2	**
HST3	2	**	PHR1	2		HST3	2	*	CTF8	2	**	MAD2	2	
HTZ1	2	***	RAD61	2	*	HTZ1	2	***	CTI6	2		MRC1	3	
KAR3	3	**	RAD9	2		KAR3	2	*	CTK1	3	**	PHR1	2	***
LSM6	2	*	RDH54	2	*	MAD3	2		DBP7	2		RAD61	3	
MMS1	2	**	REV1	3		MCK1	3		DCS1	2	*	RPB9	2	
MRC1	2	**	REV3	3	*	MEC3	2	**	DDC1	2		RPN10	3	
PHR1	2		RPB9	2	*	MIH1	2	**	DOA1	3		RTS1	2	*
RAD61	3	**	RTT107	2	**	MMS1	2	**	DOC1	3	*	SAP155	3	
RPL2B	2		SAP155	2	*	MMS22	2		DST1	2	*	SGO1	3	*
SAP155	2	***	SHP1	2		MMS4	2		DUN1	2	*	SHP1	2	*
SHP1	2	**	SRS2	3		MRC1	2	*	ELC1	2	***	SIT4	3	*
SRS2	2	***	SSN8	2	*	MSI1	2	**	ELG1	2	*	SRV2	2	*
SSN8	2		TEL1	3	*	PER1	2		ESC2	2	**	SWR1	2	
TOF1	3	**	TOF1	2		RAD17	3	*	ETR1	2		TOF1	3	
			TSA1	2	*	RAD24	3		FKH2	3		UBR1	2	*
			UBR1	2	***	RAD55	2		FUN30	2		YTA7	2	***
						RAD9	3	***	GIM4	3	*			
						RDH54	2	*	GRR1	2	*			
						RPD3	2		GSH1	2				
						RTS1	2		HOS2	2				
						RTT107	2	*	HST3	3	**			
						SAE2	2		HTZ1	2	*			
						SAP155	2	***	KAR3	3				
						SGF73	2	*	KEM1	2	*			
						SHP1	2	**	MAD1	2				
						SHU1	2	***	MAD2	2	*			
						SIN3	2	*	MCK1	3	*			
						SKY1	2		MEC3	2				
						SOD1	2	**	MMS1	3				
						SRS2	3	*	MMS2	2	*			
						SSZ1	3	**	MSH4	2	**			
						TDP1	2		MSI1	2	*			
						TEL1	3		MUS81	2	**			
						TOF1	2		NAM7	2				
						UBC12	2	*	NCS6	2	*			
						UBR1	2	*	NUP84	2				

ND			MMS			CPT			Bleomycin			Benomyl		
Gene	Number of shared screens	Significance frequency	Gene	Number of shared screens	Significance frequency	Gene	Number of shared screens	Significance frequency	Gene	Number of shared screens	Significance frequency	Gene	Number of shared screens	Significance frequency
									PER1	3				
									PHR1	2	*			
									POL32	2	*			
									PPH3	2				
									PSO2	2				
									PSY2	3				
									PSY3	2	**			
									RAD17	2				
									RAD18	2				
									RAD24	2	**			
									RAD5	3	**			
									RAD51	2				
									RAD54	2				
									RAD55	3	**			
									RAD57	2	*			
									RAD61	2	*			
									RAD9	2	*			
									RDH54	2	**			
									RGA2	2				
									RPB9	3	**			
									RPN10	2	***			
									RTC6	2	*			
									RTS1	2	*			
									RTT101	2				
									RTT107	2				
									SAP155	3	*			
									SAP4	2	**			
									SAS2	2	*			
									SEM1	3	**			
									SGF73	3				
									SGO1	2				
									SLX8	2				
									SNF4	2	*			
									SNF6	2	*			
									SOD1	2	*			
									SRS2	3	*			
									SSN3	2				
									SSZ1	2	**			
									SYF2	2	*			
									TDP1	2				
									TEL1	2	***			
									TOF1	3	*			
									TRF5	2	*			
									TSA1	2	*			
									UBR1	3				
									VPS34	2	*			

Table 4-2. List of initial hit strains and frequency of significance.

Gene hits filled in orange indicate validated negative genetic interactions. Gene hits filled in green indicate false positive hits. Number of shared interactions is based on the number a certain gene was identifies as hit out of the three screens. Frequency of significance indicates in how many screens (out of the three) the hit strain had a p-value <0.05.

A.3 Mathematical explanation of genetic interaction formula

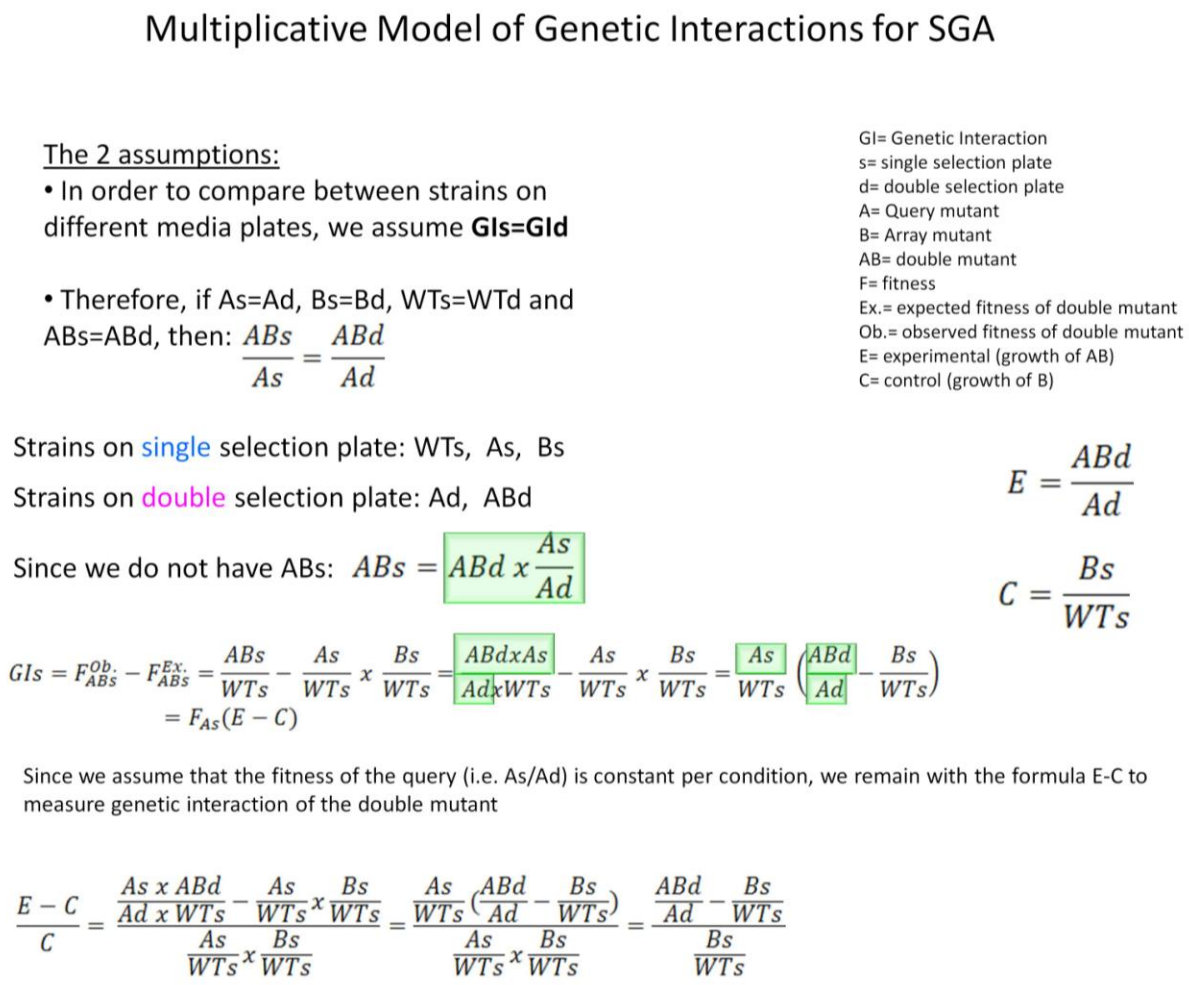

Figure 4-1. The calculation of genetic interaction in an SGA.

The fitness of a mutant strain is determined relative to the wild-type (WT) strain under the same condition. A genetic interaction between two mutated genes is determined relative to the expected combined fitness of the two single mutants, thus taking into account the growth of the WT, the observed growth of the double mutant and the growth of each single mutant, in the same environment/condition. The fitness of the query can change between conditions, therefore, the E-C calculation does not allow for comparing genetic interactions of the double mutant between conditions. The (E-C)/C calculation, which allows to account for slow growing or sensitive strains, also enables to compare double mutants between conditions, as we do not have to take into account the fitness of the query.

A.4 Final lists of validated genetic interactions with *scc1* query mutation

Gene Hit	Type of predicted GI	ScanLag score	Condition
GIM4	SL	-0.32	ND
RAD61	SL	-0.21	ND
DOC1	SL	-0.3	ND
CSM3	SL	-0.32	ND
MMS1	SL	-0.33	ND
SRS2	SL	-0.38	ND
HTZ1	SL	-0.26	ND
SAP155	SL	-0.25	ND
LSM6	SL	-0.2	ND
CIN2	SL	-0.27	ND
MRC1	SL	-0.36	ND
CTK1	SL	-0.34	ND
REV1	SC (mms)	-0.29	MMS
REV3	SC (mms)	-0.18	MMS
APN1	SC (mms)	-0.28	MMS
TEL1	SC (mms, cpt)	-0.29	MMS
TEL1	SC (mms, cpt)	-0.37	CPT
MCK1	SC (cpt, bleo)	-0.25	CPT
RAD24	SC (cpt)	-0.14	CPT
RAD9	SC (cpt)	-0.12	CPT
DOA1	SC (cpt, bleo)	-0.26	CPT
EXO1	SC (cpt)	-0.47	CPT
SIT4	SC (beno)	-0.33	Benomyl
CDH1	SC (beno)	-0.22	Benomyl
SGO1	SC (beno)	-0.32	Benomyl
SWC5	PS (ND, mms, cpt, bleo)	0.54	ND, MMS,

Gene Hit	Type of predicted GI	ScanLag score	Condition
			CPT
CLN2	PS (all 5 conditions)	0.26	ND

Table 4-3. Validated genetic interactions based on SGA data.

Gene Hit	Type of predicted GI	ScanLag score	Condition
DOA1	SC (cpt, bleo)	-0.33	Benomyl
RAD24	SC (cpt)	-0.17	Benomyl
APN1	SC (mms)	-0.26	CPT
CDH1	SC (beno)	-0.37	CPT
DBP7	SC (beno)	-0.36	CPT
FKH2	SC (bleo)	-0.21	CPT
PSY2	SC (bleo)	-0.25	CPT
RAD5	SC (bleo)	-0.16	CPT
REV3	SC (mms)	-0.15	CPT
RPN10	SC (beno)	-0.23	CPT
SGO1	SC (beno)	-0.4	CPT
SIT4	SC (beno)	-0.37	CPT
CDH1	SC (beno)	-0.17	MMS
DBP7	SC (beno)	-0.22	MMS
DOA1	SC (cpt, bleo)	-0.25	MMS
EXO1	SC (cpt)	-0.45	MMS
FKH2	SC (bleo)	-0.21	MMS
MCK1	SC (cpt, bleo)	-0.38	MMS
PER1	SC (bleo)	-0.11	MMS
PSY2	SC (bleo)	-0.11	MMS
RAD24	SC (cpt)	-0.16	MMS
SGF73	SC (bleo)	-0.11	MMS

Gene Hit	Type of predicted GI	ScanLag score	Condition
SGO1	SC (beno)	-0.38	MMS
SIT4	SC (beno)	-0.15	MMS
UBR1	SC (bleo)	-0.19	MMS
DBP7	SC (beno)	-0.24	ND
DBP7	SC (beno)	-0.24	ND
DOA1	SC (cpt, bleo)	-0.26	ND
EXO1	SC (cpt)	-0.39	ND
FKH2	SC (bleo)	-0.29	ND
FKH2	SC (bleo)	-0.29	ND
MCK1	SC (cpt, bleo)	-0.26	ND
RAD5	SC (bleo)	-0.2	ND
RAD5	SC (bleo)	-0.2	ND
RPN10	SC (beno)	-0.25	ND
RPN10	SC (beno)	-0.25	ND
SGO1	SC (beno)	-0.29	ND
SGO1	SC (beno)	-0.29	ND
SIT4	SC (beno)	-0.27	ND
SIT4	SC (beno)	-0.27	ND
TEL1	SC (mms, cpt)	-0.37	ND
UBR1	SC (bleo)	-0.28	ND
UBR1	SC (bleo)	-0.28	ND
APN1	SC (mms)	-0.3	ND

Table 4-4. New negative genetic interactions.